# Chapter 3

# SECOND-ORDER DIFFERENTIAL EQUATIONS IN ONE DIMENSION: FINITE ELEMENT MODELS



## 3.1 BACKGROUND

The traditional variational methods (e.g., the Ritz, Galerkin, and least-squares) described in Chapter 2 cease to be effective because of a serious shortcoming, namely, the difficulty in constructing the approximation functions. The approximation functions, apart from satisfying continuity, linear independence, completeness, and essential boundary conditions, are arbitrary; the selection becomes even more difficult when the given domain is geometrically complex. Since the quality of the approximation is directly affected by the choice of the approximation functions, it is discomforting to know that there exists no systematic procedure to construct them. Because of this shortcoming, despite the simplicity in obtaining approximate solutions, the traditional variational methods of approximation were never regarded as competitive computationally when compared with traditional finite difference schemes. The finite element method overcomes the shortcomings of the traditional variational methods by providing a systematic way of constructing the approximation functions.

Ideally speaking, an effective computational method should have the following features:

1. It should have a sound mathematical as well as physical basis (i.e., yield convergent solutions and be applicable to practical problems).
2. It should not have limitations with regard to the geometry, the physical composition of the domain, or the nature of the "loading."
3. The formulative procedure should be independent of the shape of the domain and the specific form of the boundary conditions.
4. It should be flexible enough to allow different degrees of approximation without reformulating the entire problem.
5. It should involve a systematic procedure that can be automated for use on digital computers.

The finite element method is a technique in which a given domain is represented as a collection of simple domains, called *finite elements*, so that it is possible to systematically construct the approximation functions needed in a variational or weighted-residual approximation of the solution of a problem over each element. Thus, the finite element method differs from the traditional Ritz, Galerkin, least-squares, collocation, and other weighted-residual methods in the manner in which the approximation functions are constructed. But this difference is responsible for the following three basic features of the finite element method:

1. *Division of whole domain into subdomains* that enable a systematic derivation of the approximation functions as well as representation of complex domains.
2. *Derivation of approximation functions* over each element. The approximation functions are often algebraic polynomials that are derived using interpolation theory. However, approximation functions need not be polynomials (like in meshless form of the finite element method).
3. *Assembly of elements* is based on continuity of the solution and balance of internal fluxes; the assemblage of elements results in a numerical analog of the mathematical model of the problem being analyzed.

These three features, which constitute three major steps of the finite element formulation, are closely related. The geometry of the elements used to represent the domain of a problem should be such that the approximation functions can be uniquely derived. The approximation functions depend not only on the geometry but also on the number and location of points, called nodes, in the element and the quantities to be interpolated (e.g., solution, or solution and its derivatives). Once the approximation functions have been derived, the procedure to obtain algebraic relations among the unknown coefficients (which give the values of the dependent variable at the nodes) is exactly the same as that used in the Ritz and weighted-residual methods. Hence, a study of Chapter 2, especially the weak-form development and the Ritz method, makes the present study easier.

The finite element method not only overcomes the shortcomings of the traditional variational methods, but it is also endowed with the features of an effective computational technique. The basic steps involved in the finite element analysis of a problem are given in Table 3.1.1.

In the sections that follow, our objective is to introduce many fundamental ideas that form the basis of the finite element method. In doing so, we postpone some issues of practical and theoretical complexity to later sections of this chapter and to Chapters 4–14. The basic steps of a finite element analysis are introduced via a model second-order differential equation.

## 3.2 BASIC STEPS OF FINITE ELEMENT ANALYSIS

### 3.2.1 Model Boundary Value Problem

Consider the problem of finding the function $u(x)$ that satisfies the differential equation

$$-\frac{d}{dx}\left(a\frac{du}{dx}\right)+cu-f=0 \quad \text{for} \quad 0<x<L \tag{3.2.1}$$

**Table 3.1.1** Steps involved in the finite element analysis of a typical problem.

1. Discretization (or representation) of the given domain into a collection of preselected finite elements. (This step can be postponed until the finite element formulation of the equation is completed.)
   (*a*) Construct the finite element mesh of preselected elements.
   (*b*) Number the nodes and the elements.
   (*c*) Generate the geometric properties (e.g., coordinates and cross-sectional areas) needed for the problem.
2. Derivation of element equations for all typical elements in the mesh.
   (*a*) Construct the variational formulation of the given differential equation over the typical element.
   (*b*) Assume that a typical dependent variable $u$ is of the form

$$u = \sum_{i=1}^{n} u_i \psi_i$$

   and substitute it into Step 2*a* to obtain element equations in the form

$$[K^e]\{u^e\} = \{F^e\}$$

   (*c*) Select, if already available in the literature, or derive element interpolation functions $\psi_i$ and compute the element matrices.
3. Assembly of element equations to obtain the equations of the whole problem.
   (*a*) Identify the interelement continuity conditions among the primary variables (relationship between the local degrees of freedom and the global degrees of freedom—connectivity of elements) by relating element nodes to global nodes.
   (*b*) Identify the "equilibrium" conditions among the secondary variables (relationship between the local source or force components and the globally specified source components).
   (*c*) Assemble element equations using Steps 3*a* and 3*b*.
4. Imposition of the boundary conditions of the problem.
   (*a*) Identify the specified global primary degrees of freedom.
   (*b*) Identify the specified global secondary degrees of freedom (if not already done in Step 3*b*).
5. Solution of the assembled equations.
6. Postprocessing of the results.
   (*a*) Compute the gradient of the solution or other desired quantities from the primary degrees of freedom computed in Step 5.
   (*b*) Represent the results in tabular and/or graphical form.

and the boundary conditions

$$u(0) = u_0, \quad \left(a\frac{du}{dx}\right)\bigg|_{x=L} = Q_0 \tag{3.2.2}$$

where $a = a(x)$, $c = c(x)$, $f = f(x)$, and $u_0$, and $Q_0$ are the *data* (i.e., known quantities) of the problem. Equation (3.2.1) arises in connection with the analytical description of many physical processes. For example, conduction and convection heat transfer in a plane wall or fin [see Fig. 3.2.1(*a*)], flow through channels and pipes, transverse deflection of cables, axial deformation of bars [see Fig. 3.2.1(*b*)], and many other physical processes are described by Eq. (3.2.1). A list of field problems described by Eq. (3.2.1) when $c(x) = 0$ are presented in Table 3.2.1 [see Reddy (2004)]. Thus, if we can develop a numerical procedure by which Eq. (3.2.1) can be solved for all possible boundary conditions, the procedure can be used to solve all field problems listed in Table 3.2.1, as well as many others. This fact provides us with the motivation to use (3.2.1) as the model second-order equation in one dimension. A step-by-step procedure for the formulation and solution of (3.2.1) by the

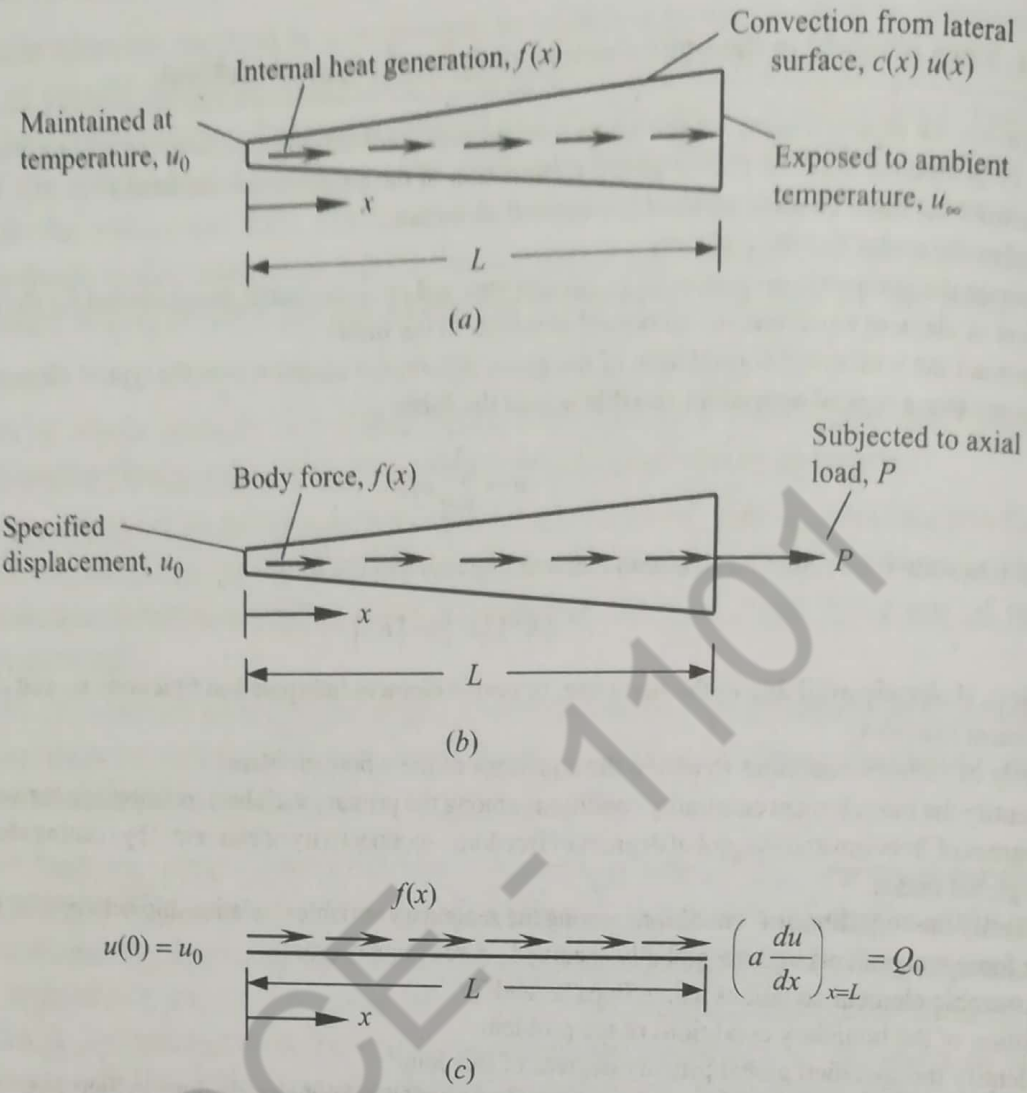


**Figure 3.2.1** ($a$) Heat transfer in a fin. ($b$) Axial deformation of a bar. ($c$) Mathematical idealization of the problem in ($a$) or ($b$).

finite element method is summarized in Table 3.1.1. The mathematical problem consists of solving the differential equation (3.2.1) in one-dimensional domain $\Omega = (0, L)$ subject to a suitable set of specified boundary conditions at the boundary points $x = 0$ and $x = L$, as shown in Fig. 3.2.1($c$). As already shown in Chapter 2, the type of boundary conditions associated with a differential equation emerges in a natural way during the weak-form development of the differential equation. A detailed discussion of these ideas is presented next.

### 3.2.2 Discretization of the Domain

In the finite element method, the domain $\Omega$ of the problem [Fig. 3.2.2($a$)] is divided into a set of subintervals, i.e., line elements, called *finite elements*. A typical element is denoted $\Omega_e$ and it is located between points $A$ and $B$ with coordinates $x_a$ and $x_b$ (i.e., of length $h_e = x_b - x_a$). The collection of finite elements in a domain is called the *finite element mesh* of the domain [see Fig. 3.2.2($b$)].

The reason for dividing a domain into a set of subdomains, i.e., finite elements, is two-fold. First, domains of most systems, by design, are a composite of geometrically and/or

**Table 3.2.1** Some examples of engineering problems governed by the second-order equation (3.2.1) (see the footnote for the meaning of some parameters*).

| Field of study | Primary variable $u$ | Problem data $a$ | Problem data $c$ | Problem data $f$ | Secondary variable $Q$ |
|---|---|---|---|---|---|
| Heat transfer | Temperature $T - T_\infty$ | Thermal conductance $kA$ | Surface convection $AP\beta$ | Heat generation $f$ | Heat $Q$ |
| Flow through porous medium | Fluid head $\phi$ | Permeability $\mu$ | 0 | Infiltraction $f$ | Point source $Q$ |
| Flow through pipes | Pressure $P$ | Pipe resistance $1/R$ | 0 | 0 | Point source $Q$ |
| Flow of viscous fluids | Velocity $v_x$ | Viscosity $\mu$ | 0 | Pressure gradient $-dP/dx$ | Shear stress $\sigma_{xz}$ |
| Elastic cables | Displacement $u$ | Tension $T$ | 0 | Transverse force $f$ | Point force $P$ |
| Elastic bars | Displacement $u$ | Axial stiffness $EA$ | 0 | Axial force $f$ | Point force $P$ |
| Torsion of bars | Angle of twist $\theta$ | Shear stiffness $GJ$ | 0 | 0 | Torque $T$ |
| Electrostatics | Electrical potential $\phi$ | Dielectric constant $\epsilon$ | 0 | Charge density $\rho$ | Electric flux $E$ |

*$k$ = thermal conductance; $\beta$ = convective film conductance; $p$ = perimeter; $P$ = pressure or force; $T_\infty$ = ambient temperature of the surrounding fluid medium; $R = 128\mu h/(\pi d^4)$ with $\mu$ being the viscosity, $h$ the length, and $d$ the diameter of the pipe; $E$ = Young's modulus; $A$ = area of cross section; $J$ = polar moment of inertia.

materially different parts, and the solution on these subdomains is represented by different functions that are continuous at the interfaces of these subdomains. Therefore, it is appropriate to seek approximation of the solution over each subdomain. Second, approximation of the solution over each element of the mesh is simpler than its approximation over the entire domain. Approximation of the geometry of the domain in the present case is not a

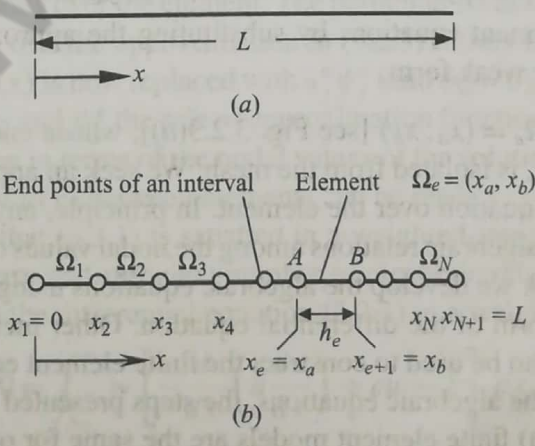


**Figure 3.2.2** (*a*) Whole domain. (*b*) Finite element discretization (mesh).

CHAPTER 3

# One-Dimensional Problems

## 3.1 INTRODUCTION

The total potential energy and the stress–strain and strain–displacement relationships are now used in developing the finite element method for a one-dimensional problem. The basic procedure is the same for two- and three-dimensional problems discussed later in the book. For the one-dimensional problem, the stress, strain, displacement, and loading depend only on the variable $x$. That is, the vectors $\mathbf{u}$, $\boldsymbol{\sigma}$, $\boldsymbol{\epsilon}$, $\mathbf{T}$, and $\mathbf{f}$ in Chapter 1 now reduce to

$$\mathbf{u} = u(x) \qquad \boldsymbol{\sigma} = \sigma(x) \qquad \boldsymbol{\epsilon} = u(x)$$
$$\mathbf{T} = T(x) \qquad \mathbf{f} = f(x) \tag{3.1}$$

Furthermore, the stress–strain and strain–displacement relations are

$$\sigma = E\epsilon \qquad \epsilon = \frac{du}{dx} \tag{3.2}$$

For one-dimensional problems, the differential volume $dV$ can be written as

$$dV = A\,dx \tag{3.3}$$

The loading consists of three types: the **body force** $f$, the **traction force** $T$, and the **point load** $P_i$. These forces are shown acting on a body in Fig. 3.1. A body force is a distributed force acting on every elemental volume of the body and has the units of force per unit volume. The self-weight due to gravity is an example of a body force. A traction force is a distributed load acting on the surface of the body. In Chapter 1, the traction force is defined as force per unit area. For the one-dimensional problem considered here, however, the traction force is defined as force per unit length. This is done by taking the traction force to be the product of the force per unit area with the perimeter of the cross section. Frictional resistance, viscous drag, and surface shear are examples of traction forces in one-dimensional problems. Finally, $P_i$ is a force acting at a point $i$ and $u_i$ is the $x$ displacement at that point.

The finite element modeling of a one-dimensional body is considered in Section 3.2. The basic idea is to discretize the region and express the displacement field in terms

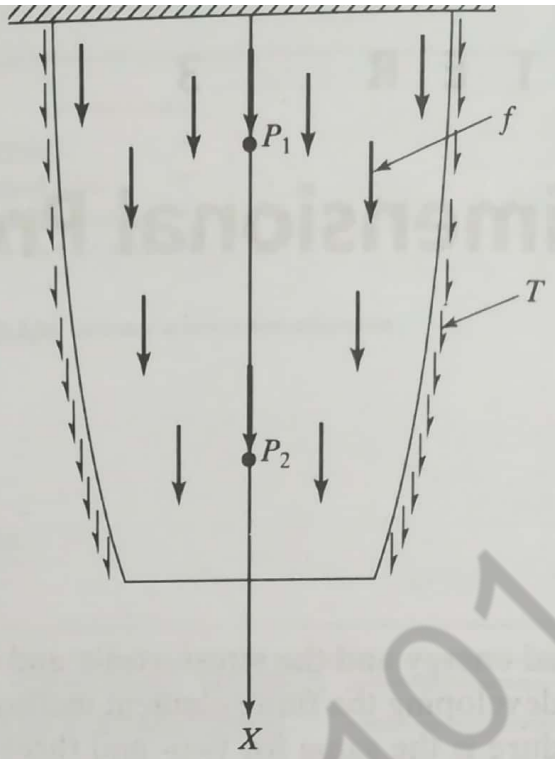


FIGURE 3.1 One-dimensional bar loaded by traction, body, and point loads.

of values at discrete points. Linear elements are introduced first. Stiffness and load concepts are developed using potential energy and Galerkin approaches. Boundary conditions are then considered. Temperature effects and quadratic elements are discussed later in this chapter.

## 3.2 FINITE ELEMENT MODELING

The steps of element division and node numbering are discussed here.

### Element Division

Consider the bar in Fig. 3.1. The first step is to **model** the bar as a *stepped shaft*, consisting of a discrete number of elements, each having a uniform cross section. Specifically, let us model the bar using four finite elements. A simple scheme for doing this is to divide the bar into four regions, as shown in Fig. 3.2a. The average cross-sectional area within each region is evaluated and then used to define an element with uniform cross section. The resulting four-element, five-node finite element model is shown in Fig. 3.2b. In the finite element model, every element connects to two nodes. In Fig. 3.2b, the element numbers are circled to distinguish them from node numbers. In addition to the cross section, traction and body forces are also (normally) treated as constant within each element. However, cross-sectional area, traction, and body forces can differ in magnitude from element to element. Better approximations are obtained by increasing the number of elements. It is convenient to define a node at each location where a point load is applied.

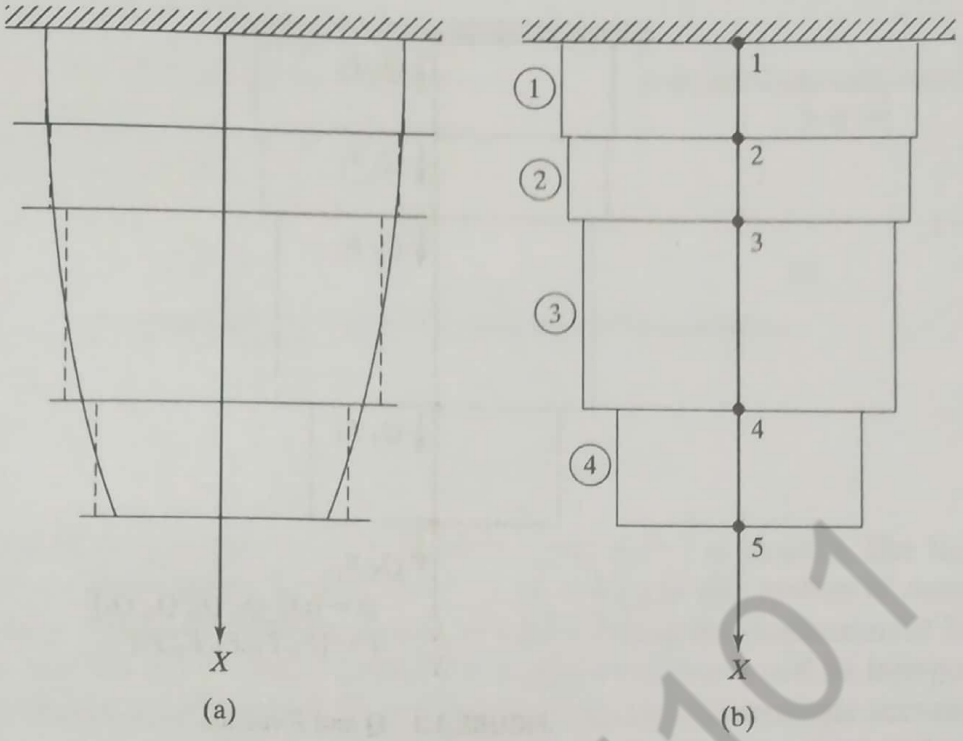


FIGURE 3.2 Finite element modeling of a bar.

### *Numbering Scheme*

We have shown how a rather complicated looking bar has been modeled using a discrete number of elements, each element having a simple geometry. The similarity of the various elements is one reason why the finite element method is easily amenable to computer implementation. For easy implementation, an orderly numbering scheme for the model has to be adopted.

In a one-dimensional problem, every node is permitted to displace only in the $\pm x$ direction. Thus, each node has only one *degree of freedom (dof)*. The five-node finite element model in Fig. 3.2b has five dofs. The displacements along each dof are denoted by $Q_1, Q_2, \ldots, Q_5$. In fact, the column vector $\mathbf{Q} = [Q_1, Q_2, \ldots, Q_5]^T$ is called the *global displacement vector*. The *global load vector* is denoted by $\mathbf{F} = [F_1, F_2, \ldots, F_5]^T$. The vectors $\mathbf{Q}$ and $\mathbf{F}$ are shown in Fig. 3.3. The sign convention used is that a displacement or load has a positive value if acting along the $+x$ direction. At this stage, conditions at the boundary are not imposed. For example, node 1 in Fig. 3.3 is fixed, which implies $Q_1 = 0$. These conditions are discussed later.

Each element has two nodes; therefore, the **element connectivity** information can be conveniently represented as shown in Fig. 3.4. Further, the element connectivity table is also given. In the connectivity table, the headings 1 and 2 refer to *local node numbers* of an element, and the corresponding node numbers on the body are called *global numbers*. Connectivity thus establishes the local–global correspondence. In this simple example, the connectivity can be easily generated since local node 1 is the same as the element number $e$, and local node 2 is $e + 1$. Other ways of numbering nodes or more complex geometries suggest the need for a connectivity table. The connectivity is introduced in the program using the array NOC.

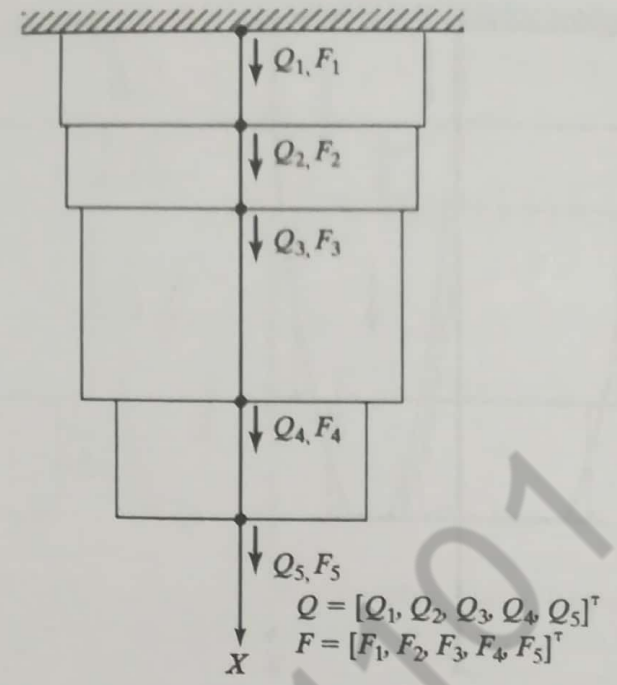


FIGURE 3.3 **Q** and **F** vectors.

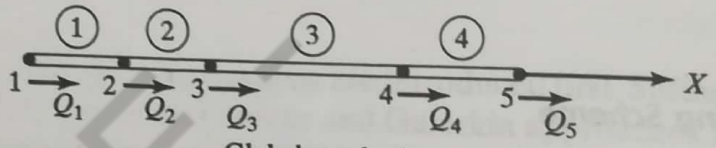


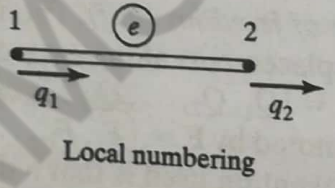


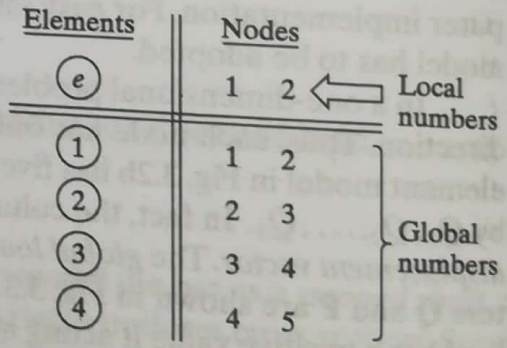


FIGURE 3.4 Element connectivity.

The concepts of dof, nodal displacements, nodal loads, and element connectivity are central to the finite element method and should be clearly understood.

## 3.3 COORDINATES AND SHAPE FUNCTIONS

Consider a typical finite element $e$ in Fig. 3.5a. In the local number scheme, the first node will be numbered 1 and the second node 2. The notation $x_1 = x$-coordinate of node 1, $x_2 = x$-coordinate of node 2 is used. We define a **natural** or **intrinsic** coordinate system, denoted by $\xi$, as

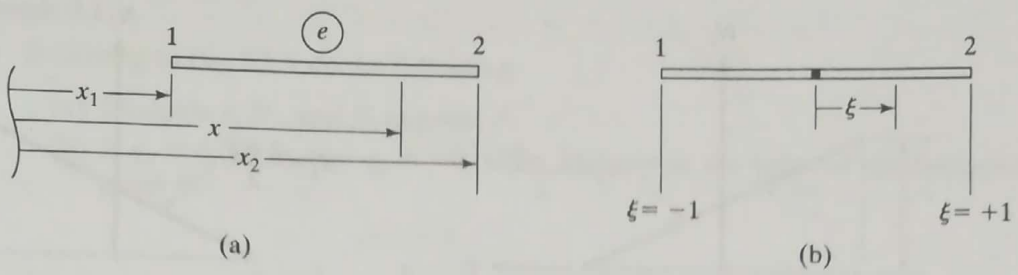


FIGURE 3.5 Typical element in $x$- and $\xi$-coordinates.

$$\xi = \frac{2}{x_2 - x_1}(x - x_1) - 1 \tag{3.4}$$

From Fig. 3.5b, we see that $\xi = -1$ at node 1 and $\xi = 1$ at node 2. The length of an element is covered when $\xi$ changes from $-1$ to 1. We use this system of coordinates in defining shape functions, which are used in interpolating the displacement field.

Now *the unknown displacement field within an element will be interpolated by a linear distribution* (Fig. 3.6). This approximation becomes increasingly accurate as more elements are considered in the model. To implement this linear interpolation, linear **shape functions** will be introduced as

$$N_1(\xi) = \frac{1 - \xi}{2} \tag{3.5}$$

$$N_2(\xi) = \frac{1 + \xi}{2} \tag{3.6}$$

The shape functions $N_1$ and $N_2$ are shown in Figs. 3.7a and b, respectively. The graph of the shape function $N_1$ in Fig. 3.7a is obtained from Eq. 3.5 by noting that $N_1 = 1$ at $\xi = -1$, $N_1 = 0$ at $\xi = 1$, and $N_1$ is a straight line between the two points. Similarly, the graph of $N_2$ in Fig. 3.7b is obtained from Eq. 3.6. Once the shape functions are defined, the linear displacement field within the element can be written in terms of the nodal displacements $q_1$ and $q_2$ as

$$u = N_1 q_1 + N_2 q_2 \tag{3.7a}$$

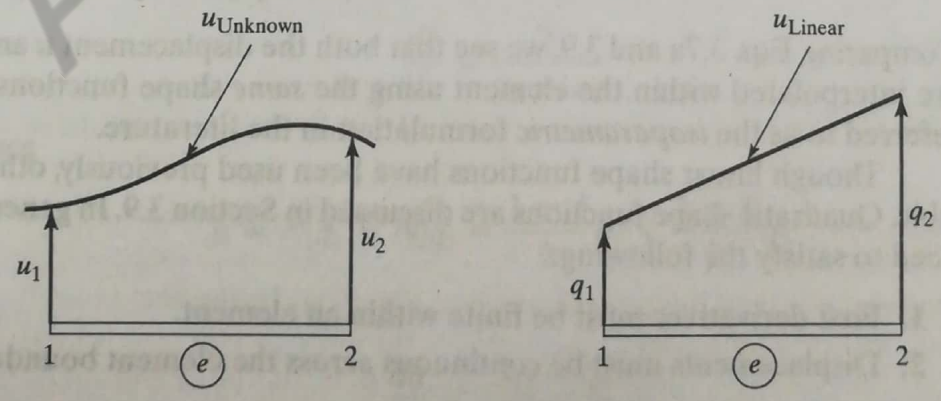


FIGURE 3.6 Linear interpolation of the displacement field within an element.

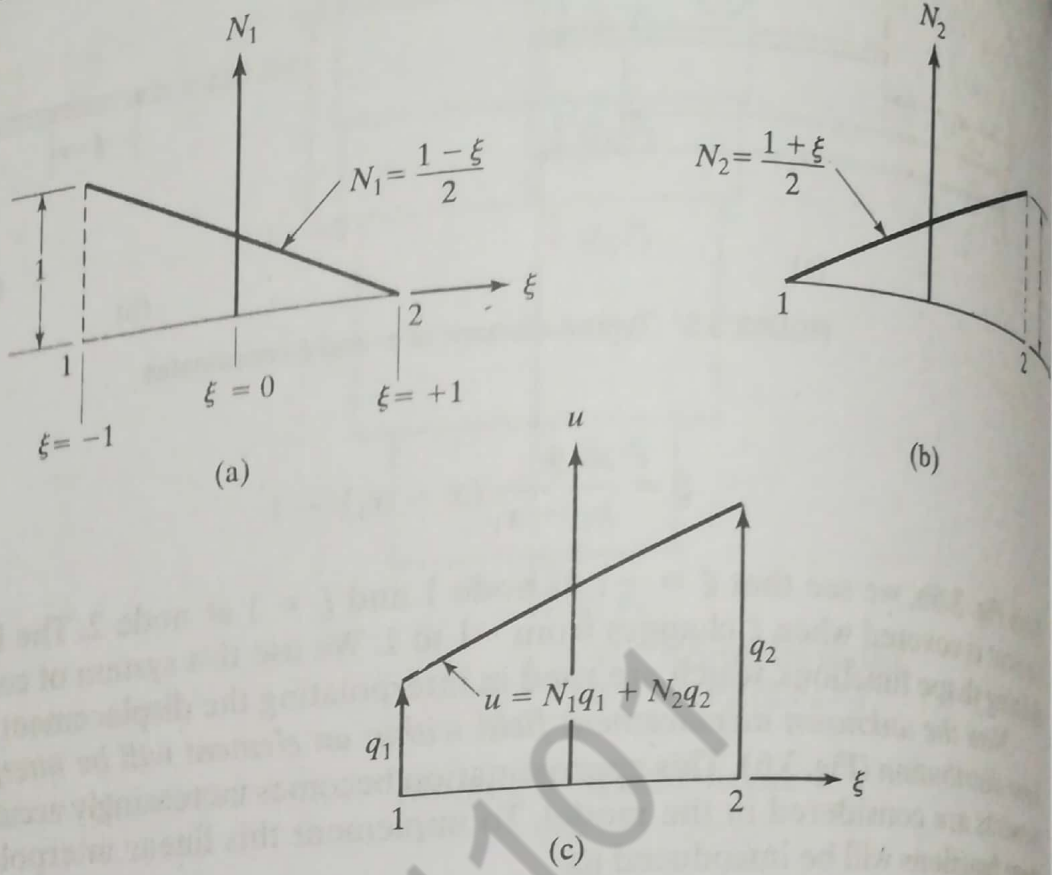


FIGURE 3.7 (a) Shape function $N_1$, (b) shape function $N_2$, and (c) linear interpolation using $N_1$ and $N_2$.

or, in matrix notation, as

$$u = \mathbf{Nq}$$

where

$$\mathbf{N} = [N_1, N_2] \quad \text{and} \quad \mathbf{q} = [q_1, q_2]^T$$

In these equations, $\mathbf{q}$ is referred to as the *element displacement vector*. It is readily verified from Eq. 3.7a that $u = q_1$ at node 1, $u = q_2$ at node 2, and that $u$ varies linearly (Fig. 3.7c).

It may be noted that the transformation from $x$ to $\xi$ in Eq. 3.4 can be written in terms of $N_1$ and $N_2$ as

$$x = N_1 x_1 + N_2 x_2$$

Comparing Eqs. 3.7a and 3.9, we see that both the displacement $u$ and the coordinate $x$ are interpolated within the element using the *same* shape functions $N_1$ and $N_2$. This is referred to as the *isoparametric* formulation in the literature.

Though linear shape functions have been used previously, other choices are also possible. Quadratic shape functions are discussed in Section 3.9. In general, shape functions need to satisfy the following:

1. First derivatives must be finite within an element.
2. Displacements must be continuous across the element boundary.

Rigid body motion should not introduce any stresses in the element.

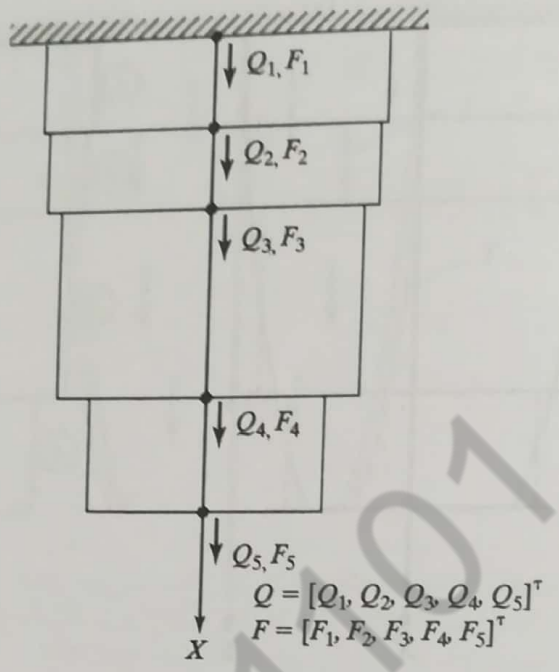


FIGURE 3.3 **Q** and **F** vectors.

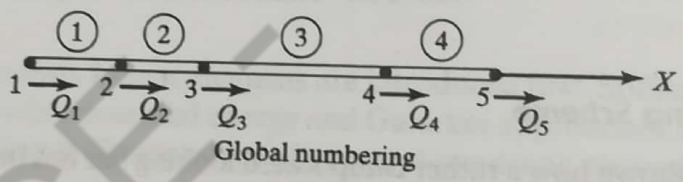


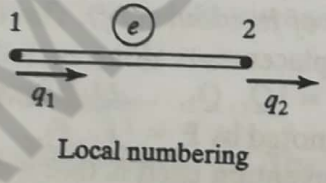


| Elements | Nodes | |
|---|---|---|
| e | 1 | 2 ⇐ Local numbers |
| 1 | 1 | 2 |
| 2 | 2 | 3 |
| 3 | 3 | 4 |
| 4 | 4 | 5 |

Global numbers

FIGURE 3.4 Element connectivity.

The concepts of dof, nodal displacements, nodal loads, and element connectivity are central to the finite element method and should be clearly understood.

## 3.3 COORDINATES AND SHAPE FUNCTIONS

Consider a typical finite element $e$ in Fig. 3.5a. In the local number scheme, the first node will be numbered 1 and the second node 2. The notation $x_1$ = $x$-coordinate of node 1, $x_2$ = $x$-coordinate of node 2 is used. We define a **natural** or **intrinsic** coordinate system, denoted by $\xi$, as

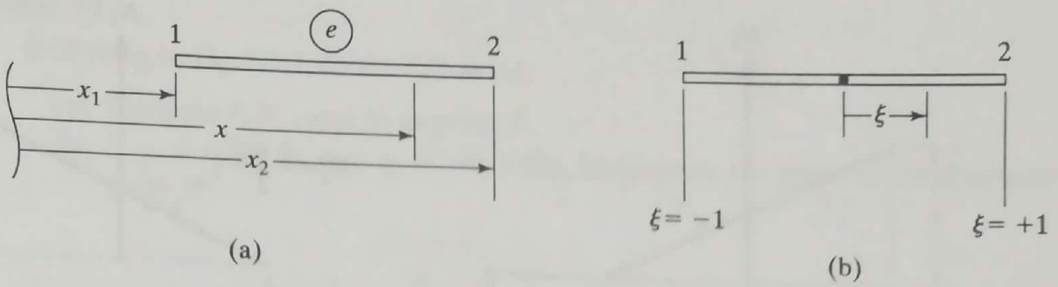


FIGURE 3.5 Typical element in $x$- and $\xi$-coordinates.

$$\xi = \frac{2}{x_2 - x_1}(x - x_1) - 1 \tag{3.4}$$

From Fig. 3.5b, we see that $\xi = -1$ at node 1 and $\xi = 1$ at node 2. The length of an element is covered when $\xi$ changes from $-1$ to 1. We use this system of coordinates in defining shape functions, which are used in interpolating the displacement field.

Now *the unknown displacement field within an element will be interpolated by a linear distribution* (Fig. 3.6). This approximation becomes increasingly accurate as more elements are considered in the model. To implement this linear interpolation, linear **shape functions** will be introduced as

$$N_1(\xi) = \frac{1 - \xi}{2} \tag{3.5}$$

$$N_2(\xi) = \frac{1 + \xi}{2} \tag{3.6}$$

The shape functions $N_1$ and $N_2$ are shown in Figs. 3.7a and b, respectively. The graph of the shape function $N_1$ in Fig. 3.7a is obtained from Eq. 3.5 by noting that $N_1 = 1$ at $\xi = -1$, $N_1 = 0$ at $\xi = 1$, and $N_1$ is a straight line between the two points. Similarly, the graph of $N_2$ in Fig. 3.7b is obtained from Eq. 3.6. Once the shape functions are defined, the linear displacement field within the element can be written in terms of the nodal displacements $q_1$ and $q_2$ as

$$u = N_1 q_1 + N_2 q_2 \tag{3.7a}$$

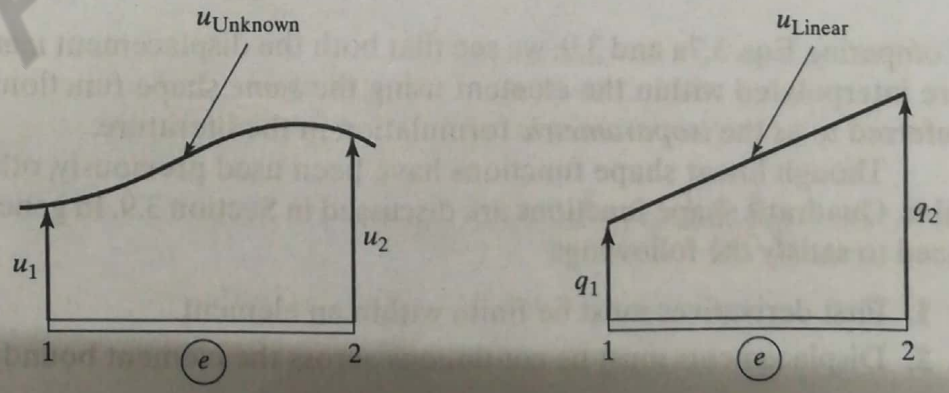


FIGURE 3.6 Linear interpolation of the displacement field within an element.

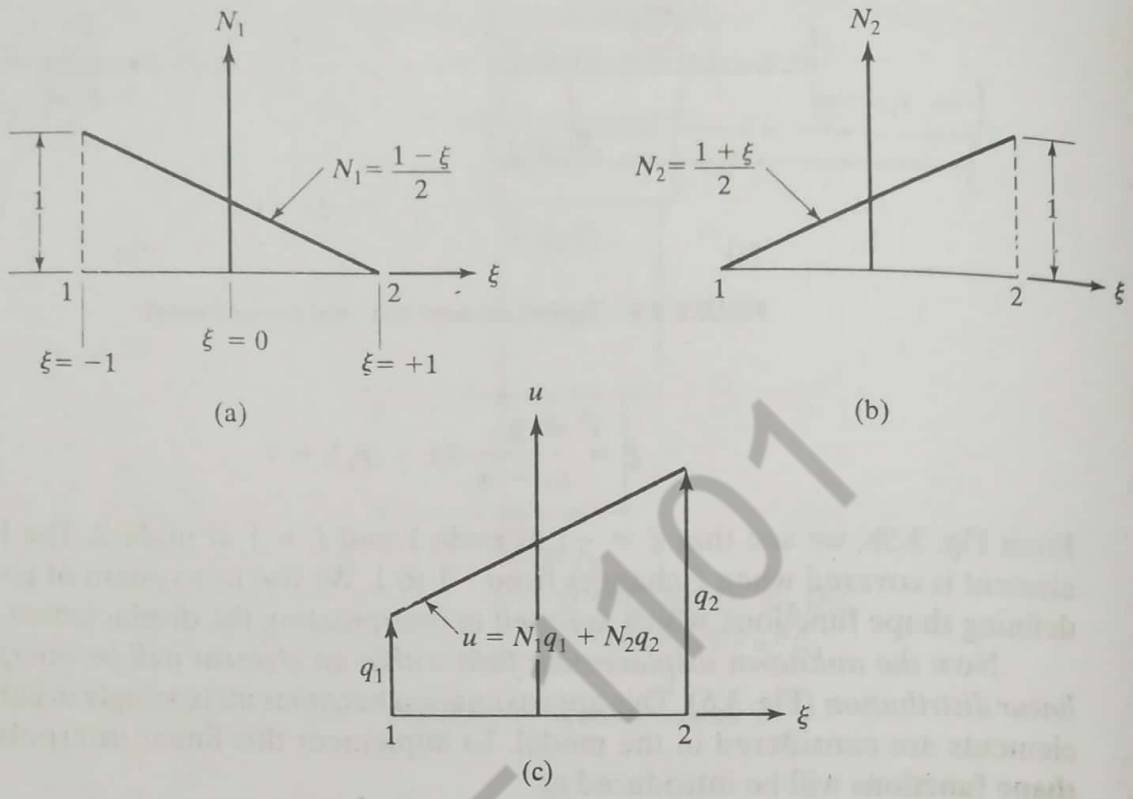


FIGURE 3.7 (a) Shape function $N_1$, (b) shape function $N_2$, and (c) linear interpolation using $N_1$ and $N_2$.

or, in matrix notation, as

$$u = \mathbf{Nq} \tag{3.7b}$$

where

$$\mathbf{N} = [N_1, N_2] \quad \text{and} \quad \mathbf{q} = [q_1, q_2]^{\mathrm{T}} \tag{3.8}$$

In these equations, $\mathbf{q}$ is referred to as the *element displacement vector*. It is readily verified from Eq. 3.7a that $u = q_1$ at node 1, $u = q_2$ at node 2, and that $u$ varies linearly (Fig. 3.7c).

It may be noted that the transformation from $x$ to $\xi$ in Eq. 3.4 can be written in terms of $N_1$ and $N_2$ as

$$x = N_1 x_1 + N_2 x_2 \tag{3.9}$$

Comparing Eqs. 3.7a and 3.9, we see that both the displacement $u$ and the coordinate $x$ are interpolated within the element using the *same* shape functions $N_1$ and $N_2$. This is referred to as the *isoparametric* formulation in the literature.

Though linear shape functions have been used previously, other choices are possible. Quadratic shape functions are discussed in Section 3.9. In general, shape functions need to satisfy the following:

1. First derivatives must be finite within an element.
2. Displacements must be continuous across the element boundary.

Rigid body motion should not introduce any stresses in the element.

**Example 3.1**

Referring to Fig. E3.1, do the following:

(a) Evaluate $\xi$, $N_1$, and $N_2$ at point $P$.

(b) If $q_1 = 0.003$ in. and $q_2 = -0.005$ in., determine the value of the displacement $q$ at point $P$.

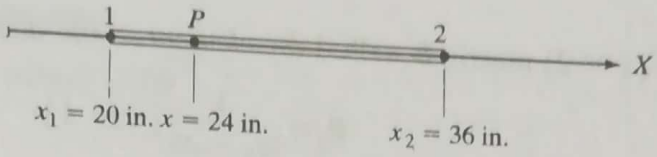


FIGURE E3.1

**Solution**

(a) Using Eq. 3.4, the $\xi$ coordinate of point $P$ is given by

$$\xi_p = \tfrac{2}{16}(24 - 20) - 1$$
$$= -0.5$$

Now Eqs. 3.5 and 3.6 yield

$$N_1 = 0.75 \quad \text{and} \quad N_2 = 0.25$$

(b) Using Eq. 3.7a, we get

$$u_p = 0.75(0.003) + 0.25(-0.005)$$
$$= 0.001 \text{ in.}$$

■

The strain–displacement relation in Eq. 3.2 is

$$\epsilon = \frac{du}{dx}$$

Upon using the chain rule of differentiation, we obtain

$$\epsilon = \frac{du}{d\xi}\frac{d\xi}{dx} \tag{3.10}$$

From the relation between $x$ and $\xi$ in Eq. 3.4, we have

$$\frac{d\xi}{dx} = \frac{2}{x_2 - x_1} \tag{3.11}$$

Also, since

$$u = N_1 q_1 + N_2 q_2 = \frac{1 - \xi}{2} q_1 + \frac{1 + \xi}{2} q_2$$

we have

$$\frac{du}{d\xi} = \frac{-q_1 + q_2}{2} \tag{3.12}$$

Thus, Eq. 3.10 yields

$$\epsilon = \frac{1}{x_2 - x_2}(-q_1 + q_2) \tag{3.}$$

The Eq. 3.13 can be written as

$$\epsilon = \mathbf{Bq} \tag{3.}$$

where the $(1 \times 2)$ matrix $\mathbf{B}$, called the *element strain–displacement matrix*, is given by

$$\mathbf{B} = \frac{1}{x_2 - x_1}[-1 \quad 1] \tag{3.}$$

*Note:* Use of linear shape functions results in a constant $\mathbf{B}$ matrix and, hence, in constant strain within the element. The stress, from Hooke's law, is

$$\sigma = E\mathbf{Bq} \tag{3.}$$

The stress given by this equation is also constant within the element. For interpolation purposes, however, the stress obtained from Eq. 3.16 can be considered to be the value at the centroid of the element.

The expressions $u = \mathbf{Nq}$, $\epsilon = \mathbf{Bq}$, and $\sigma = E\mathbf{Bq}$ relate the displacement, strain and stress, respectively, in terms of nodal values. These expressions will now be substituted into the potential-energy expression for the bar to obtain the element stiffness and load matrices.

## 3.4 THE POTENTIAL-ENERGY APPROACH

The general expression for the potential energy given in Chapter 1 is

$$\Pi = \frac{1}{2}\int_L \sigma^{\mathrm{T}}\epsilon A\,dx - \int_L u^{\mathrm{T}} f A\,dx - \int_L u^{\mathrm{T}} T\,dx - \sum_i u_i P_i \tag{3.17}$$

The quantities $\sigma$, $\epsilon$, $u$, $f$, and $T$ in Eq. 3.17 are discussed at the beginning of this chapter. In the last term, $P_i$ represents a force acting at point $i$, and $u_i$ is the $x$ displacement at that point. The summation on $i$ gives the potential energy due to all point loads.

Since the continuum has been discretized into finite elements, the expression for $\Pi$ becomes

$$\Pi = \sum_e \frac{1}{2}\int_e \sigma^{\mathrm{T}}\epsilon A\,dx - \sum_e \int_e u^{\mathrm{T}} f A\,dx - \sum_e \int_e u^{\mathrm{T}} T\,dx - \sum_i Q_i P_i \tag{3.18a}$$

The last term in Eq. 3.18a assumes that point loads $P_i$ are applied at the nodes. This assumption makes the present derivation simpler with respect to notation and is also a common modeling practice. Equation 3.18a can be written as

$$\Pi = \sum_e U_e - \sum_e \int_e u^{\mathrm{T}} f A\,dx - \sum_e \int_e u^{\mathrm{T}} T\,dx - \sum Q_i P_i \tag{3.18b}$$

where

$$U_e = \frac{1}{2}\int \sigma^T \epsilon A\, dx$$

is the element strain energy.

### *Element Stiffness Matrix*

Consider the strain energy term

$$U_e = \frac{1}{2}\int_e \sigma^T \epsilon A\, dx \tag{3.19}$$

Substituting for $\sigma = E\mathbf{Bq}$ and $\epsilon = \mathbf{Bq}$ into Eq. 3.19 yields

$$U_e = \frac{1}{2}\int_e \mathbf{q}^T\mathbf{B}^T E\mathbf{B}\mathbf{q} A\, dx \tag{3.20a}$$

or

$$U_e = \frac{1}{2}\mathbf{q}^T \int_e [\mathbf{B}^T E\mathbf{B} A\, dx]\mathbf{q} \tag{3.20b}$$

In the finite element model (Section 3.2), the cross-sectional area of element $e$, denoted by $A_e$, is constant. Also, $\mathbf{B}$ is a constant matrix. Further, the transformation from $x$ to $\xi$ in Eq. 3.4 yields

$$dx = \frac{x_2 - x_1}{2} d\xi \tag{3.21a}$$

or

$$dx = \frac{\ell_e}{2} d\xi \tag{3.21b}$$

where $-1 \le \xi \le 1$, and $\ell_e = |x_2 - x_1|$ is the length of the element.

The element strain energy $U_e$ is now written as

$$U_e = \frac{1}{2}\mathbf{q}^T\left[A_e \frac{\ell_e}{2} E_e \mathbf{B}^T\mathbf{B}\int_{-1}^{1} d\xi\right]\mathbf{q} \tag{3.22}$$

where $E_e$ is Young's modulus of element $e$. Noting that $\int_{-1}^{1} d\xi = 2$ and substituting for $\mathbf{B}$ from Eq. 3.15, we get

$$U_e = \frac{1}{2}\mathbf{q}^T A_e \ell_e E_e \frac{1}{\ell_e^2}\begin{Bmatrix} -1 \\ 1 \end{Bmatrix}[-1 \quad 1]\mathbf{q} \tag{3.23}$$

which results in

$$U_e = \frac{1}{2}\mathbf{q}^T \frac{A_e E_e}{\ell_e}\begin{bmatrix} 1 & -1 \\ -1 & 1 \end{bmatrix}\mathbf{q} \tag{3.24}$$

This equation is of the form

$$U_e = \frac{1}{2}\mathbf{q}^{\mathrm{T}}\mathbf{k}^e\mathbf{q} \tag{3.25}$$

where the **element stiffness matrix** $\mathbf{k}^e$ is given by

$$\mathbf{k}^e = \frac{E_e A_e}{\ell_e}\begin{bmatrix} 1 & -1 \\ -1 & 1 \end{bmatrix} \tag{3.26}$$

We note here the similarity of the strain energy expression in Eq. 3.26 with the strain energy in a simple spring, which is given as $U = \frac{1}{2}kQ^2$. Also, observe that $\mathbf{k}^e$ is linearly proportional to the product $A_eE_e$ and inversely proportional to the length $\ell_e$.

### *Force Terms*

The element body force term $\int_e u^{\mathrm{T}} f A\, dx$ appearing in the total potential energy is considered first. Substituting $u = N_1q_1 + N_2q_2$, we have

$$\int_e u^{\mathrm{T}} f A\, dx = A_e f \int_e (N_1q_1 + N_2q_2)\, dx \tag{3.27}$$

Recall that the body force $f$ has units of force per unit volume. In the Eq. 3.27, $A_e$ and $f$ are constant within the element and were consequently brought outside the integral. This equation can be written as

$$\int_e u^{\mathrm{T}} f A\, dx = \mathbf{q}^{\mathrm{T}}\begin{Bmatrix} A_e f \displaystyle\int_e N_1\, dx \\ A_e f \displaystyle\int_e N_2\, dx \end{Bmatrix} \tag{3.28}$$

The integrals of the shape functions described earlier can be readily evaluated by making the substitution $dx = (\ell_e/2)\, d\xi$. Thus,

$$\int_e N_1\, dx = \frac{\ell_e}{2}\int_{-1}^{1} \frac{1-\xi}{2}\, d\xi = \frac{\ell_e}{2}$$

$$\int_e N_2\, dx = \frac{\ell_e}{2}\int_{-1}^{1} \frac{1-\xi}{2}\, d\xi = \frac{\ell_e}{2} \tag{3.29}$$

Alternatively, $\int_e N_1\, dx$ is simply the area under the $N_1$ curve as shown in Fig. 3.8, which equals $\frac{1}{2}\cdot\ell_e\cdot 1 = \ell_e/2$. Similarly, $\int N_2\, dx = \frac{1}{2}\cdot\ell_e\cdot 1 = \ell_e/2$. The body force term in Eq. 3.28 reduces to

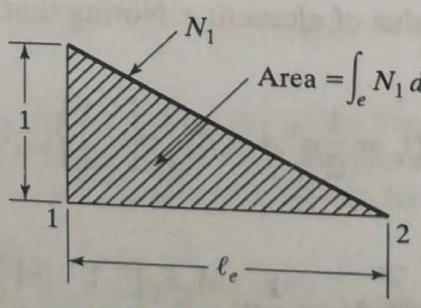


FIGURE 3.8 Integral of a shape function.

$$\int_e u^T f A \, dx = \mathbf{q}^T \frac{A_e}{2} \ell_e f \begin{Bmatrix} 1 \\ 1 \end{Bmatrix} \tag{3.30a}$$

which is of the form

$$\int_e u^T f A \, dx = \mathbf{q}^T \mathbf{f}^e \tag{3.30b}$$

The right side of this equation is of the form Displacement × Force. Thus, the **element body force vector**, $\mathbf{f}^e$, is identified as

$$\mathbf{f}^e = \frac{A_e \ell_e f}{2} \begin{Bmatrix} 1 \\ 1 \end{Bmatrix} \tag{3.31}$$

The element body force vector above has a simple physical explanation. Since $A_e \ell_e$ is the volume of the element and $f$ is the body force per unit volume, we see that $A_e \ell_e f$ gives the total body force acting on the element. The factor $\frac{1}{2}$ in Eq. 3.31 tells us that this total body force is equally distributed to the two nodes of the element.

The element *traction force term* $\int_e u^T T \, dx$ appearing in the total potential energy is now considered. We have

$$\int_e u^T T \, dx = \int_e (N_1 q_1 + N_2 q_2) T \, dx \tag{3.32}$$

Since the traction force $T$ is constant within the element, we have

$$\int_e u^T T \, dx = q^T \begin{Bmatrix} T \int_e N_1 \, dx \\ T \int_e N_2 \, dx \end{Bmatrix} \tag{3.33}$$

We have already shown that $\int_e N_1 \, dx = \int_e N_2 \, dx = \ell_e/2$. Thus, Eq. 3.33 is of the form

$$\int_e u^T T \, dx = \mathbf{q}^T \mathbf{T}^e \tag{3.34}$$

where the element traction-force vector is given by

$$\mathbf{T}^e = \frac{T \ell_e}{2} \begin{Bmatrix} 1 \\ 1 \end{Bmatrix} \tag{3.35}$$

We can provide a physical explanation for this equation as was given for the element body force vector.

At this stage, element matrices $\mathbf{k}^e$, $\mathbf{f}^e$, and $\mathbf{T}^e$ have been obtained. After we account for the element convectivity (in Fig. 3.3, for example, $\mathbf{q} = [Q_1, Q_2]^T$ for element 1, $\mathbf{q} = [Q_2, Q_3]^T$ for element 2, etc.), the total potential energy in Eq. 3.18b can be written as

$$\Pi = \tfrac{1}{2} \mathbf{Q}^T \mathbf{K} \mathbf{Q} - \mathbf{Q}^T \mathbf{F} \tag{3.36}$$

where $\mathbf{K}$ is the *global stiffness matrix*, $\mathbf{F}$ is the global load vector, and $\mathbf{Q}$ is the global displacement vector. For example, in the finite element model in Fig. 3.2b, $\mathbf{K}$ is a $(5 \times 5)$

matrix, and $\mathbf{Q}$ and $\mathbf{F}$ are each $(5 \times 1)$ vectors. $\mathbf{K}$ is obtained as follows: Using the element connectivity information, the elements of each $\mathbf{k}^e$ are placed in the appropriate locations in the larger $\mathbf{K}$ matrix, and overlapping elements are then summed. The $\mathbf{F}$ vector is similarly assembled. This process of assembling $\mathbf{K}$ and $\mathbf{F}$ from element stiffness and force matrices is discussed in detail in Section 3.6.

## 3.5 THE GALERKIN APPROACH

Following the concepts introduced in Chapter 1, we introduce a virtual displacement field

$$\phi = \phi(x) \tag{3.37}$$

and associated virtual strain

$$\epsilon(\phi) = \frac{d\phi}{dx} \tag{3.38}$$

where $\phi$ is an arbitrary or virtual displacement consistent with the boundary conditions. Galerkin's variational form, given in Eq. 1.43, for the one-dimensional problem considered here, is

$$\int_L \sigma^{\mathrm{T}} \epsilon(\phi) A \, dx - \int_L \phi^{\mathrm{T}} f A \, dx - \int_L \phi^{\mathrm{T}} T \, dx - \sum_i \phi_i P_i = 0 \tag{3.39a}$$

This equation should hold for every $\phi$ consistent with the boundary conditions. The first term represents the internal virtual work, while the load terms represent the external virtual work.

On the discretized region, Eq. 3.39a becomes

$$\sum_e \int_e \epsilon^{\mathrm{T}} E \epsilon(\phi) A \, dx - \sum_e \int_e \phi^{\mathrm{T}} f A \, dx - \sum_e \int_e \phi^{\mathrm{T}} T \, dx - \sum_i \phi_i P_i = 0 \tag{3.39b}$$

Note that $\epsilon$ is the strain due to the actual loads in the problem, while $\epsilon(\phi)$ is a virtual strain. Similar to the interpolation steps in Eqs. 3.7b, 3.14, and 3.16, we express

$$\begin{aligned} \phi &= \mathbf{N}\boldsymbol{\psi} \\ \epsilon(\phi) &= \mathbf{B}\boldsymbol{\psi} \end{aligned} \tag{3.40}$$

where $\boldsymbol{\psi} = [\psi_1, \psi_2]^{\mathrm{T}}$ represents the arbitrary nodal displacements of element $e$. Also, the global virtual displacements at the nodes are represented by

$$\boldsymbol{\Psi} = [\psi_1, \psi_2, \ldots, \psi_N]^{\mathrm{T}} \tag{3.41}$$

### Element Stiffness

Consider the first term, representing internal virtual work, in Eq. 3.39b. Substituting Eq. 3.40 into Eq. 3.39b, and noting that $\epsilon = \mathbf{Bq}$, we get

$$\int_e \epsilon^{\mathrm{T}} E \epsilon(\phi) A \, dx = \int_e \mathbf{q}^{\mathrm{T}} \mathbf{B}^{\mathrm{T}} E \, \mathbf{B}\boldsymbol{\psi} \, A \, dx \tag{3.42}$$

In the finite element model (Section 3.2), the cross-sectional area of element $e$, denoted by $A_e$, is constant. Also, $\mathbf{B}$ is a constant matrix. Further, $dx = (\ell_e/2)\, d\xi$. Thus,

$$\int_e \epsilon^T E \epsilon(\phi) A \, dx = \mathbf{q}^T \left[ E_e A_e \frac{\ell_e}{2} \mathbf{B}^T \mathbf{B} \int_{-1}^{1} d\xi \right] \boldsymbol{\psi} \tag{3.43a}$$

$$= \mathbf{q}^T \mathbf{k}^e \boldsymbol{\psi} \tag{3.43b}$$

$$= \boldsymbol{\psi}^T \mathbf{k}^e \mathbf{q}$$

where $\mathbf{k}^e$ is the (symmetric) element stiffness matrix given by

$$\mathbf{k}^e = E_e A_e \ell_e \mathbf{B}^T \mathbf{B} \tag{3.44}$$

Substituting $\mathbf{B}$ from Eq. 3.15, we have

$$\mathbf{k}^e = \frac{E_e A_e}{\ell_e} \begin{bmatrix} 1 & -1 \\ -1 & 1 \end{bmatrix} \tag{3.45}$$

### *Force Terms*

Consider the second term in Eq. 3.39a, representing the virtual work done by the body force in an element. Using $\phi = \mathbf{N}\boldsymbol{\psi}$ and $dx = \ell_e/2\, d_\xi$, and noting that the body force in the element is assumed constant, we have

$$\int_e \phi^T f A \, dx = \int_{-1}^{1} \boldsymbol{\psi}^T \mathbf{N}^T f A_e \frac{\ell_e}{2} d\xi \tag{3.46a}$$

$$= \boldsymbol{\psi}^T \mathbf{f}^e \tag{3.46b}$$

where

$$\mathbf{f}^e = \frac{A_e \ell_e f}{2} \begin{Bmatrix} \int_{-1}^{1} N_1 \, d\xi \\ \int_{-1}^{1} N_2 \, d\xi \end{Bmatrix} \tag{3.47a}$$

is called the element body force vector. Substituting for $N_1 = (1 - \xi)/2$ and $N_2 = (1 + \xi)/2$, we obtain $\int_{-1}^{1} N_1 \, d\xi = 1$. Alternatively, $\int_{-1}^{1} N_1 \, d\xi$ is the area under the $N_1$ curve $= \frac{1}{2} \times 2 \times 1 = 1$ and $\int_{-1}^{1} N_2 \, d\xi = 1$. Thus,

$$\mathbf{f}^e = \frac{A_e \ell_e f}{2} \begin{Bmatrix} 1 \\ 1 \end{Bmatrix} \tag{3.47b}$$

The element traction term then reduces to

$$\int_e \phi^T T \, dx = \boldsymbol{\psi}^T \mathbf{T}^e \tag{3.48}$$

where the element traction-force vector is given by

$$\mathbf{T}^e = \frac{T \ell_e}{2} \begin{Bmatrix} 1 \\ 1 \end{Bmatrix} \tag{3.49}$$

At this stage, the element matrices $\mathbf{k}^e$, $\mathbf{f}^e$, and $\mathbf{T}^e$ have been obtained. After accounting for the element connectivity (in Fig. 3.3, for example, $\boldsymbol{\psi} = [\psi_1, \psi_2]^T$ for element 1, $\boldsymbol{\psi} = [\Psi_2, \Psi_3]^T$ for element 2, etc.), the variational form

$$\sum_e \boldsymbol{\psi}^T \mathbf{k}^e \mathbf{q} - \sum_e \boldsymbol{\psi}^T \mathbf{f}^e - \sum_e \boldsymbol{\psi}^T \mathbf{T}^e - \sum_i \Psi_i P_i = 0 \tag{3.50}$$

can be written as

$$\Psi^T(\mathbf{KQ} - \mathbf{F}) = 0 \tag{3.51}$$

which should hold for every $\Psi$ consistent with the boundary conditions. Methods for handling boundary conditions are discussed shortly. The global stiffness matrix $\mathbf{K}$ is assembled from element matrices $\mathbf{k}^e$ using element connectivity information. Likewise, $\mathbf{F}$ is assembled from element matrices $\mathbf{f}^e$ and $\mathbf{T}^e$. This assembly is discussed in detail in the next section.

## 3.6 ASSEMBLY OF THE GLOBAL STIFFNESS MATRIX AND LOAD VECTOR

We noted earlier that the total potential energy written in the form

$$\Pi = \sum_e \frac{1}{2}\mathbf{q}^T \mathbf{k}^e \mathbf{q} - \sum_e \mathbf{q}^T \mathbf{f}^e - \sum_e \mathbf{q}^T \mathbf{T}^e - \sum_i P_i Q_i$$

can be written in the form

$$\Pi = \tfrac{1}{2}\mathbf{Q}^T \mathbf{K} \mathbf{Q} - \mathbf{Q}^T \mathbf{F}$$

by taking element connectivity into account. This step involves assembling $\mathbf{K}$ and $\mathbf{F}$ from element stiffness and force matrices. The assembly of the structural stiffness matrix $\mathbf{K}$ from element stiffness matrices $\mathbf{k}^e$ will first be shown here.

Referring to the finite element model in Fig. 3.2b, let us consider the strain energy in, say, element 3. We have

$$U_3 = \tfrac{1}{2}\mathbf{q}^T \mathbf{k}^3 \mathbf{q} \tag{3.52a}$$

or, substituting for $\mathbf{k}^3$,

$$U_3 = \frac{1}{2}\mathbf{q}^T \frac{E_3 A_3}{\ell_3} \begin{bmatrix} 1 & -1 \\ -1 & 1 \end{bmatrix} \mathbf{q} \tag{3.52b}$$

For element 3, we have $\mathbf{q} = [Q_3, Q_4]^T$. Thus, we can write $U_3$ as

$$U_3 = \tfrac{1}{2}[Q_1, Q_2, Q_3, Q_4, Q_5] \begin{bmatrix} 0 & 0 & 0 & 0 & 0 \\ 0 & 0 & 0 & 0 & 0 \\ 0 & 0 & \dfrac{E_3 A_3}{\ell_3} & \dfrac{-E_3 A_3}{\ell_3} & 0 \\ 0 & 0 & \dfrac{-E_3 A_3}{\ell_3} & \dfrac{E_3 A_3}{\ell_3} & 0 \\ 0 & 0 & 0 & 0 & 0 \end{bmatrix} \begin{Bmatrix} Q_1 \\ Q_2 \\ Q_3 \\ Q_4 \\ Q_5 \end{Bmatrix} \tag{3.53}$$

From the previous equations, we see that elements of the matrix $\mathbf{k}^3$ occupy the third and fourth rows and columns of the $\mathbf{K}$ matrix. Consequently, when adding element-strain energies, the elements of $\mathbf{k}^e$ are placed in the appropriate locations of the global $\mathbf{K}$ matrix, based on the element connectivity; overlapping elements are simply added. We can denote this assembly symbolically as

$$\mathbf{K} \leftarrow \sum_e \mathbf{k}^e \tag{3.54a}$$

Similarly, the global load vector $\mathbf{F}$ is assembled from element-force vectors and point loads as

$$\mathbf{F} \leftarrow \sum_e (\mathbf{f}^e + \mathbf{T}^e) + \mathbf{P} \tag{3.54b}$$

The Galerkin approach also gives us the same assembly procedure. An example is now given to illustrate this assembly procedure in detail. In actual computation, $\mathbf{K}$ is stored in banded or skyline form to take advantage of symmetry and sparsity. This aspect is discussed in Section 3.7 and in greater detail in Chapter 4.

**Example 3.2**

Consider the bar as shown in Fig. E3.2. For each element $i$, $A_i$ and $\ell_i$ are the cross-sectional area and length, respectively. Each element $i$ is subjected to a traction force $T_i$ per unit length and a body force $f$ per unit volume. The units of $T_i$, $f$, $A_i$, and so on are assumed to be consistent. The Young's modulus of the material is $E$. A concentrated load $P_2$ is applied at node 2. The structural stiffness matrix and nodal load vector will now be assembled.

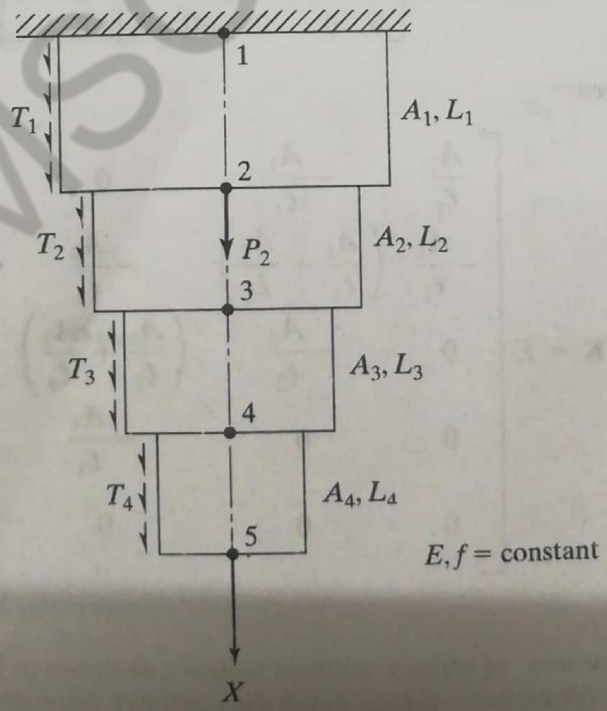


FIGURE E3.2

The element stiffness matrix for each element $i$ is obtained from Eq. 3.26 as

$$[k^{(i)}] = \frac{EA_i}{\ell_i}\begin{bmatrix} 1 & -1 \\ -1 & 1 \end{bmatrix}$$

The element connectivity table is the following:

| Element | 1 | 2 |
|---|---|---|
| 1 | 1 | 2 |
| 2 | 2 | 3 |
| 3 | 3 | 4 |
| 4 | 4 | 5 |

The element stiffness matrices can be "expanded" using the connectivity table and then summed (or assembled) to obtain the structural stiffness matrix as follows:*

$$\mathbf{K} = \frac{EA_1}{\ell_1}\begin{bmatrix} 1 & -1 & 0 & 0 & 0 \\ -1 & 1 & 0 & 0 & 0 \\ 0 & 0 & 0 & 0 & 0 \\ 0 & 0 & 0 & 0 & 0 \\ 0 & 0 & 0 & 0 & 0 \end{bmatrix} + \frac{EA_2}{\ell_2}\begin{bmatrix} 0 & 0 & 0 & 0 & 0 \\ 0 & 1 & -1 & 0 & 0 \\ 0 & -1 & 1 & 0 & 0 \\ 0 & 0 & 0 & 0 & 0 \\ 0 & 0 & 0 & 0 & 0 \end{bmatrix}$$

$$+ \frac{EA_3}{\ell_3}\begin{bmatrix} 0 & 0 & 0 & 0 & 0 \\ 0 & 0 & 0 & 0 & 0 \\ 0 & 0 & 1 & -1 & 0 \\ 0 & 0 & -1 & 1 & 0 \\ 0 & 0 & 0 & 0 & 0 \end{bmatrix} + \frac{EA_4}{\ell_4}\begin{bmatrix} 0 & 0 & 0 & 0 & 0 \\ 0 & 0 & 0 & 0 & 0 \\ 0 & 0 & 0 & 0 & 0 \\ 0 & 0 & 0 & 1 & -1 \\ 0 & 0 & 0 & -1 & 1 \end{bmatrix}$$

which gives

$$\mathbf{K} = E\begin{bmatrix} \frac{A_1}{\ell_1} & -\frac{A_1}{\ell_1} & 0 & 0 & 0 \\ -\frac{A_1}{\ell_1} & \left(\frac{A_1}{\ell_1}+\frac{A_2}{\ell_2}\right) & -\frac{A_2}{\ell_2} & 0 & 0 \\ 0 & -\frac{A_2}{\ell_2} & \left(\frac{A_2}{\ell_2}+\frac{A_3}{\ell_3}\right) & -\frac{A_3}{\ell_3} & 0 \\ 0 & 0 & -\frac{A_3}{\ell_3} & \left(\frac{A_3}{\ell_3}+\frac{A_4}{\ell_4}\right) & -\frac{A_4}{\ell_4} \\ 0 & 0 & 0 & -\frac{A_4}{\ell_4} & \frac{A_4}{\ell_4} \end{bmatrix}$$

*This "expansion" of element stiffness matrices as shown in Example 3.2 is merely for illustration purposes and is never explicitly carried out in the computer, since storing zeroes is inefficient. Instead, $\mathbf{K}$ is assembled directly from $\mathbf{k}^e$ using the connectivity table.

The global load vector is assembled as

$$\mathbf{F} = \begin{Bmatrix} \frac{A_1\ell_1 f}{2} + \frac{\ell_1 T_1}{2} \\ \left(\frac{A_1\ell_1 f}{2} + \frac{\ell_1 T_1}{2}\right) + \left(\frac{A_2\ell_2 f}{2} + \frac{\ell_2 T_2}{2}\right) \\ \left(\frac{A_2\ell_2 f}{2} + \frac{\ell_2 T_2}{2}\right) + \left(\frac{A_3\ell_3 f}{2} + \frac{\ell_3 T_3}{2}\right) \\ \left(\frac{A_3\ell_3 f}{2} + \frac{\ell_3 T_3}{2}\right) + \left(\frac{A_4\ell_4 f}{2} + \frac{\ell_4 T_4}{2}\right) \\ \frac{A_4\ell_4 f}{2} + \frac{\ell_4 T_4}{2} \end{Bmatrix} + \begin{Bmatrix} 0 \\ P_2 \\ 0 \\ 0 \\ 0 \end{Bmatrix}$$

■

## 3.7 PROPERTIES OF K

Several important comments will now be made regarding the global stiffness matrix for the linear one-dimensional problem discussed earlier:

1. The dimension of the global stiffness **K** is $(N \times N)$, where $N$ is the number of nodes. This follows from the fact that each node has only one degree of freedom.
2. **K** is symmetric.
3. **K** is a banded matrix. That is, all elements outside of the band are zero. This can be seen in Example 3.2, just considered. In this example, **K** can be compactly represented in banded form as

$$\mathbf{K}_{\text{banded}} = E \begin{bmatrix} \frac{A_1}{\ell_1} & -\frac{A_1}{\ell_1} \\ \frac{A_1}{\ell_1} + \frac{A_2}{\ell_2} & -\frac{A_2}{\ell_2} \\ \frac{A_2}{\ell_2} + \frac{A_3}{\ell_3} & -\frac{A_3}{\ell_3} \\ \frac{A_3}{\ell_3} + \frac{A_4}{\ell_4} & -\frac{A_4}{\ell_4} \\ \frac{A_4}{\ell_4} & 0 \end{bmatrix}$$

Note that $\mathbf{K}_{\text{banded}}$ is of dimension $[N \times \text{NBW}]$, where NBW is the half-bandwidth. In many one-dimensional problems such as the example just considered, the connectivity of element $i$ is $i, i+1$. In such cases, the banded matrix has only two columns (NBW = 2). In two and three dimensions, the direct formation of **K** in banded or skyline

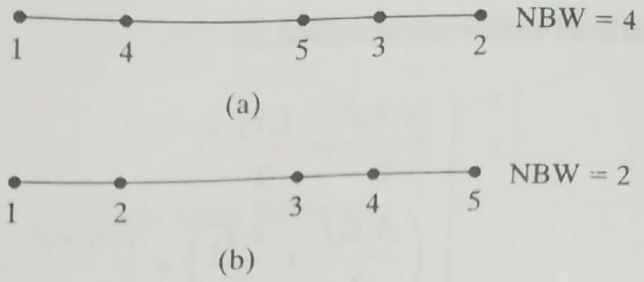


FIGURE 3.9 Node numbering and its effect on the half-bandwidth.

form from the element matrices involves some bookkeeping. This is discussed in detail at the end of Chapter 4. The reader should verify the following general formula for the half-bandwidth:

$$\text{NBW} = \max\begin{pmatrix}\text{Difference between dof numbers}\\ \text{connecting an element}\end{pmatrix} + 1 \tag{3.55}$$

For example, consider a four-element model of a bar that is numbered as shown in Fig. 3.9a. Using Eq. 3.55, we have

$$\text{NBW} = \max(4-1, 5-4, 5-3, 3-2) + 1 = 4$$

The numbering scheme in Fig. 3.9a is bad since $\mathbf{K}$ is almost "filled up" and consequently requires more computer storage and computation. Figure 3.9b shows the optimum numbering for minimum NBW.

Now the potential energy or Galerkin's approach has to be applied, noting the boundary conditions of the problem, to yield the finite element (equilibrium) equations. Solution of these equations yields the global displacement vector $\mathbf{Q}$. The stresses and reaction forces can then be recovered. These steps will now be discussed in the next section.

## 3.8 THE FINITE ELEMENT EQUATIONS; TREATMENT OF BOUNDARY CONDITIONS

Finite element equations are now developed after a consistent treatment of the boundary conditions.

### Types of Boundary Conditions

After using a discretization scheme to model the continuum, we have obtained an expression for the total potential energy in the body as

$$\Pi = \tfrac{1}{2}\mathbf{Q}^{\mathrm{T}}\mathbf{K}\mathbf{Q} - \mathbf{Q}^{\mathrm{T}}\mathbf{F}$$

where $\mathbf{K}$ is the structural stiffness matrix, $\mathbf{F}$ is the global load vector, and $\mathbf{Q}$ is the global displacement vector. As discussed previously, $\mathbf{K}$ and $\mathbf{F}$ are assembled from element stiffness and force matrices, respectively. We now must arrive at the equations of equilibrium, from which we can determine nodal displacements, element stresses, and support reactions.

The minimum potential-energy theorem (Chapter 1) is now invoked. This theorem is stated as follows: *Of all possible displacements that satisfy the boundary conditions of a structural system, those corresponding to equilibrium configurations make the total potential energy assume a minimum value.* Consequently, the equations of equilibrium can be obtained by minimizing, with respect to $\mathbf{Q}$, the potential energy $\Pi = \frac{1}{2}\mathbf{Q}^{\mathrm{T}}\mathbf{K}\mathbf{Q} - \mathbf{Q}^{\mathrm{T}}\mathbf{F}$ *subject to boundary conditions.* Boundary conditions are usually of the type

$$Q_{p_1} = a_1, Q_{p_2} = a_2, \ldots, Q_{p_r} = a_r \tag{3.56}$$

That is, the displacements along dofs $p_1, p_2, \ldots, p_r$ are specified to be equal to $a_1, a_2, \ldots, a_r$, respectively. In other words, there are $r$ number of supports in the structure, with each support node given a specified displacement. For example, consider the bar in Fig. 3.2b. There is only one boundary condition in this problem, $Q_1 = 0$.

It is noted here that *the treatment of boundary conditions in this section is applicable to two- and three-dimensional problems as well.* For this reason, the term dof is used here instead of node, since a two-dimensional stress problem will have two degrees of freedom per node. The steps described in this section will be used in all subsequent chapters. Furthermore, a Galerkin-based argument leads to the same steps for handling boundary conditions as the energy approach used subsequently.

There are *multipoint constraints* of the type

$$\beta_1 Q_{p_1} + \beta_2 Q_{p_2} = \beta_0 \tag{3.57}$$

where $\beta_0$, $\beta_1$, and $\beta_2$ are known constants. These types of boundary conditions are used in modeling inclined roller supports, rigid connections, or shrink fits.

It should be emphasized that improper specification of boundary conditions can lead to erroneous results. Boundary conditions eliminate the possibility of the structure moving as a rigid body. Further, boundary conditions should accurately model the physical system. Two approaches will now be discussed for handling specified displacement boundary conditions of the type given in Eq. 3.56: the **elimination approach** and the **penalty approach**. For multipoint constraints in Eq. 3.57, only the penalty approach will be given, because it is simpler to implement.

### Elimination Approach

To illustrate the basic idea, consider the single boundary condition $Q_1 = a_1$. The equilibrium equations are obtained by minimizing $\Pi$ with respect to $\mathbf{Q}$, subject to the boundary condition $Q_1 = a_1$. For an $N$ − dof structure, we have

$$\mathbf{Q} = [Q_1, Q_2, \ldots, Q_N]^{\mathrm{T}}$$
$$\mathbf{F} = [F_1, F_2, \ldots, F_N]^{\mathrm{T}}$$

The global stiffness matrix is of the form

$$\mathbf{K} = \begin{bmatrix} K_{11} & K_{12} & \cdots & K_{1N} \\ K_{21} & K_{22} & \cdots & K_{2N} \\ \vdots & & & \\ K_{N1} & K_{N2} & \cdots & K_{NN} \end{bmatrix} \tag{3.58}$$

Note that $K$ is a symmetric matrix. The potential energy $\Pi = \frac{1}{2}\mathbf{Q}^T\mathbf{K}\mathbf{Q} - \mathbf{Q}^T\mathbf{F}$ can be written in expanded form as

$$\begin{aligned}\Pi = \tfrac{1}{2}(&Q_1K_{11}Q_1 + Q_1K_{12}Q_2 + \cdots + Q_1K_{1N}Q_N\\ &+ Q_2K_{21}Q_1 + Q_2K_{22}Q_2 + \cdots + Q_2K_{2N}Q_N\\ &\cdots\cdots\cdots\cdots\cdots\cdots\cdots\cdots\cdots\cdots\cdots\cdots\\ &+ Q_NK_{N1}Q_1 + Q_NK_{N2}Q_2 + \cdots + Q_NK_{NN}Q_N)\\ &- (Q_1F_1 + Q_2F_2 + \cdots + Q_NF_N)\end{aligned} \tag{3.59}$$

If we now substitute the boundary condition $Q_1 = a_1$ into this expression for $\Pi$, we obtain

$$\begin{aligned}\Pi = \tfrac{1}{2}(&a_1K_{11}a_1 + a_1K_{12}Q_2 + \cdots + a_1K_{1N}Q_N\\ &+ Q_2K_{21}a_1 + Q_2K_{22}Q_2 + \cdots + Q_2K_{2N}Q_N\\ &\cdots\cdots\cdots\cdots\cdots\cdots\cdots\cdots\cdots\cdots\cdots\cdots\\ &+ Q_NK_{N1}a_1 + Q_NK_{N2}Q_2 + \cdots + Q_NK_{NN}Q_N)\\ &- (a_1F_1 + Q_2F_2 + \cdots + Q_NF_N)\end{aligned} \tag{3.60}$$

Note that the displacement $Q_1$ *has been eliminated* in the potential-energy expression. Consequently, the requirement that $\Pi$ take on a minimum value implies that

$$\frac{d\Pi}{dQ_i} = 0 \qquad i = 2, 3, \ldots, N \tag{3.61}$$

We thus obtain, from Eqs. 3.60 and 3.61,

$$\begin{aligned}K_{22}Q_2 + K_{23}Q_3 + \cdots + K_{2N}Q_N &= F_2 - K_{21}a_1\\ K_{32}Q_2 + K_{33}Q_3 + \cdots + K_{3N}Q_N &= F_3 - K_{31}a_1\\ \cdots\cdots\cdots\cdots\cdots\cdots\cdots\cdots\cdots\cdots\cdots\cdots\\ K_{N2}Q_2 + K_{N3}Q_3 + \cdots + K_{NN}Q_N &= F_N - K_{N1}a_1\end{aligned} \tag{3.62}$$

These *finite element equations* can be expressed in matrix form as

$$\begin{bmatrix} K_{22} & K_{23} & \cdots & K_{2N} \\ K_{32} & K_{33} & \cdots & K_{3N} \\ \vdots & & & \\ K_{N2} & K_{N3} & \cdots & K_{NN} \end{bmatrix} \begin{Bmatrix} Q_2 \\ Q_3 \\ \vdots \\ Q_N \end{Bmatrix} = \begin{Bmatrix} F_2 - K_{21}a_1 \\ F_3 - K_{31}a_1 \\ \vdots \\ F_N - K_{N1}a_1 \end{Bmatrix} \tag{3.63}$$

We now observe that the $(N - 1 \times N - 1)$ stiffness matrix is obtained simply by deleting or *eliminating* the first row and column (in view of $Q_1 = a_1$) from the original $(N \times N)$ stiffness matrix. Equation 3.63 may be denoted as

$$\mathbf{K}\mathbf{Q} = \mathbf{F} \tag{3.64}$$

where **K** is a reduced stiffness matrix obtained by eliminating the row and column corresponding to the specified or "support" dof. Equation 3.64 can be solved for the displacement vector **Q** using Gaussian elimination. Note that the reduced **K** matrix is nonsingular, provided the boundary conditions have been specified properly; the original **K** matrix, on the other hand, is a singular matrix. Once **Q** has been determined, the element stress can be evaluated using Eq. 3.16: $\sigma = E\mathbf{Bq}$, where **q** for each element is extracted from **Q** using element connectivity information.

Assume that displacements and stresses have been determined. It is now necessary to calculate the **reaction force** $R_1$ at the support. This reaction force can be obtained from the finite element equation (or equilibrium equation) for node 1:

$$K_{11}Q_1 + K_{12}Q_2 + \cdots + K_{1N}Q_N = F_1 + R_1 \tag{3.65}$$

Here, $Q_1, Q_2, \ldots, Q_N$ are known. $F_1$, which equals the load applied at the support (if any), is also known. Consequently, the reaction force at the node that maintains equilibrium, is

$$R_1 = K_{11}Q_1 + K_{12}Q_2 + \cdots + K_{1N}Q_N - F_1 \tag{3.66}$$

Note that the elements $K_{11}, K_{12}, \ldots, K_{1N}$, which form the first row of **K**, need to be *stored separately*. This is because **K** in Eq. 3.64 is obtained by deleting this row and column from the original **K**.

The modifications to **K** and **F** discussed earlier are also derivable using Galerkin's variational formulation. We have Eq. 3.51 in which

$$\Psi^{\mathrm{T}}(\mathbf{KQ} - \mathbf{F}) = 0 \tag{3.67}$$

for every $\Psi$ consistent with the boundary conditions of the problem. Specifically, consider the constraint

$$Q_1 = a_1 \tag{3.68}$$

Then, we require

$$\Psi_1 = 0 \tag{3.69}$$

Choosing virtual displacements $\Psi = [0, 1, 0, \ldots, 0]$, $\Psi = [0, 0, 1, 0, \ldots, 0]^{\mathrm{T}}, \ldots$, $\Psi = [0, 0, \ldots, 0, 1]^{\mathrm{T}}$, and substituting each of these into Eq. 3.67, we obtain precisely the equilibrium equations given in Eqs. 3.63.

The preceding discussion addressed the boundary condition $Q_1 = a_1$. This procedure can readily be generalized to handle multiple boundary conditions. The general procedure is summarized subsequently. Again, this procedure is also applicable to two- and three-dimensional problems.

**Summary: Elimination Approach**

Consider the boundary conditions

$$Q_{p_1} = a_1, Q_{p_2} = a_2, \ldots, Q_{p_r} = a_r$$

Step 1. Store the $p_1$th, $p_2$th, ..., and $p_r$th rows of the global stiffness matrix **K** and force vector **F**. These rows will be used subsequently.

Step 2. Delete the $p_1$th row and column, the $p_2$th row and column, ..., and the $p_r$th row and column from the **K** matrix. The resulting stiffness matrix **K** is of dimension $(N - r, N - r)$. Similarly, the corresponding load vector **F** is of dimension $(N - r, 1)$. Modify each load component as

$$F_i = F_i - (K_{i,p_1}a_1 + K_{i,p_2}a_2 + \cdots + K_{i,p_r}a_r) \tag{3.70}$$

for each dof $i$ that is not a support. Solve

$$\mathbf{KQ} = \mathbf{F}$$

for the displacement vector **Q**.

Step 3. For each element, extract the element displacement vector **q** from the **Q** vector, using element connectivity, and determine element stresses.

Step 4. Using the information stored in step 1, evaluate the reaction forces at each support dof from

$$\begin{aligned} R_{p_1} &= K_{p_1,1}Q_1 + K_{p_1,2}Q_2 + \cdots + K_{p_1,N}Q_N - F_{p_1} \\ R_{p_2} &= K_{p_2,1}Q_1 + K_{p_2,2}Q_2 + \cdots + K_{p_2,N}Q_N - F_{p_2} \\ &\cdots\cdots\cdots\cdots\cdots\cdots\cdots\cdots\cdots\cdots\cdots\cdots\cdots\cdots\cdots\cdots\cdots\cdots \\ R_{p_r} &= K_{p_r,1}Q_1 + K_{p_r,2}Q_2 + \cdots + K_{p_r,N}Q_N - F_{p_r} \end{aligned} \tag{3.71}$$

**Example 3.3**

Consider the thin (steel) plate in Fig. E3.3a. The plate has a uniform thickness $t = 1$ in., Young's modulus $E = 30 \times 10^6$ psi, and weight density $\rho = 0.2836$ lb/in.$^3$. In addition to its self-weight, the plate is subjected to a point load $P = 100$ lb at its midpoint.

(a) Model the plate with two finite elements.

(b) Write down expressions for the element stiffness matrices and element body force vectors.

(c) Assemble the structural stiffness matrix **K** and global load vector **F**.

(d) Using the elimination approach, solve for the global displacement vector **Q**.

(e) Evaluate the stresses in each element.

(f) Determine the reaction force at the support.

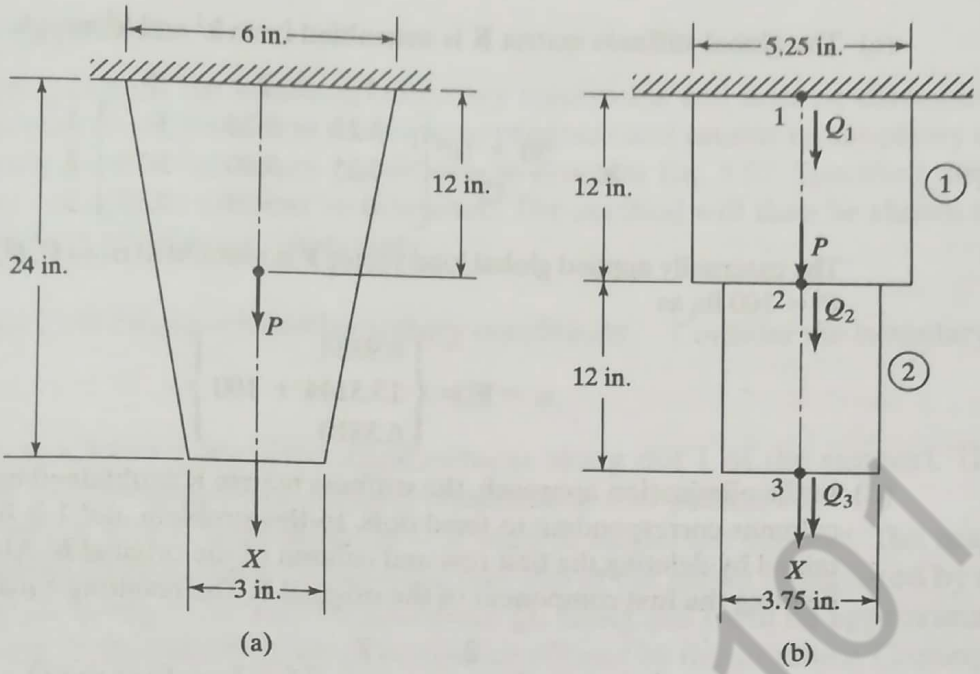


FIGURE E3.3

**Solution**

(a) Using two elements, each of 12 in. in length, we obtain the finite element model in Fig. E3.3b. Nodes and elements are numbered as shown. Note that the area at the midpoint of the plate in Fig. E3.3a is 4.5 in.$^2$. Consequently, the average area of element 1 is $A_1 = (6 + 4.5)/2 = 5.25$ in.$^2$, and the average area of element 2 is $A_2 = (4.5 + 3)/2 = 3.75$ in.$^2$. The boundary condition for this model is $Q_1 = 0$.

(b) From Eq. 3.26, we can write down expressions for the element stiffness matrices of the two elements as

$$\mathbf{k}^1 = \frac{30 \times 10^6 \times 5.25}{12} \begin{matrix} \\ 1 \\ 2 \end{matrix} \overset{\begin{matrix} 1 & 2 \end{matrix} \leftarrow \text{Global dof}}{\begin{bmatrix} 1 & -1 \\ -1 & 1 \end{bmatrix}} \begin{matrix} \downarrow \\ 1 \\ 2 \end{matrix}$$

and

$$\mathbf{k}^2 = \frac{30 \times 10^6 \times 3.75}{12} \overset{\begin{matrix} 2 & 3 \end{matrix}}{\begin{bmatrix} 1 & -1 \\ -1 & 1 \end{bmatrix}} \begin{matrix} 2 \\ 3 \end{matrix}$$

Using Eq. 3.31, the element body force vectors are

$$\mathbf{f}^1 = \frac{5.25 \times 12 \times 0.2836}{2} \overset{\text{Global dof} \downarrow}{\begin{Bmatrix} 1 \\ 1 \end{Bmatrix}} \begin{matrix} 1 \\ 2 \end{matrix}$$

and

$$\mathbf{f}^2 = \frac{3.75 \times 12 \times 0.2836}{2} \begin{Bmatrix} 1 \\ 1 \end{Bmatrix} \begin{matrix} 2 \\ 3 \end{matrix}$$

(c) The global stiffness matrix $\mathbf{K}$ is assembled from $\mathbf{k}^1$ and $\mathbf{k}^2$ as

$$\mathbf{K} = \frac{30 \times 10^6}{12} \begin{array}{c} \\ 1 \\ 2 \\ 3 \end{array} \begin{array}{c} \begin{array}{ccc} 1 & 2 & 3 \end{array} \\ \begin{bmatrix} 5.25 & -5.25 & 0 \\ -5.25 & 9.00 & -3.75 \\ 0 & -3.75 & 3.75 \end{bmatrix} \end{array}$$

The externally applied global load vector $\mathbf{F}$ is assembled from $\mathbf{f}^1$, $\mathbf{f}^2$, and the point load $P = 100$ lb; as

$$\mathbf{F} = \begin{Bmatrix} 8.9334 \\ 15.3144 + 100 \\ 6.3810 \end{Bmatrix}$$

(d) In the elimination approach, the stiffness matrix $\mathbf{K}$ is obtained by deleting rows and columns corresponding to fixed dofs. In this problem, dof 1 is fixed. Thus, $\mathbf{K}$ is obtained by deleting the first row and column of the original $\mathbf{K}$. Also, $\mathbf{F}$ is obtained by deleting the first component of the original $\mathbf{F}$. The resulting equations are

$$\frac{30 \times 10^6}{12} \begin{array}{c} \begin{array}{cc} 2 & 3 \end{array} \\ \begin{bmatrix} 9.00 & -3.75 \\ -3.75 & 3.75 \end{bmatrix} \end{array} \begin{Bmatrix} Q_2 \\ Q_3 \end{Bmatrix} = \begin{Bmatrix} 115.3144 \\ 6.3810 \end{Bmatrix}$$

Solution of these equations yields

$$Q_2 = 0.9272 \times 10^{-5} \text{ in.}$$
$$Q_3 = 0.9953 \times 10^{-5} \text{ in.}$$

Thus, $Q = [0, 0.9272 \times 10^{-5}, 0.9953 \times 10^{-5}]^T$ in.

(e) Using Eqs. 3.15 and 3.16, we obtain the stress in each element:

$$\sigma_1 = 30 \times 10^6 \times \tfrac{1}{12}[-1 \quad 1] \begin{Bmatrix} 0 \\ 0.9272 \times 10^{-5} \end{Bmatrix}$$
$$= 23.18 \text{ psi}$$

and

$$\sigma_2 = 30 \times 10^6 \times \tfrac{1}{12}[-1 \quad 1] \begin{Bmatrix} 0.9272 \times 10^{-5} \\ 0.9953 \times 10^{-5} \end{Bmatrix}$$
$$= 1.70 \text{ psi}$$

(f) The reaction force $R_1$ at node 1 is obtained from Eq. 3.71. This calculation requires the first row of $\mathbf{K}$ from part (c). Also, from part (c), note that the externally applied load (due to the self-weight) at note 1 is $F_1 = 8.9334$ lb. Thus,

$$R_1 = \frac{30 \times 10^6}{12}[5.25 \quad -5.25 \quad 0] \begin{Bmatrix} 0 \\ 0.9272 \times 10^{-5} \\ 0.9953 \times 10^{-5} \end{Bmatrix} - 8.9334$$
$$= -130.6 \text{ lb}$$

Evidently, the reaction is equal and opposite to the total downward load on the plate. ■

# HEAT TRANSFER AND MASS TRANSPORT ▲

## CHAPTER OBJECTIVES

- To derive the basic differential equation for one-dimensional heat conduction.
- To include heat transfer by convection in the one-dimensional heat transfer model.
- To introduce typical units used for heat transfer.
- To list typical thermal conductivities of materials and heat transfer coefficients based on common modes of free air convection through condensation of water vapor.
- To derive the one-dimensional finite element formulation for heat transfer by conduction and convection.
- To introduce the steps for solving a heat transfer problem by the finite element method.
- To illustrate by examples how to solve one-dimensional heat transfer problems.
- To develop the two-dimensional heat transfer finite element formulation and illustrate an example of a two-dimensional solution.
- To describe how to deal with point or line sources of heat generation.
- To demonstrate when three-dimensional finite element models must be used.
- To introduce the one-dimensional heat transfer with mass transport of the fluid.
- To derive the finite element formulation of heat transfer with mass transport by using Galerkin's method.
- To present a flowchart of two- and three-dimensional heat transfer process.
- To show examples of two- and three-dimensional problems that have been solved using a computer program.

## Introduction

In this chapter, we present the first use in this text of the finite element method for solution of nonstructural problems. We first consider the heat-transfer problem, although many similar problems, such as seepage through porous media, torsion of shafts, and magnetostatics [3], can also be treated by the same form of equations (but with different physical characteristics) as that for heat transfer.

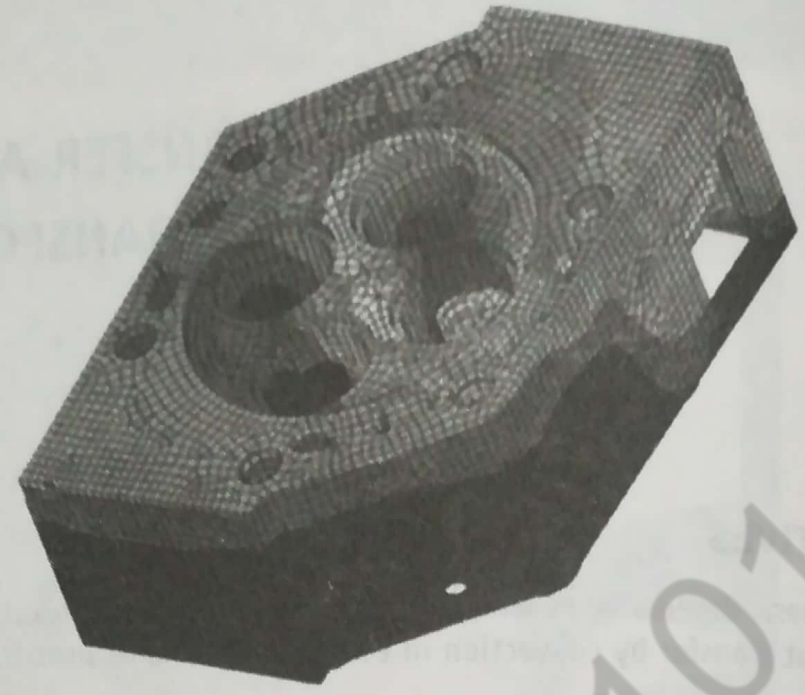

**Figure 13–1** Finite element results of cylinder head showing temperature distribution (brick elements were used in the model) (Courtesy of Algor, Inc.) (See the full-color insert for a color version of this figure.)

Familiarity with the heat-transfer problem makes possible determination of the temperature distribution within a body. We can then determine the amount of heat moving into or out of the body and the thermal stresses. Figure 13–1 is an illustration of a three-dimensional model of a cylinder head with the temperature distribution shown throughout the head. The cylinder head is made of stainless steel AISI 410 and is part of a diesel engine that would provide reduced heat rejection and increased power density. The resulting temperature distribution reveals the high temperature of 815 °C in red color at the interface between the two exhaust ports. These temperatures were then fed into the linear stress analyzer to obtain the thermal stresses ranging from 585 MPa to 1380 MPa. The linear stress analysis confirmed the behavior that the engineers saw in the initial prototype tests. The highest thermal stresses coincided with the part of the cylinder head that had been leaking in the preliminary prototypes.

We begin with a derivation of the basic differential equation for heat conduction in one dimension and then extend this derivation to the two-dimensional case. We will then review the units used for the physical quantities involved in heat transfer.

In preceding chapters dealing with stress analysis, we used the principle of minimum potential energy to derive the element equations, where an assumed displacement function within each element was used as a starting point in the derivation. We will now use a similar procedure for the nonstructural heat-transfer problem. We define an assumed temperature function within each element. Instead of minimizing a potential energy functional, we minimize a similar functional to obtain the element equations. Matrices analogous to the stiffness and force matrices of the structural problem result.

We will consider one-, two-, and three-dimensional finite element formulations of the heat-transfer problem and provide illustrative examples of the determination

of the temperature distribution along the length of a rod and within a two-dimensional body and show some three-dimensional heat transfer examples as well.

Next, we will consider the contribution of fluid mass transport. The one-dimensional mass-transport phenomenon is included in the basic heat-transfer differential equation. Because it is not readily apparent that a variational formulation is possible for this problem, we will apply Galerkin's residual method directly to the differential equation to obtain the finite element equations. (You should note that the mass transport stiffness matrix is asymmetric.) We will compare an analytical solution to the finite element solution for a heat exchanger design/analysis problem to show the excellent agreement.

Finally, we will present some computer program results for both two- and three-dimensional heat transfer.

## 13.1 Derivation of the Basic Differential Equation

### One-Dimensional Heat Conduction (without Convection)

We now consider the derivation of the basic differential equation for the one-dimensional problem of heat conduction without convection. The purpose of this derivation is to present a physical insight into the heat-transfer phenomena, which must be understood so that the finite element formulation of the problem can be fully understood. (For additional information on heat transfer, consult texts such as References [1] and [2].) We begin with the control volume shown in Figure 13–2. By conservation of energy, we have

$$E_{\text{in}} + E_{\text{generated}} = \Delta U + E_{\text{out}} \tag{13.1.1}$$

or

$$q_x A\,dt + QA\,dx\,dt = \Delta U + q_{x+dx} A\,dt \tag{13.1.2}$$

where

$E_{\text{in}}$ is the energy entering the control volume, in units of joules (J) or kW · h.

$\Delta U$ is the change in stored energy, in units of kW · h (kWh).

$q_x$ is the heat conducted (heat flux) into the control volume at surface edge $x$, in units of kW/m$^2$.

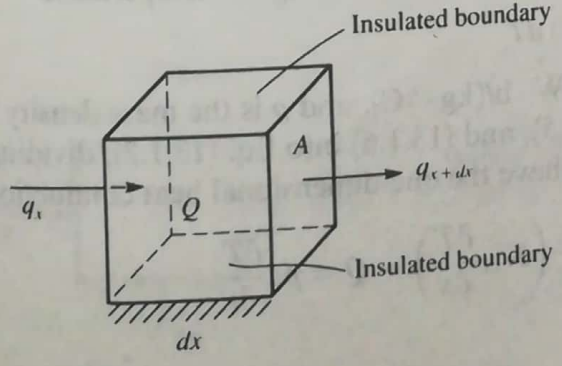


Figure 13–2 Control volume for one-dimensional heat conduction

$q_{x+dx}$ is the heat conducted out of the control volume at the surface edge $x + dx$.

$t$ is time, in h or s.

$Q$ is the internal heat source (heat generated per unit time per unit volume is positive), in kW/m$^3$ (a heat sink, heat drawn out of the volume, is negative).

$A$ is the cross-sectional area perpendicular to heat flow $q$, in m$^2$.

By Fourier's law of heat conduction,

$$q_x = -K_{xx}\frac{dT}{dx} \tag{13.1.3}$$

where

$K_{xx}$ is the thermal conductivity in the $x$ direction, in kW/(m · °C).

$T$ is the temperature, in °C.

$dT/dx$ is the temperature gradient, in °C/m.

Equation (13.1.3) states that the heat flux in the $x$ direction is proportional to the gradient of temperature in the $x$ direction. The minus sign in Eq. (13.1.3) implies that, by convention, heat flow is positive in the direction opposite the direction of temperature increase. Equation (13.1.3) is analogous to the one-dimensional stress–strain law for the stress analysis problem—that is, to $\sigma_x = E(du/dx)$. Similarly,

$$q_{x+dx} = -K_{xx}\frac{dT}{dx}\bigg|_{x+dx} \tag{13.1.4}$$

where the gradient in Eq. (13.1.4) is evaluated at $x + dx$. By Taylor series expansion, for any general function $f(x)$, we have

$$f_{x+dx} = f_x + \frac{df}{dx}dx + \frac{d^2f}{dx^2}\frac{dx^2}{2} + \cdots$$

Therefore, using a two-term Taylor series, Eq. (13.1.4) becomes

$$q_{x+dx} = -\left[K_{xx}\frac{dT}{dx} + \frac{d}{dx}\left(K_{xx}\frac{dT}{dx}\right)dx\right] \tag{13.1.5}$$

The change in stored energy can be expressed by

$$\begin{aligned}\Delta U &= \text{specific heat} \times \text{mass} \times \text{change in temperature} \\ &= c(\rho A\,dx)\,dT\end{aligned} \tag{13.1.6}$$

where $c$ is the specific heat in kW · h/(kg · °C), and $\rho$ is the mass density in kg/m$^3$. On substituting Eqs. (13.1.3), (13.1.5), and (13.1.6) into Eq. (13.1.2), dividing Eq. (13.1.2) by $A\,dx\,dt$, and simplifying, we have the one-dimensional heat conduction equation as

$$\frac{\partial}{\partial x}\left(K_{xx}\frac{\partial T}{\partial x}\right) + Q = \rho c\frac{\partial T}{\partial t} \tag{13.1.7}$$

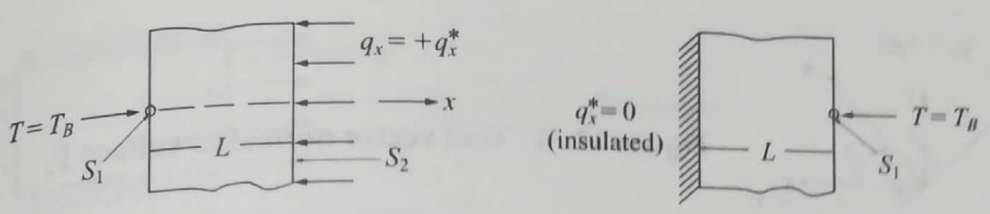


**Figure 13–3** Examples of boundary conditions in one-dimensional heat conduction

For steady state, any differentiation with respect to time is equal to zero, so Eq. (13.1.7) becomes

$$\frac{d}{dx}\left(K_{xx}\frac{dT}{dx}\right) + Q = 0 \tag{13.1.8}$$

For constant thermal conductivity and steady state, Eq. (13.1.7) becomes

$$K_{xx}\frac{d^2T}{dx^2} + Q = 0 \tag{13.1.9}$$

The boundary conditions are of the form

$$T = T_B \qquad \text{on } S_1 \tag{13.1.10}$$

where $T_B$ represents a known boundary temperature and $S_1$ is a surface where the temperature is known, and

$$q_x^* = -K_{xx}\frac{dT}{dx} = \text{constant} \qquad \text{on } S_2 \tag{13.1.11}$$

where $S_2$ is a surface where the prescribed heat flux $q_x^*$ or temperature gradient is known. On an insulated boundary, $q_x^* = 0$. These different boundary conditions are shown in Figure 13–3, where by sign convention, positive $q_x^*$ occurs when heat is flowing into the body, and negative $q_x^*$ when heat is flowing out of the body.

### Two-Dimensional Heat Conduction (Without Convection)

Consider the two-dimensional heat conduction problem in Figure 13–4. In a manner similar to the one-dimensional case, for steady-state conditions, we can show that for material properties coinciding with the global $x$ and $y$ directions,

$$\frac{\partial}{\partial x}\left(K_{xx}\frac{\partial T}{\partial x}\right) + \frac{\partial}{\partial y}\left(K_{yy}\frac{\partial T}{\partial y}\right) + Q = 0 \tag{13.1.12}$$

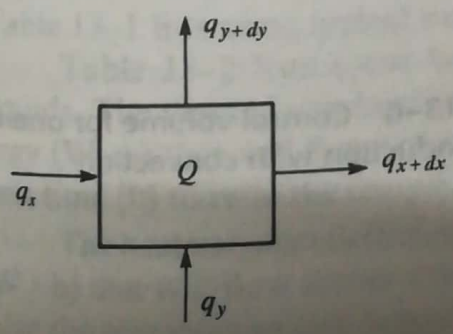


**Figure 13–4** Control volume for two-dimensional heat conduction

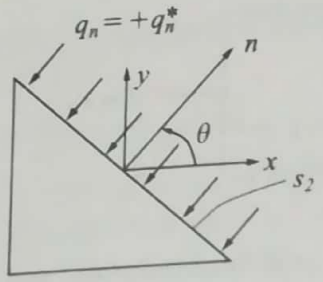


Figure 13–5 Unit vector normal to surface $S_2$

with boundary conditions

$$T = T_B \qquad \text{on } S_1 \tag{13.1.13}$$

$$q_n = q_n^* = K_{xx}\frac{\partial T}{\partial x}C_x + K_{yy}\frac{\partial T}{\partial y}C_y = \text{constant} \qquad \text{on } S_2 \tag{13.1.14}$$

where $C_x$ and $C_y$ are the direction cosines of the unit vector $\boldsymbol{n}$ normal to the surface $S_2$ shown in Figure 13–5. Again, $q_n^*$ is by sign convention, positive if heat is flowing into the edge of the body.

## ▲ 13.2 Heat Transfer with Convection

For a conducting solid in contact with a fluid, there will be a heat transfer taking place between the fluid and solid surface when a temperature difference occurs.

The fluid will be in motion either through external pumping action (**forced convection**) or through the buoyancy forces created within the fluid by the temperature differences within it (**natural** or **free convection**).

We will now consider the derivation of the basic differential equation for one-dimensional heat conduction with convection. Again we assume the temperature change is much greater in the $x$ direction than in the $y$ and $z$ directions. Figure 13–6 shows the control volume used in the derivation. Again, by Eq. (13.1.1) for conservation of energy, we have

$$q_x A\,dt + QA\,dx\,dt = c(\rho A\,dx)\,dT + q_{x+dx}A\,dt + q_h P\,dx\,dt \tag{13.2.1}$$

In Eq. (13.2.1), all terms have the same meaning as in Section 13.1, except the heat flow by convective heat transfer is given by Newton's law of cooling

$$q_h = h(T - T_\infty) \tag{13.2.2}$$

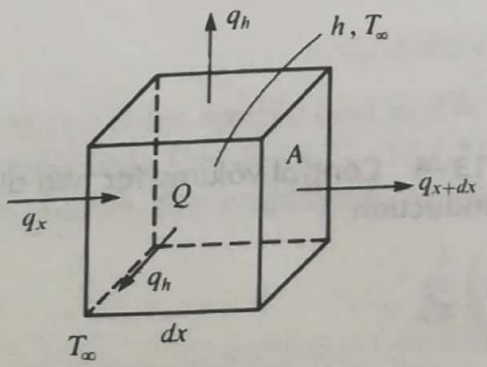


Figure 13–6 Control volume for one-dimensional heat conduction with convection

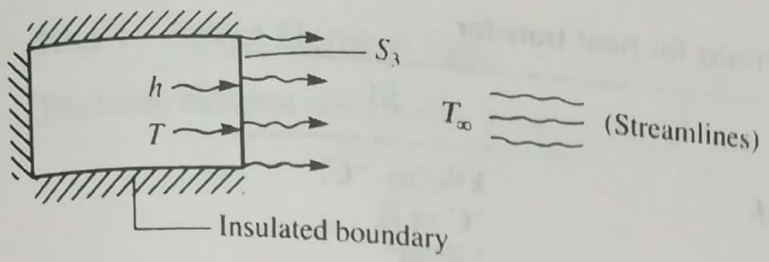


**Figure 13–7** Model illustrating convective heat transfer (arrows on surface $S_3$ indicate heat transfer by convection)

where

$h$ is the heat-transfer or convection coefficient, in kW/(m$^2$ · °C).

$T$ is the temperature of the solid surface at the solid/fluid interface.

$T_\infty$ is the temperature of the fluid (here the free-stream fluid temperature).

$P$ in Eq. (13.2.1) denotes the perimeter around the constant cross-sectional area $A$.

Again, using Eqs. (13.1.3) through (13.1.6) and (13.2.2) in Eq. (13.2.1), dividing by $A\,dx\,dt$, and simplifying, we obtain the differential equation for one-dimensional heat conduction with convection as

$$\frac{\partial}{\partial x}\left(K_{xx}\frac{\partial T}{\partial x}\right)+Q=\rho c\frac{\partial T}{\partial t}+\frac{hP}{A}(T-T_\infty) \tag{13.2.3}$$

with possible boundary conditions on (1) temperature, given by Eq. (13.1.10), and/or (2) temperature gradient, given by Eq. (13.1.11), and/or (3) loss of heat by convection from the ends of the one-dimensional body, as shown in Figure 13–7. Equating the heat flow in the solid wall to the heat flow in the fluid at the solid/fluid interface, we have

$$-K_{xx}\frac{dT}{dx}=h(T-T_\infty) \qquad \text{on } S_3 \tag{13.2.4}$$

as a boundary condition for the problem of heat conduction with convection.

## 13.3 Typical Units; Thermal Conductivities, $K$; and Heat-Transfer Coefficients, $h$

Table 13–1 lists some typical units used for the heat-transfer problem.

Table 13–2 lists some typical thermal conductivities of various solids and liquids. The thermal conductivity $K$, in W/(m · °C), measures the amount of heat energy (W · h) that will flow through a unit length (ft or m) of a given substance in a unit time (h) to raise the temperature one degree (°C).

The heat transfer coefficient $h$, in W/(m$^2$ · °C), measures the amount of heat energy (W · h) that will flow across a unit area (m$^2$) of a given substance in a unit time (h) to raise the temperature one degree (C).

**Table 13–1** Typical units for heat transfer

| Variable | SI |
|---|---|
| Thermal conductivity, $K$ | $kW/(m \cdot °C)$ |
| Temperature, $T$ | °C or K |
| Internal heat source, $Q$ | $kW/m^3$ |
| Heat flux, $q$ | $kW/m^2$ |
| Heat flow, $\bar{q}$ | kW |
| Convection coefficient, $h$ | $kW/(m^2 \cdot °C)$ |
| Energy, $E$ | $kW \cdot h$ |
| Specific heat, $c$ | $(kW \cdot h)/(kg \cdot °C)$ |
| Mass density, $\rho$ | $kg/m^3$ |

**Table 13–2** Typical thermal conductivities of some solids and fluids

| Material | K [W/(m · °C)] |
|---|---|
| Solids | |
| Aluminum, 0 °C (32 °F) | 202 |
| Steel (1% carbon), 0 °C | 35 |
| Fiberglass, 20 °C (68 °F) | 0.035 |
| Concrete, 0 °C | 0.81–1.40 |
| Earth, coarse gravelly, 20 °C | 0.520 |
| Wood, oak, radial direction, 20 °C | 0.17 |
| Fluids | |
| Engine oil, 20 °C | 0.145 |
| Dry air, atmospheric pressure, 20 °C | 0.0243 |

**Natural** or **free convection** occurs when, for instance, a heated plate is exposed to ambient room air without an external source of motion. This movement of the air, experienced as a result of the density gradients near the plate, is called *natural* or *free convection*. **Forced convection** is experienced, for instance, in the case of a fan blowing air over a plate.

## 13.4 One-Dimensional Finite Element Formulation Using a Variational Method

The temperature distribution influences the amount of heat moving into or out of a body and also influences the stresses in a body. Thermal stresses occur in all bodies that experience a temperature gradient from some equilibrium state but are not free to expand in all directions. To evaluate thermal stresses, we need to know the temperature distribution in the body. The finite element method is a realistic method for predicting quantities such as temperature distribution and thermal stresses in a body. In this section, we formulate the one-dimensional heat-transfer equations using a variational method. Examples are included to illustrate the solution of this type of problem.

### Step 1 Select Element Type

The basic element with nodes 1 and 2 is shown in Figure 13–8(a).

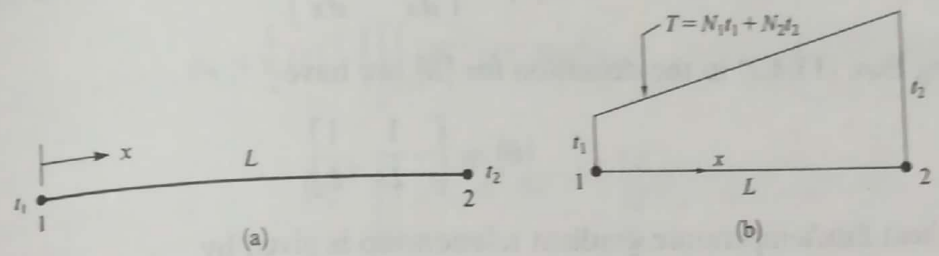


Figure 13–8 (a) Basic one-dimensional temperature element and (b) temperature variation along length of element

### Step 2 Choose a Temperature Function

We choose the temperature function $T$ [Figure 13–8(b)] within each element similar to the displacement function of Chapter 3, as

$$T(x) = N_1 t_1 + N_2 t_2 \tag{13.4.1}$$

where $t_1$ and $t_2$ are the nodal temperatures to be determined, and

$$N_1 = 1 - \frac{x}{L} \qquad N_2 = \frac{x}{L} \tag{13.4.2}$$

are again the same shape functions as used for the bar element. The $[N]$ matrix is then given by

$$[N] = \begin{bmatrix} 1 - \dfrac{x}{L} & \dfrac{x}{L} \end{bmatrix} \tag{13.4.3}$$

and the nodal temperature matrix is

$$\{t\} = \begin{Bmatrix} t_1 \\ t_2 \end{Bmatrix} \tag{13.4.4}$$

In matrix form, we express Eq. (13.4.1) as

$$\{T\} = [N]\{t\} \tag{13.4.5}$$

### Step 3 Define the Temperature Gradient/Temperature and Heat Flux/Temperature Gradient Relationships

The temperature gradient matrix $\{g\}$, analogous to the strain matrix $\{\varepsilon\}$, is given by

$$\{g\} = \begin{Bmatrix} \dfrac{dT}{dx} \end{Bmatrix} = [B]\{t\} \tag{13.4.6}$$

where $[B]$ is obtained by substituting Eq. (13.4.1) for $T(x)$ into Eq. (13.4.6) and differentiating with respect to $x$, that is,

$$[B] = \begin{bmatrix} \dfrac{dN_1}{dx} & \dfrac{dN_2}{dx} \end{bmatrix}$$

Using Eqs. (13.4.2) in the definition for $[B]$, we have

$$[B] = \begin{bmatrix} -\dfrac{1}{L} & \dfrac{1}{L} \end{bmatrix} \tag{13.4.7}$$

The heat flux/temperature gradient relationship is given by

$$q_x = -[D]\{g\} \tag{13.4.8}$$

where the material property matrix is now given by

$$[D] = [K_{xx}] \tag{13.4.9}$$

**Step 4** Derive the Element Conduction Matrix and Equations

Equations (13.1.9) through (13.1.11) and (13.2.3) can be shown to be derivable (as shown, for instance, in References [4–6]) by the minimization of the following functional (analogous to the potential energy functional $\pi_p$):

$$\pi_h = U + \Omega_Q + \Omega_q + \Omega_h \tag{13.4.10}$$

where

$$U = \frac{1}{2}\iiint_V \left[ K_{xx}\left(\frac{dT}{dx}\right)^2 \right] dV$$

$$\Omega_Q = -\iiint_V QT\, dV \qquad \Omega_q = -\iint_{S_2} q^* T\, dS \qquad \Omega_h = \frac{1}{2}\iint_{S_3} h(T - T_\infty)^2\, dS \tag{13.4.11}$$

and where $S_2$ and $S_3$ are separate surface areas over which heat flow (flux) $q^*$ ($q^*$ is positive into the surface) and convection loss $h(T - T_\infty)$ are specified. We cannot specify $q^*$ and $h$ on the same surface because they cannot occur simultaneously on the same surface, as indicated by Eqs. (13.4.11).

Using Eqs. (13.4.5), (13.4.6), and (13.4.9) in Eq. (13.4.11) and then using Eq. (13.4.10), we can write $\pi_h$ in matrix form as

$$\pi_h = \frac{1}{2}\iiint_V [\{g\}^T[D]\{g\}]\, dV - \iiint_V \{t\}^T[N]^T Q\, dV$$
$$- \iint_{S_2} \{t\}^T[N]^T q^*\, dS + \frac{1}{2}\iint_{S_3} h[(\{t\}^T[N]^T - T_\infty)^2]\, dS \tag{13.4.12}$$

On substituting Eq. (13.4.6) into Eq. (13.4.12) and using the fact that the nodal temperatures $\{t\}$ are independent of the general coordinates $x$ and $y$ and can therefore be taken outside the integrals, we have

$$\pi_h = \frac{1}{2}\{t\}^T \iiint_V [B]^T[D][B]\,dV\{t\} - \{t\}^T \iiint_V [N]^T Q\,dV$$
$$- \{t\}^T \iint_{S_2} [N]^T q^*\,dS + \frac{1}{2}\iint_{S_3} h[\{t\}^T[N]^T[N]\{t\}$$
$$- (\{t\}^T[N]^T + [N]\{t\})T_\infty + T_\infty^2]\,dS \tag{13.4.13}$$

In Eq. (13.4.13), the minimization is most easily accomplished by explicitly writing the surface integral $S_3$ with $\{t\}$ left inside the integral as shown. On minimizing Eq. (13.4.13) with respect to $\{t\}$, we obtain

$$\frac{\partial \pi_h}{\partial\{t\}} = \iiint_V [B]^T[D][B]\,dV\{t\} - \iiint_V [N]^T Q\,dV$$
$$- \iint_{S_2} [N]^T q^*\,dS + \iint_{S_3} h[N]^T[N]\,dS\{t\}$$
$$- \iint_{S_3} [N]^T hT_\infty\,dS = 0 \tag{13.4.14}$$

where the last term $hT_\infty^2$ in Eq. (13.4.13) is a constant that drops out while minimizing $\pi_h$. Simplifying Eq. (13.4.14), we obtain

$$\left[\iiint_V [B]^T[D][B]\,dV + \iint_{S_3} h[N]^T[N]\,ds\right]\{t\} = \{f_Q\} + \{f_q\} + \{f_h\} \tag{13.4.15}$$

where the force matrices have been defined by

$$\{f_Q\} = \iiint_V [N]^T Q\,dV \qquad \{f_q\} = \iint_{S_2} [N]^T q^*\,dS$$
$$\{f_h\} = \iint_{S_3} [N]^T hT_\infty\,dS \tag{13.4.16}$$

In Eq. (13.4.16), the first term $\{f_Q\}$ (heat source positive, sink negative) is of the same form as the body-force term, and the second term $\{f_q\}$ (heat flux, positive into the surface) and third term $\{f_h\}$ (heat transfer or convection) are similar to surface tractions

(distributed loading) in the stress analysis problem. You can observe this fact by comparing Eq. (13.4.16) with Eq. (6.2.46). Because we are formulating element equations of the form $\{f\} = [k]\{t\}$, we have the element conduction matrix[1] for the heat-transfer problem given in Eq. (13.4.15) by

$$[k] = \iiint_V [B]^T[D][B]\,dV + \iint_{S_3} h[N]^T[N]\,dS \tag{13.4.17}$$

where the first and second integrals in Eq. (13.4.17) are the contributions of conduction and convection, respectively. Using Eq. (13.4.17) in Eq. (13.4.15), for each element, we have

$$\{f\} = [k]\{t\} \tag{13.4.18}$$

Using the first term of Eq. (13.4.17), along with Eqs. (13.4.7) and (13.4.9), the conduction part of the $[k]$ matrix for the one-dimensional element becomes

$$[k_c] = \iiint_V [B]^T[D][B]\,dV = \int_0^L \begin{Bmatrix} -\frac{1}{L} \\ \frac{1}{L} \end{Bmatrix} [K_{xx}] \begin{bmatrix} -\frac{1}{L} & \frac{1}{L} \end{bmatrix} A\,dx$$

$$= \frac{AK_{xx}}{L^2} \int_0^L \begin{bmatrix} 1 & -1 \\ -1 & 1 \end{bmatrix} dx \tag{13.4.19}$$

or, finally,

$$[k_c] = \frac{AK_{xx}}{L} \begin{bmatrix} 1 & -1 \\ -1 & 1 \end{bmatrix} \tag{13.4.20}$$

The convection part of the $[k]$ matrix becomes

$$[k_h] = \iint_{S_3} h[N]^T[N]\,dS = hP \int_0^L \begin{Bmatrix} 1 - \frac{x}{L} \\ \frac{x}{L} \end{Bmatrix} \begin{bmatrix} 1 - \frac{x}{L} & \frac{x}{L} \end{bmatrix} dx$$

or, on integrating,

$$[k_h] = \frac{hPL}{6} \begin{bmatrix} 2 & 1 \\ 1 & 2 \end{bmatrix} \tag{13.4.21}$$

where

$$dS = P\,dx$$

[1] The element conduction matrix is often called the *stiffness matrix* because *stiffness matrix* is becoming a generally accepted term used to describe the matrix of known coefficients multiplied by the unknown degrees of freedom, such as temperatures, displacements, and so on.

and $P$ is the perimeter of the element (assumed to be constant). Therefore, adding Eqs. (13.4.20) and (13.4.21), we find that the $[k]$ matrix is

$$[k] = \frac{AK_{xx}}{L}\begin{bmatrix} 1 & -1 \\ -1 & 1 \end{bmatrix} + \frac{hPL}{6}\begin{bmatrix} 2 & 1 \\ 1 & 2 \end{bmatrix} \tag{13.4.22}$$

When $h$ is zero on the boundary of an element, the second term on the right side of Eq. (13.4.22) (convection portion of $[k]$) is zero. This corresponds, for instance, to an insulated boundary.

The force matrix terms, on simplifying Eq. (13.4.16) and assuming $Q$, $q^*$, and product $hT_\infty$ to be constant are

$$\{f_Q\} = \iiint_V [N]^T Q\, dV = QA\int_0^L \begin{Bmatrix} 1 - \dfrac{x}{L} \\ \dfrac{x}{L} \end{Bmatrix} dx = \frac{QAL}{2}\begin{Bmatrix} 1 \\ 1 \end{Bmatrix} \tag{13.4.23}$$

and

$$\{f_q\} = \iint_{S_2} q^*[N]^T\, dS = q^*P\int_0^L \begin{Bmatrix} 1 - \dfrac{x}{L} \\ \dfrac{x}{L} \end{Bmatrix} dx = \frac{q^*PL}{2}\begin{Bmatrix} 1 \\ 1 \end{Bmatrix} \tag{13.4.24}$$

and

$$\{f_h\} = \iint_{S_3} hT_\infty[N]^T\, dS = \frac{hT_\infty PL}{2}\begin{Bmatrix} 1 \\ 1 \end{Bmatrix} \tag{13.4.25}$$

Therefore, adding Eqs. (13.4.23) through (13.4.25), we obtain

$$\{f\} = \frac{QAL + q^*PL + hT_\infty PL}{2}\begin{Bmatrix} 1 \\ 1 \end{Bmatrix} \tag{13.4.26}$$

Equation (13.4.26) indicates that one-half of the assumed uniform heat source $Q$ goes to each node, one-half of the prescribed uniform heat flux $q^*$ (positive $q^*$ enters the body) goes to each node, and one-half of the convection from the perimeter surface $hT_\infty$ goes to each node of an element.

Finally, we must consider the convection from the free end of an element. For simplicity's sake, we will assume convection occurs only from the right end of the element, as shown in Figure 13–9. The additional convection term contribution to the stiffness matrix is given by

$$[k_h]_{\text{end}} = \iint_{S_{\text{end}}} h[N]^T[N]\, dS \tag{13.4.27}$$

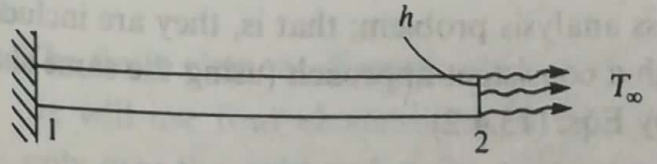


**Figure 13–9** Convection force from the end of an element

Now $N_1 = 0$ and $N_2 = 1$ at the right end of the element. Substituting the $N$'s into Eq. (13.4.27), we obtain

$$[k_h]_{\text{end}} = \iint_{S_{\text{end}}} h \begin{Bmatrix} 0 \\ 1 \end{Bmatrix} [0 \quad 1]\, dS = hA \begin{bmatrix} 0 & 0 \\ 0 & 1 \end{bmatrix} \tag{13.4.28}$$

The convection force from the free end of the element is obtained from the application of Eq. (13.4.25) with the shape functions now evaluated at the right end (where convection occurs) and with $S_3$ (the surface over which convection occurs) now equal to the cross-sectional area $A$ of the rod. Hence,

$$\{f_h\}_{\text{end}} = hT_\infty A \begin{Bmatrix} N_1(x = L) \\ N_2(x = L) \end{Bmatrix} = hT_\infty A \begin{Bmatrix} 0 \\ 1 \end{Bmatrix} \tag{13.4.29}$$

represents the convective force from the right end of an element where $N_1(x = L)$ represents $N_1$ *evaluated at* $x = L$, and so on.

### Step 5 Assemble the Element Equations to Obtain the Global Equations and Introduce Boundary Conditions

We obtain the global or total structure conduction matrix using the same procedure as for the structural problem (called the *direct stiffness method* as described in Section 2.4); that is,

$$[K] = \sum_{e=1}^{N} [k^{(e)}] \tag{13.4.30}$$

typically in units of kW/°C or Btu/(h-°F). The global force matrix is the sum of all element heat sources and is given by

$$\{F\} = \sum_{e=1}^{N} \{f^{(e)}\} \tag{13.4.31}$$

typically in units of kW or Btu/h. The global equations are then

$$\{F\} = [K]\{t\} \tag{13.4.32}$$

with the prescribed nodal temperature boundary conditions given by Eq. (13.1.13). Note that the boundary conditions on heat flux, Eq. (13.1.11), and convection, Eq. (13.2.4), are actually accounted for in the same manner as distributed loading was accounted for in the stress analysis problem; that is, they are included in the column of force matrices through a consistent approach (using the same shape functions used to derive $[k]$), as given by Eqs. (13.4.2).

The heat-transfer problem is now amenable to solution by the finite element method. The procedure used for solution is similar to that for the stress analysis problem. In Section 13.5, we will derive the specific equations used to solve the two-dimensional heat-transfer problem.

### Step 6 Solve for the Nodal Temperatures

We now solve for the global nodal temperature, $\{t\}$, where the appropriate nodal temperature boundary conditions, Eq. (13.1.13), are specified.

### Step 7 Solve for the Element Temperature Gradients and Heat Fluxes

Finally, we calculate the element temperature gradients from Eq. (13.4.6), and the heat fluxes, typically from Eq. (13.4.8).

To illustrate the use of the equations developed in this section, we will now solve some one-dimensional heat-transfer problems.

---

**Example 13.1**

Determine the temperature distribution along the length of the rod shown in Figure 13–10 with an insulated perimeter. The temperature at the left end is a constant 40 °C and the free-stream temperature is −10 °C. Let $h = 55$ W/(m$^2$ · °C) and $K_{xx} = 35$ W/(m · °C). The value of $h$ is typical for forced air convection and the value of $K_{xx}$ is a typical conductivity for carbon steel (Tables 13–2 and 13–3).

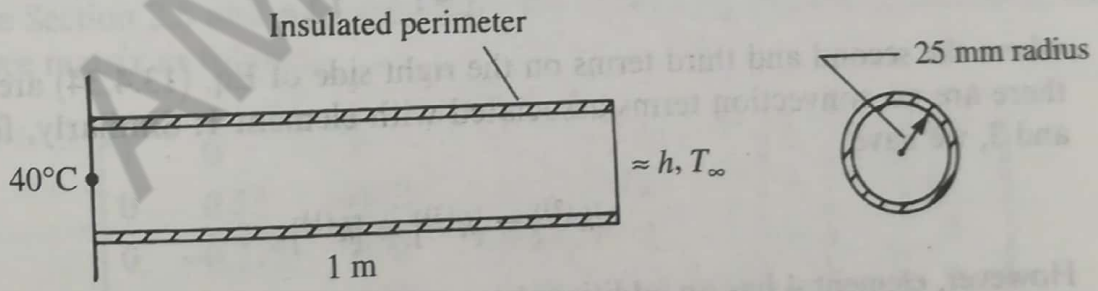


**Figure 13–10** One-dimensional rod subjected to temperature variation

**SOLUTION:**

The finite element discretization is shown in Figure 13–11. For simplicity's sake, we will use four elements, each 0.25 m long. There will be convective heat loss only over the right end of the rod because we consider the left end to have a known

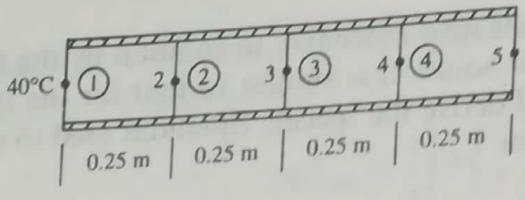


**Figure 13–11** Finite element discretized rod

temperature and the perimeter to be insulated. We calculate the stiffness matrices for each element as follows:

$$\frac{AK_{xx}}{L} = \frac{\pi(0.025\text{ m})^2[35\text{ W/(m}\cdot\text{°C)}]}{(0.25\text{ m})}$$
$$= 0.275\text{ W/°C}$$

$$\frac{hPL}{6} = \frac{[55\text{ W/(m}\cdot\text{°C)}](2\pi)}{6}(0.025\text{ m})(0.25\text{ m}) \tag{13.4.33}$$
$$= 0.36\text{ W/°C}$$

$$hT_\infty PL = [55\text{ W/(m}\cdot\text{°C)}](-10\text{ °C})(2\pi)(0.025\text{ m})(0.25\text{ m})$$
$$= -21.6\text{ W/°C}$$

In general, from Eqs. (13.4.22) and (13.4.27), we have

$$[k] = \frac{AK_{xx}}{L}\begin{bmatrix}1 & -1\\ -1 & 1\end{bmatrix} + \frac{hPL}{6}\begin{bmatrix}2 & 1\\ 1 & 2\end{bmatrix} + \iint_{S_{\text{end}}} h[N]^T[N]\,dS \tag{13.4.34}$$

Substituting Eqs. (13.4.33) into Eq. (13.4.34) for element 1, we have

$$[k^{(1)}] = 0.275\begin{bmatrix}1 & -1\\ -1 & 1\end{bmatrix}\text{ W/°C} \tag{13.4.35}$$

where the second and third terms on the right side of Eq. (13.4.34) are zero because there are no convection terms associated with element 1. Similarly, for elements 2 and 3, we have

$$[k^{(2)}] = [k^{(3)}] = [k^{(1)}] \tag{13.4.36}$$

However, element 4 has an additional (convection) term owing to heat loss from the flat surface at its right end. Hence, using Eq. (13.4.28), we have

$$[k^{(4)}] = [k^{(1)}] + hA\begin{bmatrix}0 & 0\\ 0 & 1\end{bmatrix}$$
$$= 0.275\begin{bmatrix}1 & -1\\ -1 & 1\end{bmatrix} + [55\text{ W/(m}^2\cdot\text{°C)}]\pi(0.025\text{ m})^2\begin{bmatrix}0 & 0\\ 0 & 1\end{bmatrix}$$
$$= \begin{bmatrix}0.275 & -0.275\\ -0.275 & 0.386\end{bmatrix}\text{ W/°C} \tag{13.4.37}$$

In general, we would use Eqs. (13.4.23) through (13.4.25), and (13.4.29) to obtain the element force matrices. However, in this example, $Q = 0$ (no heat source), $q^* = 0$ (no heat flux), and there is no convection except from the right end. Therefore,

$$\{f^{(1)}\} = \{f^{(2)}\} = \{f^{(3)}\} = 0 \tag{13.4.38}$$

and

$$\begin{aligned}\{f^{(4)}\} &= hT_\infty A\begin{Bmatrix}0\\1\end{Bmatrix}\\ &= [55\ \text{W/(m}^2\cdot{}^\circ\text{C})](-10\,^\circ\text{C})\pi(0.025\ \text{m})^2\begin{Bmatrix}0\\1\end{Bmatrix}\\ &= -1.8\begin{Bmatrix}0\\1\end{Bmatrix}\ \text{W/}^\circ\text{C}\end{aligned} \tag{13.4.39}$$

The assembly of the element stiffness matrices [Eqs. (13.4.35) through (13.4.37)] and the element force matrices [Eqs. (13.4.38) and (13.4.39)], using the direct stiffness method, produces the following system of equations:

$$\begin{bmatrix} 0.275 & -0.275 & 0 & 0 & 0\\ -0.275 & 0.55 & -0.275 & 0 & 0\\ 0 & -0.275 & 0.55 & -0.275 & 0\\ 0 & 0 & -0.275 & 0.55 & -0.275\\ 0 & 0 & 0 & -0.275 & 0.383 \end{bmatrix}\begin{Bmatrix} t_1\\ t_2\\ t_3\\ t_4\\ t_5\end{Bmatrix} = \begin{Bmatrix} F_1\\ 0\\ 0\\ 0\\ -1.8\end{Bmatrix} \tag{13.4.40}$$

where $F_1$ corresponds to an unknown rate of heat flow at node 1 (analogous to an unknown support force in the stress analysis problem). We have a known nodal temperature boundary condition of $t_1 = 40\,^\circ\text{C}$. This nonhomogeneous boundary condition must be treated in the same manner as was described for the stress analysis problem (see Section 2.5 and Appendix B.4). We modify the stiffness (conduction) matrix and force matrix as follows:

$$\begin{bmatrix} 1 & 0 & 0 & 0 & 0\\ 0 & 0.55 & -0.275 & 0 & 0\\ 0 & -0.275 & 0.55 & -0.275 & 0\\ 0 & 0 & -0.275 & 0.55 & -0.275\\ 0 & 0 & 0 & -0.275 & 0.383 \end{bmatrix}\begin{Bmatrix} t_1\\ t_2\\ t_3\\ t_4\\ t_5\end{Bmatrix} = \begin{Bmatrix} 40\\ 11\\ 0\\ 0\\ -1.8\end{Bmatrix} \tag{13.4.41}$$

where the terms in the first row and column of the stiffness matrix corresponding to the known temperature condition, $t_1 = 40\,^\circ\text{C}$, have been set equal to 0 except for the main diagonal, which has been set equal to 1, and the first row of the force matrix has been set equal to the known nodal temperature at node 1. Also, the term $(-0.275) \times (40\,^\circ\text{C}) = -11$ on the left side of the second equation of Eq. (13.4.40) has been transposed to the right side in the second row (as +11) of Eq. (13.4.41). The second through fifth equations of Eq. (13.4.41) corresponding to the rows of unknown

nodal temperatures can now be solved (typically by Gaussian elimination). The resulting solution is given by

$$t_2 = 32.36\,^\circ\text{C} \qquad t_3 = 24.72\,^\circ\text{C} \qquad t_4 = 17.09\,^\circ\text{C} \qquad t_5 = 9.45\,^\circ\text{C} \tag{13.4.42}$$

For this elementary problem, the closed-form solution of the differential equation for conduction, Eq. (13.1.9), with the left-end boundary condition given by Eq. (13.1.10) and the right-end boundary condition given by Eq. (13.2.4) yields a linear temperature distribution through the length of the rod. The evaluation of this linear temperature function at 10-in. intervals (corresponding to the nodal points used in the finite element model) yields the same temperatures as obtained in this example by the finite element method. Because the temperature function was assumed to be linear in each finite element, this comparison is as expected. Note that $F_1$ could be determined by the first of Eqs. (13.4.40). ∎

---

**Example 13.2**

To illustrate more fully the use of the equations developed in Section 13.4, we will now solve the heat-transfer problem shown in Figure 13–12. For the one-dimensional rod, determine the temperatures at 75 mm increments along the length of the rod and the rate of heat flow through element 1. Let $K_{xx} = 60\ \text{W/(m}\cdot\,^\circ\text{C)}$, $h = 800\ \text{W/(m}^2\cdot\,^\circ\text{C)}$, and $T_\infty = 10\,^\circ\text{C}$. The temperature at the left end of the rod is constant at 100 °C.

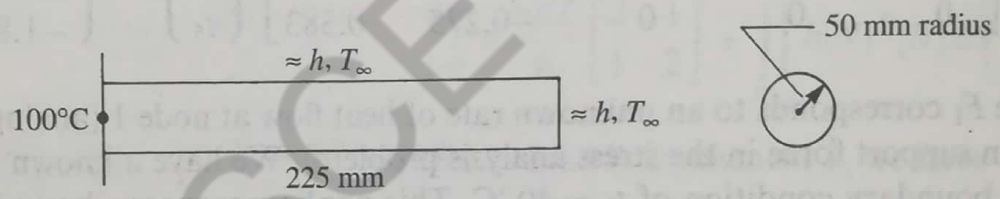


**Figure 13–12** One-dimensional rod subjected to temperature variation

**SOLUTION:**

The finite element discretization is shown in Figure 13–13. Three elements are sufficient to enable us to determine temperatures at the four points along the rod, although more elements would yield answers more closely approximating the analytical solution obtained by solving the differential equation such as Eq. (13.2.3) with the partial derivative with respect to time equal to zero. There will be convective heat loss over the perimeter and the right end of the rod. The left end will not have convective

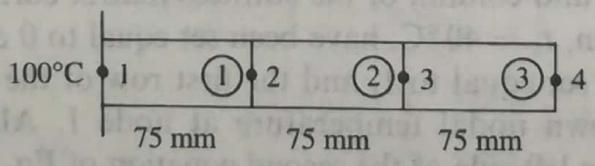


**Figure 13–13** Finite element discretized rod of Figure 13–12

heat loss. Using Eqs. (13.4.22) and (13.4.28), we calculate the stiffness matrices for the elements as follows:

$$\frac{AK_{xx}}{L} = \frac{(\pi \times 0.05^2)(60)}{0.075} = 2\pi \text{ W/°C}$$
$$\frac{hPL}{6} = \frac{(800)(2\pi \times 0.05)(0.075)}{6} = \pi \text{ W/°C} \tag{13.4.43}$$
$$hA = (800)(\pi \times 0.05^2) = 2\pi \text{ W/°C}$$

Substituting the results of Eqs. (13.4.43) into Eq. (13.4.22), we obtain the stiffness matrix for element 1 as

$$[k^{(1)}] = 2\pi \begin{bmatrix} 1 & -1 \\ -1 & 1 \end{bmatrix} + \pi \begin{bmatrix} 2 & 1 \\ 1 & 2 \end{bmatrix}$$
$$= 2\pi \begin{bmatrix} 2 & -\frac{1}{2} \\ -\frac{1}{2} & 2 \end{bmatrix} \text{ W/°C} \tag{13.4.44}$$

Because there is no convection across the ends of element 1 (its left end has a known temperature and its right end is inside the whole rod and thus not exposed to fluid motion), the contribution to the stiffness matrix owing to convection from an end of the element, such as given by Eq. (13.4.28), is zero. Similarly,

$$[k^{(2)}] = [k^{(1)}] = 2\pi \begin{bmatrix} 2 & -\frac{1}{2} \\ -\frac{1}{2} & 2 \end{bmatrix} \text{ W/°C} \tag{13.4.45}$$

However, element 3 has an additional (convection) term owing to heat loss from the exposed surface at its right end. Therefore, Eq. (13.4.28) yields a contribution to the element 3 stiffness matrix, which is then given by

$$[k^{(3)}] = [k^{(1)}] + hA \begin{bmatrix} 0 & 0 \\ 0 & 1 \end{bmatrix} = 2\pi \begin{bmatrix} 2 & -\frac{1}{2} \\ -\frac{1}{2} & 2 \end{bmatrix} + 2\pi \begin{bmatrix} 0 & 0 \\ 0 & 1 \end{bmatrix}$$
$$= 2\pi \begin{bmatrix} 2 & -\frac{1}{2} \\ -\frac{1}{2} & 3 \end{bmatrix} \text{ W/°C} \tag{13.4.46}$$

In general, we calculate the force matrices by using Eqs. (13.4.26) and (13.4.29). Because $Q = 0$ and $q^* = 0$, we only have force terms from $hT_\infty$ as given by Eq. (13.4.25). Therefore,

$$\{f^{(1)}\} = \{f^{(2)}\} = \frac{hT_\infty PL}{2} \begin{Bmatrix} 1 \\ 1 \end{Bmatrix} = \frac{(800 \text{ W/(m}^2 \cdot \text{°C})\,(10\,\text{°C})\,(2\pi \times 0.05)\,(0.075)}{2} \begin{Bmatrix} 1 \\ 1 \end{Bmatrix} \tag{13.4.47a}$$
$$= 2\pi \begin{Bmatrix} 15 \\ 15 \end{Bmatrix}$$

Element 3 has convection from both the perimeter and the right end. Therefore,

$$\{f^{(3)}\} = \{f^{(1)}\} + hT_\infty A\begin{Bmatrix}0\\1\end{Bmatrix} = 2\pi\begin{Bmatrix}15\\15\end{Bmatrix} + (800\,\text{W/m}^2\cdot{}^\circ\text{C})\,(10\,^\circ\text{C})\pi(0.05\,\text{m})^2\begin{Bmatrix}0\\1\end{Bmatrix}$$

$$= 2\pi\begin{Bmatrix}15\\25\end{Bmatrix} \tag{13.4.47b}$$

The assembly of the element stiffness matrices, Eqs. (13.4.44) through (13.4.46), and the force matrices, Eqs. (13.4.47a) and (13.4.47b), using the direct stiffness method, produces the following system of equations (where the $2\pi$ term has been divided out of both sides of Eq. (13.4.48)):

$$\begin{bmatrix} 2 & -\frac{1}{2} & 0 & 0 \\ -\frac{1}{2} & 4 & -\frac{1}{2} & 0 \\ 0 & -\frac{1}{2} & 4 & -\frac{1}{2} \\ 0 & 0 & -\frac{1}{2} & 3 \end{bmatrix}\begin{Bmatrix} t_1 = 100 \\ t_2 \\ t_3 \\ t_4 \end{Bmatrix} = \begin{Bmatrix} F_1' + 15 \\ 15 + 15 \\ 15 + 15 \\ 25 \end{Bmatrix} \tag{13.4.48}$$

Where $F_1' = F_1/2\pi$.

Expressing the second through fourth of Eqs. (13.4.48) in explicit form, we have

$$\begin{aligned} 4t_2 - 0.5t_3 + 0t_4 &= 50 + 30 \\ -0.5t_2 + 4t_3 - 0.5t_4 &= 30 \\ 0t_2 - 0.5t_3 + 3t_4 &= 25 \end{aligned} \tag{13.4.49}$$

Solving for the nodal temperatures $t_2 - t_4$ we obtain

$$t_2 = 21.43\,^\circ\text{C} \qquad t_3 = 11.46\,^\circ\text{C} \qquad t_4 = 10.24\,^\circ\text{C} \tag{13.4.50}$$

Next, we determine the heat flux for element 1 by using Eqs. (13.4.6) and (13.4.9) in Eq. (13.4.8) as

$$q^{(1)} = -K_{xx}[B]\{t\} \tag{13.4.51}$$

Using Eq. (13.4.7) in Eq. (13.4.51), we have

$$q^{(1)} = -K_{xx}\begin{bmatrix}-\frac{1}{L} & \frac{1}{L}\end{bmatrix}\begin{Bmatrix}t_1\\t_2\end{Bmatrix} \tag{13.4.52}$$

Substituting the numerical values for $t_1$ and $t_2$ into Eq. (13.4.52), we obtain

$$q^{(1)} = -60\begin{bmatrix}-\frac{1}{0.075} & \frac{1}{0.075}\end{bmatrix}\begin{Bmatrix}100\\21.43\end{Bmatrix}$$

or

$$q^{(1)} = 62856\ \text{W/m}^2 \tag{13.4.53}$$

We then determine the rate of heat flow $\bar{q}$ by multiplying Eq. (13.4.53) by the cross-sectional area over which $q$ acts. Therefore,

$$\bar{q}^{(1)} = 62856(\pi \times 0.05^2) = 493.7\ \text{W}$$

Here positive heat flow indicates heat flow from node 1 to node 2 (to the right). ■

**Example 13.3**

The plane wall shown in Figure 13–14 is 1 m thick. The left surface of the wall ($x = 0$) is maintained at a constant temperature of 200 °C, and the right surface ($x = L = 1$ m) is insulated. The thermal conductivity is $K_{xx} = 25$ W/(m · °C) and there is a uniform generation of heat inside the wall of $Q = 400$ W/m$^3$. Determine the temperature distribution through the wall thickness.

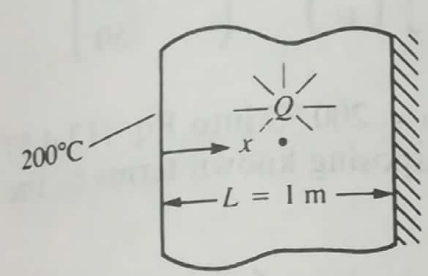


**Figure 13–14** Conduction in a plane wall subjected to uniform heat generation

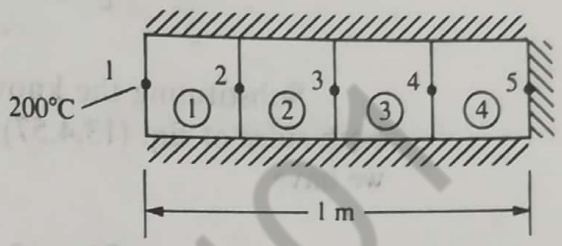


**Figure 13–15** Discretized model of Figure 13–14

**SOLUTION:**

This problem is assumed to be approximated as a one-dimensional heat-transfer problem. The discretized model of the wall is shown in Figure 13–15. For simplicity, we use four equal-length elements all with unit cross-sectional area ($A = 1$ m$^2$). The unit area represents a typical cross section of the wall. The perimeter of the wall model is then insulated to obtain the correct conditions.

Using Eqs. (13.4.22) and (13.4.28), we calculate the element stiffness matrices as follows:

$$\frac{AK_{xx}}{L} = \frac{(1 \text{ m}^2)[25 \text{ W/(m} \cdot \text{°C)}]}{0.25 \text{ m}} = 100 \text{ W/°C}$$

For each identical element, we have

$$[k] = 100 \begin{bmatrix} 1 & -1 \\ -1 & 1 \end{bmatrix} \text{ W/°C} \tag{13.4.54}$$

Because no convection occurs, $h$ is equal to zero; therefore, there is no convection contribution to $[k]$.

The element force matrices are given by Eq. (13.4.26). With $Q = 400$ W/m$^3$, $q = 0$, and $h = 0$, Eq. (13.4.26) becomes

$$\{f\} = \frac{QAL}{2} \begin{Bmatrix} 1 \\ 1 \end{Bmatrix} \tag{13.4.55}$$

Evaluating Eq. (13.4.55) for a typical element, such as element 1, we obtain

$$\begin{Bmatrix} f_{1x} \\ f_{2x} \end{Bmatrix} = \frac{(400 \text{ W/m}^3)(1 \text{ m}^2)(0.25 \text{ m})}{2} \begin{Bmatrix} 1 \\ 1 \end{Bmatrix} = \begin{Bmatrix} 50 \\ 50 \end{Bmatrix} \text{ W} \tag{13.4.56}$$

The force matrices for all other elements are equal to Eq. (13.4.56).

The assemblage of the element matrices, Eqs. (13.4.54) and (13.4.56) and the other force matrices similar to Eq. (13.4.56), yields

$$100\begin{bmatrix} 1 & -1 & 0 & 0 & 0 \\ -1 & 2 & -1 & 0 & 0 \\ 0 & -1 & 2 & -1 & 0 \\ 0 & 0 & -1 & 2 & -1 \\ 0 & 0 & 0 & -1 & 1 \end{bmatrix}\begin{Bmatrix} t_1 \\ t_2 \\ t_3 \\ t_4 \\ t_5 \end{Bmatrix} = \begin{Bmatrix} F_1 + 50 \\ 100 \\ 100 \\ 100 \\ 50 \end{Bmatrix} \tag{13.4.57}$$

Substituting the known temperature $t_1 = 200\,^\circ\text{C}$ into Eq. (13.4.57), dividing both sides of Eq. (13.4.57) by 100, and transposing known terms to the right side, we have

$$\begin{bmatrix} 1 & 0 & 0 & 0 & 0 \\ 0 & 2 & -1 & 0 & 0 \\ 0 & -1 & 2 & -1 & 0 \\ 0 & 0 & -1 & 2 & -1 \\ 0 & 0 & 0 & -1 & 1 \end{bmatrix}\begin{Bmatrix} t_1 \\ t_2 \\ t_3 \\ t_4 \\ t_5 \end{Bmatrix} = \begin{Bmatrix} 200\,^\circ\text{C} \\ 201 \\ 1 \\ 1 \\ 0.5 \end{Bmatrix} \tag{13.4.58}$$

The second through fifth equations of Eq. (13.4.58) can now be solved simultaneously to yield

$$t_2 = 203.5\,^\circ\text{C} \qquad t_3 = 206\,^\circ\text{C} \qquad t_4 = 207.5\,^\circ\text{C} \qquad t_5 = 208\,^\circ\text{C} \tag{13.4.59}$$

Using the first of Eqs. (13.4.57) yields the rate of heat flow out the left end:

$$F_1 = 100(t_1 - t_2) - 50$$
$$F_1 = 100(200 - 203.5) - 50$$
$$F_1 = -400\ \text{W}$$

The closed-form solution of the differential equation for conduction, Eq. (13.1.9), with the left-end boundary condition given by Eq. (13.1.10) and the right-end boundary condition given by Eq. (13.1.11), and with $q_x^* = 0$, is shown in Reference [2] to yield a parabolic temperature distribution through the wall. Evaluating the expression for the temperature function given in Reference [2] for values of $x$ corresponding to the node points of the finite element model, we obtain

$$t_2 = 203.5\,^\circ\text{C} \qquad t_3 = 206\,^\circ\text{C} \qquad t_4 = 207.5\,^\circ\text{C} \qquad t_5 = 208\,^\circ\text{C} \tag{13.4.60}$$

Figure 13–16 is a plot of the closed-form solution and the finite element solution for the temperature variation through the wall. The finite element nodal values and the closed-form values are equal, because the consistent equivalent force matrix has been used. (This was also discussed in Sections 3.10 and 3.11 for the axial bar subjected to distributed loading, and in Section 4.5 for the beam subjected to distributed

## 13.5 Two-Dimensional Finite Element Formulation

Because many bodies can be modeled as two-dimensional heat-transfer problems, now develop the equations for an element appropriate for these problems. Example using this element then follow.

### Step 1 Select Element Type

The three-noded triangular element with nodal temperatures shown in Figure 13–20 the basic element for solution of the two-dimensional heat-transfer problem.

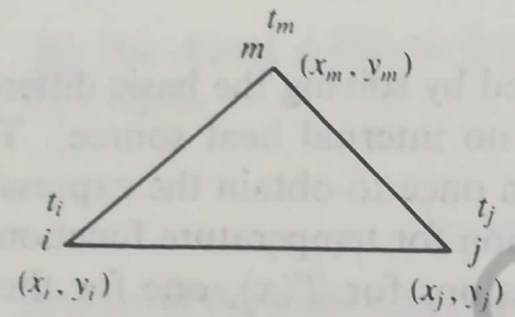


**Figure 13–20** Basic triangular element with nodal temperatures

### Step 2 Select a Temperature Function

The temperature function is given by

$$\{T\} = [N_i \quad N_j \quad N_m] \begin{Bmatrix} t_i \\ t_j \\ t_m \end{Bmatrix} \tag{13.5.1}$$

where $t_i$, $t_j$, and $t_m$ are the nodal temperatures, and the shape functions are again given by Eqs. (6.2.18); that is,

$$N_i = \frac{1}{2A}(\alpha_i + \beta_i x + \gamma_i y) \tag{13.5.2}$$

with similar expressions for $N_j$ and $N_m$. Here the $\alpha$'s, $\beta$'s, and $\gamma$'s are defined by Eqs. (6.2.10).

Unlike the CST element of Chapter 6 where there are 2 degrees of freedom per node (an $x$ and a $y$ displacement), in the heat transfer three-noded triangular element only a single scalar value (nodal temperature) is the primary unknown at each node, as shown by Eq. (13.5.1). This holds true for the three-dimensional elements as well, as shown in Section 13.7. Hence, the heat-transfer problem is sometimes known as a scalar-valued boundary value problem.

**Step 3** Define the Temperature Gradient/Temperature and Heat Flux/Temperature Gradient Relationships

We define the gradient matrix analogous to the strain matrix used in the stress analysis problem as

$$\{g\} = \begin{Bmatrix} \dfrac{\partial T}{\partial x} \\ \dfrac{\partial T}{\partial y} \end{Bmatrix} \tag{13.5.3}$$

Using Eq. (13.5.1) in Eq. (13.5.3), we have

$$\{g\} = \begin{bmatrix} \dfrac{\partial N_i}{\partial x} & \dfrac{\partial N_j}{\partial x} & \dfrac{\partial N_m}{\partial x} \\ \dfrac{\partial N_i}{\partial y} & \dfrac{\partial N_j}{\partial y} & \dfrac{\partial N_m}{\partial y} \end{bmatrix} \begin{Bmatrix} t_i \\ t_j \\ t_m \end{Bmatrix} \tag{13.5.4}$$

The gradient matrix $\{g\}$, written in compact matrix form analogously to the strain matrix $\{\varepsilon\}$ of the stress analysis problem, is given by

$$\{g\} = [B]\{t\} \tag{13.5.5}$$

where the $[B]$ matrix is obtained by substituting the three equations suggested by Eq. (13.5.2) in the rectangular matrix on the right side of Eq. (13.5.4) as

$$[B] = \frac{1}{2A}\begin{bmatrix} \beta_i & \beta_j & \beta_m \\ \gamma_i & \gamma_j & \gamma_m \end{bmatrix} \tag{13.5.6}$$

The heat flux/temperature gradient relationship is now

$$\begin{Bmatrix} q_x \\ q_y \end{Bmatrix} = -[D]\{g\} \tag{13.5.7}$$

where the material property matrix is

$$[D] = \begin{bmatrix} K_{xx} & 0 \\ 0 & K_{yy} \end{bmatrix} \tag{13.5.8}$$

**Step 4** Derive the Element Conduction Matrix and Equations

The element stiffness matrix from Eq. (13.4.17) is

$$[k] = \iiint_V [B]^T[D][B]\,dV + \iint_{S_3} h[N]^T[N]\,dS \tag{13.5.9}$$

where

$$[k_c] = \iiint_V [B]^T[D][B]\,dV$$

$$= \iiint_V \frac{1}{4A^2}\begin{bmatrix}\beta_i & \gamma_i\\ \beta_j & \gamma_j\\ \beta_m & \gamma_m\end{bmatrix}\begin{bmatrix}K_{xx} & 0\\ 0 & K_{yy}\end{bmatrix}\begin{bmatrix}\beta_i & \beta_j & \beta_m\\ \gamma_i & \gamma_j & \gamma_m\end{bmatrix} dV \tag{13.5.10}$$

Assuming constant thickness in the element and noting that all terms of the integrand of Eq. (13.5.10) are constant, we have

$$[k_c] = \iiint_V [B]^T[D][B]\,dV = tA[B]^T[D][B] \tag{13.5.11}$$

Equation (13.5.11) is the true conduction portion of the total stiffness matrix Eq. (13.5.9). The second integral of Eq. (13.5.9) (the convection portion of the total stiffness matrix) is defined by

$$[k_h] = \iint_{S_3} h[N]^T[N]\,dS \tag{13.5.12}$$

We can explicitly multiply the matrices in Eq. (13.5.12) to obtain

$$[k_h] = h\iint_{S_3}\begin{bmatrix}N_iN_i & N_iN_j & N_iN_m\\ N_jN_i & N_jN_j & N_jN_m\\ N_mN_i & N_mN_j & N_mN_m\end{bmatrix} dS \tag{13.5.13}$$

To illustrate the use of Eq. (13.5.13), consider the side between nodes $i$ and $j$ of the triangular element to be subjected to convection (Figure 13–21). Then $N_m = 0$ along side $i$-$j$, and we obtain

$$[k_h] = \frac{hL_{i\text{-}j}t}{6}\begin{bmatrix}2 & 1 & 0\\ 1 & 2 & 0\\ 0 & 0 & 0\end{bmatrix} \tag{13.5.14}$$

where $L_{i\text{-}j}$ is the length of side $i$-$j$.

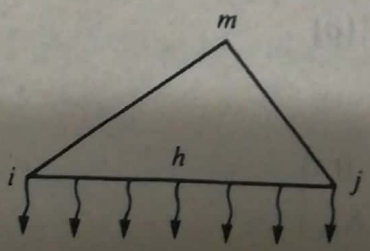


**Figure 13–21** Heat loss by convection from side $i$-$j$

The evaluation of the force matrix integrals in Eq. (13.4.16) is as follows:

$$\{f_Q\} = \iiint_V Q[N]^T \, dV = Q \iiint_V [N]^T \, dV \tag{13.5.15}$$

for constant heat source $Q$. Thus it can be shown (left to your discretion) that this integral is equal to

$$\{f_Q\} = \frac{QV}{3} \begin{Bmatrix} 1 \\ 1 \\ 1 \end{Bmatrix} \tag{13.5.16}$$

where $V = At$ is the volume of the element. Equation (13.5.16) indicates that heat is generated by the body in three equal parts to the nodes (like body forces in the elasticity problem). The second force matrix in Eq. (13.4.16) is

$$\{f_q\} = \iint_{S_2} q^* [N]^T \, dS = \iint_{S_2} q^* \begin{Bmatrix} N_i \\ N_j \\ N_m \end{Bmatrix} dS \tag{13.5.17}$$

This reduces to

$$\frac{q^* L_{i\text{-}j} t}{2} \begin{Bmatrix} 1 \\ 1 \\ 0 \end{Bmatrix} \quad \text{on side } i\text{-}j \tag{13.5.18}$$

$$\frac{q^* L_{j\text{-}m} t}{2} \begin{Bmatrix} 0 \\ 1 \\ 1 \end{Bmatrix} \quad \text{on side } j\text{-}m \tag{13.5.19}$$

$$\frac{q^* L_{m\text{-}i} t}{2} \begin{Bmatrix} 1 \\ 0 \\ 1 \end{Bmatrix} \quad \text{on side } m\text{-}i \tag{13.5.20}$$

where $L_{i\text{-}j}$, $L_{j\text{-}m}$, and $L_{m\text{-}i}$ are the lengths of the sides of the element, and the heat flux $q^*$ is assumed constant over each edge. The integral $\iint_{S_3} hT_\infty [N]^T \, dS$ can be found in a manner similar to Eq. (13.5.17) by simply replacing $q^*$ with $hT_\infty$ in Eqs. (13.5.18) through (13.5.20).

### Steps 5 through 7

Steps 5 through 7 are identical to those described in Section 13.4.

To illustrate the use of the equations presented in Section 13.5, we will now solve some two-dimensional heat-transfer problems.

### Transverse Deflections of Membranes

Suppose that a membrane, with fixed edges, occupies the region $\Omega$ in the $(x, y)$ plane. Initially the membrane is stretched so that the tension $a$ in the membrane is uniform and $a$ is so large that it is not appreciably altered when the membrane is deflected by a distributed transverse force, $f(x, y)$. The equation governing the transverse deflection $u$ of the membrane is given by

$$-a\left(\frac{\partial^2 u}{\partial x^2}+\frac{\partial^2 u}{\partial y^2}\right)=f(x, y) \quad \text{in } \Omega \tag{8.5.63a}$$

with

$$u=0 \quad \text{on } \Gamma \tag{8.5.63b}$$

Note that (8.5.63$a$) and (8.5.63$b$) have the same form as the equations used to describe torsion of cylindrical bars [see Eq. (8.5.60)]. The finite element model of the equation is obvious. In view of the close analogy between this problem and the torsion of cylindrical bars, we will not consider any numerical examples here (see Examples 8.3.1 and 8.5.6).

**Example 8.5.6** (Torsion of a Square Cross-Sectional Bar)

Here we consider torsion of a square ($a \times a$) cross-section bar. Note that the problem is antisymmetric as far as the loading and stress distribution are concerned; however, the stress function, being a scalar function governed by the Poisson equation (8.5.60), is symmetric about the $x$ and $y$ axes as well as the diagonal lines. When using rectangular elements, one quadrant of the bar cross section can be used in the finite element analysis. The biaxial symmetry about the $x$ and $y$ axes requires imposition of the following boundary conditions on $\Psi$ (see Example 8.3.1):

$$\frac{\partial \Psi}{\partial x} = 0 \quad \text{on the line } x = 0, \qquad \frac{\partial \Psi}{\partial y} = 0 \quad \text{on the line } y = 0$$

In addition, on the actual boundary we have the condition $\Psi = 0$ on lines $x = a$ and $y = b = a$.

**Example 8.3.1**

Consider a problem described by the Poisson equation

$$-\nabla^2 u = f_0 \quad \text{or} \quad -\left(\frac{\partial^2 u}{\partial x^2} + \frac{\partial^2 u}{\partial y^2}\right) = f_0 \quad \text{in } \Omega \tag{8.3.1}$$

in a square region [see Fig. 8.3.1(*a*)]

$$\Omega = \{(x, y) : -A < x < A,\ -A < y < A\}$$

where $u(x, y)$ is the dependent unknown and $f_0$ is the uniformly distributed source. We shall consider the following boundary conditions for the problem:

$$u = 0 \text{ on the entire boundary } \Gamma \tag{8.3.2}$$

We wish to use the finite element method to determine $u(x, y)$ everywhere in $\Omega$.

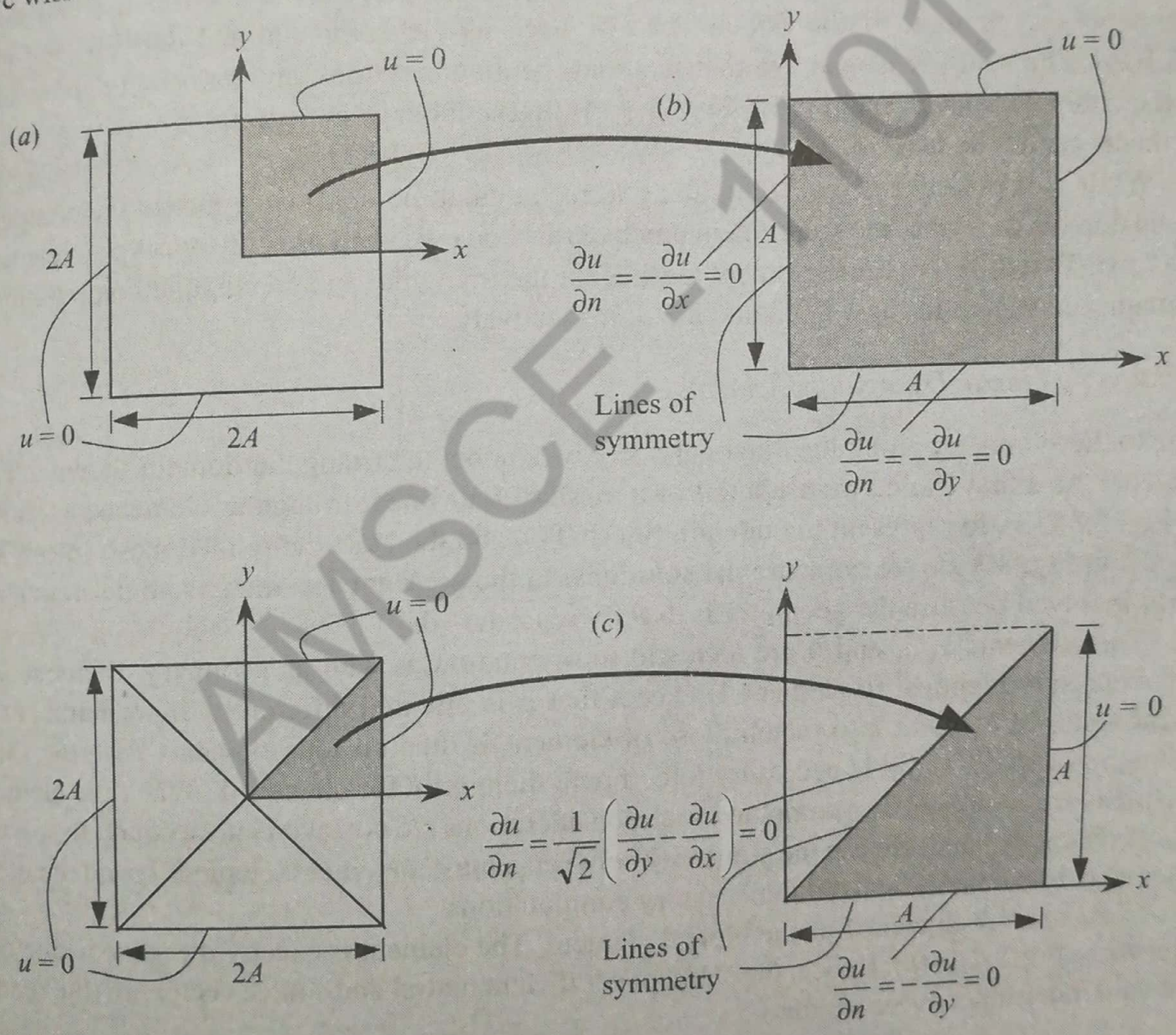


**Figure 8.3.1** Finite element analysis of the Poisson equation in a square region: (*a*) Geometry of the actual domain with boundary conditions. (*b*) Computational domain based on biaxial symmetry. (*c*) Computational domain based on biaxial as well as diagonal symmetry.

*Selection of the Computational Domain*

When the given domain $\Omega$ exhibits solution symmetries, it is sufficient to solve the problem on a portion of $\Omega$ that provides the solution on the entire domain. A problem possesses symmetry of the solution about a line only when symmetry of the ($a$) geometry, ($b$) material properties, ($c$) source variation, and ($d$) boundary conditions exist about the line. Whenever a portion of the domain is modeled to exploit symmetries available in the problem, the lines of symmetries become a portion of the boundary of the computational domain. On lines of symmetry, the normal derivative of the solution (i.e., derivative of the solution with respect to the coordinate normal to the line of symmetry) is zero:

$$q_n = \frac{\partial u}{\partial n} = \frac{\partial u}{\partial x} n_x + \frac{\partial u}{\partial y} n_y = 0 \tag{8.3.2}$$

The problem at hand has the geometric symmetry about the $x=0$ and $y=0$ axes; since the coefficients describing the material behavior, $a_{ij}$, are either zero or unity, material symmetry about the $x=0$ and $y=0$ axes is automatically met. The symmetry of source variation is dictated by $f$. Since it is uniform, i.e., $f=f_0$, constant, the data is symmetric with respect to the $x=0$ and $y=0$ axes. Lastly, the boundary conditions are symmetric with respect to the $x=0$ and $y=0$ axes. Thus, the solution is symmetric about the $x=0$ and $y=0$ axes, and hence, a quadrant of the domain can be used as the computational domain [see Fig. 8.3.1($b$)]. The solution is also symmetric about the diagonal lines, and an octant can be used as the computational domain [see Fig. 8.3.1($c$)]. In the latter case, a mesh of only rectangular elements cannot be used.

While it is possible to mix triangular and rectangular elements to represent the computational domain as well as the solution, in much of this book we shall use only one type of element at a time. Two different finite element meshes for the triangular and rectangular computational domains are shown in Figs. 8.3.2 and 8.3.3, respectively.

*Solution by Linear Triangular Elements*

Due to the symmetry along the diagonal $x=y$, we model the triangular domain shown in Fig. 8.3.1($c$). As a first choice we use a uniform mesh of four linear triangular elements, as shown in Fig. 8.3.2($a$), to represent the domain (mesh T1), and then use the refined mesh (mesh T2) shown in Fig. 8.3.2($b$) to compare the solutions. In the present case, there is no discretization error involved because the geometry is exactly represented.

The elements 1, 3, and 4 are identical in orientation as well as geometry. Element 2 is geometrically identical to element 1, except that it is oriented differently. If we number the local nodes of element 2 to match those of element 1, then all four elements have the same element matrices, and it is necessary to compute them only for element 1. When the element matrices are computed on a computer, such considerations are not taken into account. In solving the problem by hand, we use the similarity between a master element (element 1) and the other elements in the mesh to avoid unnecessary computations.

We consider element 1 as the typical element. The element is exactly the same as the one shown in Fig. 8.2.11($b$). Hence, the element coefficient matrix and source vector are (the reader should independently verify this)

$$[K^1] = \frac{1}{2ab}\begin{bmatrix} b^2 & -b^2 & 0 \\ -b^2 & a^2+b^2 & -a^2 \\ 0 & -a^2 & a^2 \end{bmatrix}, \quad \{f^1\} = \frac{f_0 ab}{6}\begin{Bmatrix} 1 \\ 1 \\ 1 \end{Bmatrix} \tag{8.3.4}$$

where in the present case $a=b=A/2=0.5$.

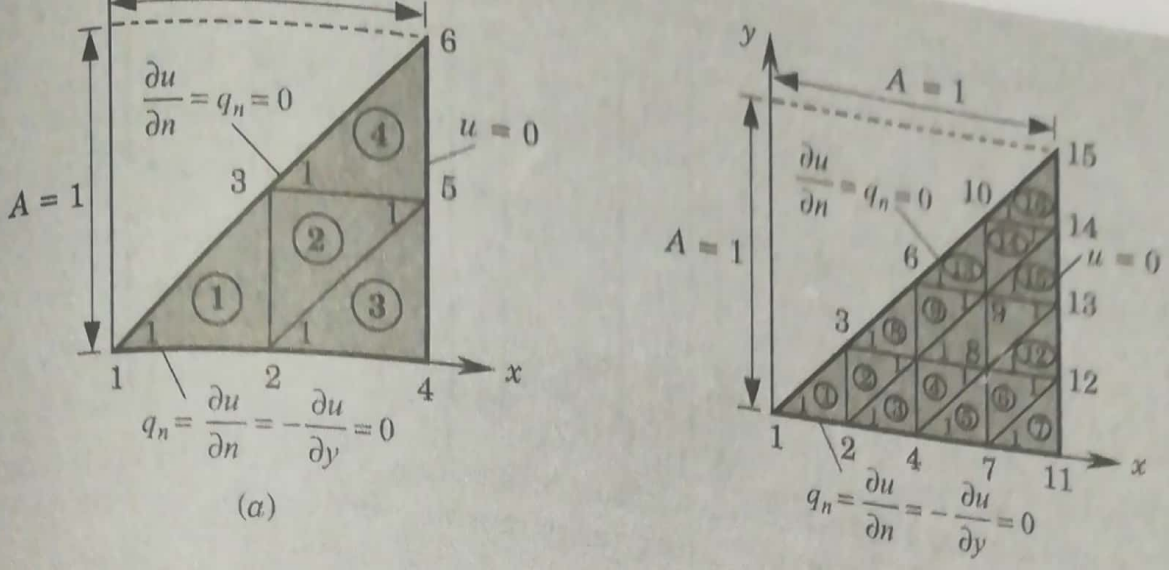


**Figure 8.3.2** (*a*) Mesh T1 of triangular elements. (*b*) Mesh T2 of triangular elements.

The element matrix in (8.3.4) is valid for the Laplace operator $-\nabla^2$ on any right-angle triangle with sides $a$ and $b$ in which the right angle is at node 2, and the diagonal line of the triangle connects node 3 to node 1. Note that the off-diagonal coefficient associated with the nodes on the diagonal line is zero for a right-angled triangle.

In summary, for the mesh shown in Fig. 8.3.2(*a*), we have

$$[K^1]=[K^2]=[K^3]=[K^4], \quad \{f^1\}=\{f^2\}=\{f^3\}=\{f^4\}$$

with

$$[K^e]=\frac{1}{2}\begin{bmatrix} 1 & -1 & 0 \\ -1 & 2 & -1 \\ 0 & -1 & 1 \end{bmatrix}, \quad \{f^e\}=\frac{f_0}{24}\begin{Bmatrix} 1 \\ 1 \\ 1 \end{Bmatrix} \tag{8.3.5}$$

The assembled coefficient matrix for the finite element mesh is $6 \times 6$, because there are six global nodes with one unknown per node. The assembled matrix can be obtained directly by using the correspondence between the global nodes and the local nodes, expressed through the connectivity matrix,

$$[B]=\begin{bmatrix} 1 & 2 & 3 \\ 5 & 3 & 2 \\ 2 & 4 & 5 \\ 3 & 5 & 6 \end{bmatrix} \tag{8.3.6}$$

A few representative global coefficients are given below in terms of the element coefficients.

$$K_{11}=K_{11}^1=\frac{1}{2}, \quad K_{12}=K_{12}^1=-\frac{1}{2}, \quad K_{22}=K_{22}^1+K_{33}^2+K_{11}^3=\frac{2}{2}+\frac{1}{2}+\frac{1}{2}$$

$$K_{13}=K_{13}^1=0, \quad K_{14}=0, \quad K_{15}=0, \quad K_{16}=0, \quad K_{23}=K_{23}^1+K_{32}^2=-\frac{1}{2}-\frac{1}{2}$$

$$K_{33}=K_{33}^1+K_{22}^2+K_{11}^4=\frac{1}{2}+\frac{2}{2}+\frac{1}{2}, \quad F_1=F_1^1=Q_1^1+f_1^1 \tag{8.3.7}$$

$$F_2=(Q_2^1+Q_3^2+Q_1^3)+(f_2^1+f_3^2+f_1^3), \quad F_3=(Q_3^1+Q_2^2+Q_1^4)+(f_3^1+f_2^2+f_1^4)$$

$$F_4=F_2^3=Q_2^3+f_2^3, \quad F_5=(Q_1^2+Q_3^3+Q_2^4)+(f_1^2+f_3^3+f_2^4), \quad F_6=F_3^4=Q_3^4+f_3^4$$

The assembled system of equations associated with mesh T1 are

$$\frac{1}{2}\begin{bmatrix} 1 & -1 & 0 & 0 & 0 & 0 \\ -1 & 4 & -2 & -1 & 0 & 0 \\ 0 & -2 & 4 & 0 & -2 & 0 \\ 0 & -1 & 0 & 2 & -1 & 0 \\ 0 & 0 & -2 & -1 & 4 & -1 \\ 0 & 0 & 0 & 0 & -1 & 1 \end{bmatrix} \begin{Bmatrix} U_1 \\ U_2 \\ U_3 \\ U_4 \\ U_5 \\ U_6 \end{Bmatrix} = \frac{f_0}{24} \begin{Bmatrix} 1 \\ 3 \\ 3 \\ 1 \\ 3 \\ 1 \end{Bmatrix} + \begin{Bmatrix} Q_1^1 \\ Q_2^1 + Q_3^2 + Q_1^3 \\ Q_3^1 + Q_2^2 + Q_1^4 \\ Q_2^3 \\ Q_1^2 + Q_3^3 + Q_2^4 \\ Q_3^4 \end{Bmatrix} \tag{8.3.8}$$

Note that at nodes 4 and 6, both $u$ and $q_n$ are specified (a type of singularity in the specified data). However, we shall give priority to the primary variable over the secondary variable. Thus, we assume that

$$U_4 = U_5 = U_6 = 0 \tag{8.3.9}$$

and $Q_4$, $Q_5$, and $Q_6$, assumed to be unknown, are determined in the postcomputation. The specified secondary degrees of freedom are (all due to symmetry)

$$Q_1 = Q_1^1 = 0, \quad Q_2 = Q_2^1 + Q_3^2 + Q_1^3 = 0, \quad Q_3 = Q_3^1 + Q_2^2 + Q_1^4 = 0 \tag{8.3.10}$$

For example, consider the sum

$$\begin{aligned} Q_2^1 + Q_3^2 + Q_1^3 &= (Q_{21}^1 + Q_{22}^1) + (Q_{32}^2 + Q_{33}^2) + (Q_{11}^3 + Q_{13}^3) \\ &= Q_{21}^1 + (Q_{22}^1 + Q_{32}^2) + (Q_{33}^2 + Q_{13}^3) + Q_{11}^3 = 0 + 0 + 0 + 0 \end{aligned}$$

where $Q_{21}^1$ and $Q_{11}^3$ are zero because of $q_n = 0$ and $Q_{22}^1 + Q_{32}^2$ and $Q_{33}^2 + Q_{13}^3$ are zero because of the balance of fluxes between neighboring elements.

Since the only unknown primary variables for mesh T1 are $U_1$, $U_2$, and $U_3$, the condensed equations for the primary unknowns can be obtained by deleting rows and columns 4, 5, and 6 from the system (8.3.8). In retrospect, it would have been sufficient to write the finite element equations associated with the global nodes 1, 2, and 3:

$$\begin{aligned} K_{11}U_1 + K_{12}U_2 + K_{13}U_3 &= F_1 \\ K_{21}U_1 + K_{22}U_2 + K_{23}U_3 + K_{24}U_4 + K_{25}U_5 &= F_2 \\ K_{31}U_1 + K_{32}U_2 + K_{33}U_3 + K_{35}U_5 + K_{36}U_6 &= F_3 \end{aligned}$$

Noting that $U_4 = U_5 = U_6 = 0$, we can write the above equations in terms of the element coefficients:

$$\begin{bmatrix} K_{11}^1 & K_{12}^1 & K_{13}^1 \\ K_{21}^1 & K_{22}^1 + K_{33}^2 + K_{11}^3 & K_{23}^1 + K_{32}^2 \\ K_{31}^1 & K_{32}^1 + K_{23}^2 & K_{33}^1 + K_{22}^2 + K_{11}^4 \end{bmatrix} \begin{Bmatrix} U_1 \\ U_2 \\ U_3 \end{Bmatrix} = \begin{Bmatrix} f_1^1 \\ f_2^1 + f_3^2 + f_1^3 \\ f_3^1 + f_2^2 + f_1^4 \end{Bmatrix} \tag{8.3.11}$$

The unknown secondary variables $Q_4$, $Q_5$, and $Q_6$ can be computed from the element equations

$$\begin{Bmatrix} Q_4 \\ Q_5 \\ Q_6 \end{Bmatrix} = -\begin{Bmatrix} f_2^3 \\ f_1^2 + f_3^3 + f_2^4 \\ f_3^4 \end{Bmatrix} + \begin{bmatrix} 0 & K_{21}^3 & 0 \\ 0 & K_{13}^2 + K_{31}^3 & K_{12}^2 + K_{21}^4 \\ 0 & 0 & K_{31}^4 \end{bmatrix} \begin{Bmatrix} U_1 \\ U_2 \\ U_3 \end{Bmatrix} \tag{8.3.12}$$

For example, we have

$$\begin{aligned} Q_4 = Q_2^3 &= Q_{21}^3 + Q_{22}^3 + Q_{23}^3 \\ &= \int_{1-2} q_n^3 \psi_2^3 \, dx + \int_{2-3} q_n^3 \psi_2^3 \, dy + \int_{3-1} q_n^3 \psi_2^3 \, ds \end{aligned} \tag{8.3.13a}$$

where

$$\begin{aligned} (q_n^3)_{1-2} &= \left( \frac{\partial u}{\partial x} n_x + \frac{\partial u}{\partial y} n_y \right)_{1-2} = 0 \quad \left( n_x = 0, \quad \frac{\partial u}{\partial y} = 0 \right) \\ (q_n^3)_{2-3} &= \left( \frac{\partial u}{\partial x} n_x + \frac{\partial u}{\partial y} n_y \right)_{2-3} = \frac{\partial u}{\partial x} \quad (n_x = 1, \quad n_y = 0) \\ (\psi_2^3)_{2-3} &= 1 - \frac{y}{h_{23}}, \quad (\psi_2^3)_{3-1} = 0 \end{aligned} \tag{8.3.13b}$$

Thus, we have

$$Q_4 = Q_{22}^3 = \int_0^{h_{23}} \frac{\partial u}{\partial x} \left( 1 - \frac{y}{h_{23}} \right) dy$$

where $\partial u / \partial x$ is calculated using $\partial u_h / \partial x$ from the finite element interpolation

$$\frac{\partial u_h}{\partial x} = \sum_{j=1}^{3} u_j^3 \frac{\beta_j^3}{2A_3}$$

We obtain ($h_{23} = a = 0.5$, $\beta_1^3 = -a = -0.5$, $2A_3 = a^2 = 0.25$, $U_4 = U_5 = 0$),

$$Q_4 = \frac{h_{23}}{4A_3} \sum_{j=1}^{3} u_j^3 \beta_j^3 = \frac{h_{23}}{4A_3} \left( \beta_1^3 U_2 + \beta_2^3 U_4 + \beta_3^3 U_5 \right) = -0.5 U_2 \tag{8.3.14}$$

Using the numerical values of the coefficients $K_{ij}^e$ and $f_i^e$, (with $f_0 = 1$), we write the condensed equations for $U_1$, $U_2$, and $U_3$ as

$$\begin{bmatrix} 0.5 & -0.5 & 0.0 \\ -0.5 & 2.0 & -1.0 \\ 0.0 & -1.0 & 2.0 \end{bmatrix} \begin{Bmatrix} U_1 \\ U_2 \\ U_3 \end{Bmatrix} = \frac{1}{24} \begin{Bmatrix} 1 \\ 3 \\ 3 \end{Bmatrix} \tag{8.3.15}$$

Solving (8.3.15) for $U_i$ ($i = 1, 2, 3$), we obtain

$$\begin{Bmatrix} U_1 \\ U_2 \\ U_3 \end{Bmatrix} = \frac{1}{24} \begin{bmatrix} 3 & 1 & 0.5 \\ 1 & 1 & 0.5 \\ 0.5 & 0.5 & 0.75 \end{bmatrix} \begin{Bmatrix} 1 \\ 3 \\ 3 \end{Bmatrix} = \frac{1}{24} \begin{Bmatrix} 7.5 \\ 5.5 \\ 4.25 \end{Bmatrix} = \begin{Bmatrix} 0.31250 \\ 0.22917 \\ 0.17708 \end{Bmatrix} \tag{8.3.16}$$

## Natural Vibration of Beams

*Euler–Bernoulli Beam Theory*

For the Euler–Bernoulli beam theory, the equation of motion is of the form [see Reddy (2002), pp. 193–196]

$$\rho A\frac{\partial^2 w}{\partial t^2}-\rho I\frac{\partial^4 w}{\partial t^2\partial x^2}+\frac{\partial^2}{\partial x^2}\left(EI\frac{\partial^2 w}{\partial x^2}\right)=q(x,t) \tag{6.1.36}$$

where $\rho$ denotes the mass density per unit length, $A$ the area of cross section, $E$ the modulus, and $I$ the second moment of area (see Chapter 5). The expression involving $\rho I$ is called

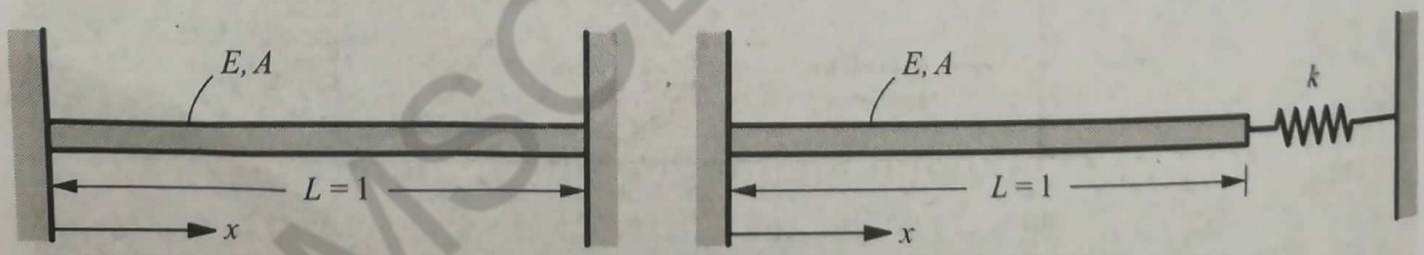


Set 1: $U(0) = 0$, $U(L) = 0$

Set 2: $U(0) = 0$, $\left[\frac{dU}{dx} + HU\right]_{x=L} = 0$

**Figure 6.1.3** Uniform bar with two sets of boundary conditions.

*rotary inertia* term. Equation (6.1.36) can be formulated as an eigenvalue problem in the interest of finding the frequency of natural vibration by assuming periodic motion

$$w(x,t) = W(x)e^{-i\omega t} \tag{6.1.37}$$

where $\omega$ is the frequency of natural transverse motion and $W(x)$ is the mode shape of the transverse motion. Substitution of Eq. (6.1.37) into (6.1.36) yields

$$\frac{d^2}{dx^2}\left(EI\frac{d^2W}{dx^2}\right) - \lambda\left(\rho AW - \rho I\frac{d^2W}{dx^2}\right) = 0 \tag{6.1.38}$$

where $\lambda = \omega^2$.

The weak form of Eq. (6.1.38) is given by

$$\begin{aligned} 0 = \int_{x_a}^{x_b} \left(EI\frac{d^2v}{dx^2}\frac{d^2W}{dx^2} - \lambda\rho Avw - \lambda\rho I\frac{dv}{dx}\frac{dW}{dx}\right)dx \\ + \left\{v\left[\frac{d}{dx}\left(EI\frac{d^2W}{dx^2}\right) + \lambda\rho I\frac{dW}{dx}\right]\right\}_{x_a}^{x_b} + \left[\left(-\frac{dv}{dx}\right)EI\frac{d^2W}{dx^2}\right]_{x_a}^{x_b} \end{aligned} \tag{6.1.39}$$

where $v$ is the weight function. Note that the rotary inertia term contributes to the shear force term, giving rise to an effective shear force that must be known at a boundary point when the deflection is unknown at the point.

To obtain the finite element model of Eq. (6.1.39), assume finite element approximation of the form

$$W(x) = \sum_{j=1}^{4} \Delta_j^e \phi_j^e(x) \tag{6.1.40}$$

where $\phi_j^e$ are the Hermite cubic polynomials [see Eqs. (5.2.11) and (5.2.12)], and obtain the finite element model

$$\left([K^e] - \omega^2[M^e]\right)\{\Delta^e\} = \{Q^e\} \tag{6.1.41a}$$

where

$$K_{ij}^e = \int_{x_a}^{x_b} EI\frac{d^2\phi_i^e}{dx^2}\frac{d^2\phi_j^e}{dx^2}\,dx, \quad M_{ij}^e = \int_{x_a}^{x_b}\left(\rho A\,\phi_i^e\,\phi_j^e + \rho I\,\frac{d\phi_i^e}{dx}\frac{d\phi_j^e}{dx}\right)dx \tag{6.1.41b}$$

$$\begin{aligned} Q_1^e &\equiv \left[\frac{d}{dx}\left(EI\frac{d^2W}{dx^2}\right) + \lambda\rho I\frac{dW}{dx}\right]\Bigg|_{x_a}, \qquad Q_2^e \equiv \left(EI\frac{d^2W}{dx^2}\right)\Bigg|_{x_a} \\ Q_3^e &\equiv -\left[\frac{d}{dx}\left(EI\frac{d^2W}{dx^2}\right) + \lambda\rho I\frac{dW}{dx}\right]\Bigg|_{x_b}, \quad Q_4^e \equiv -\left(EI\frac{d^2W}{dx^2}\right)\Bigg|_{x_b} \end{aligned} \tag{6.1.41c}$$

For constant values of $EI$ and $\rho A$, the stiffness matrix $[K^e]$ and mass matrix $[M^e]$ are

$$[K^e] = \frac{2E_eI_e}{h_e^3}\begin{bmatrix} 6 & -3h_e & -6 & -3h_e \\ -3h_e & 2h_e^2 & 3h_e & h_e^2 \\ -6 & 3h_e & 6 & 3h_e \\ -3h_e & h_e^2 & 3h_e & 2h_e^2 \end{bmatrix}$$

$$[M^e] = \frac{\rho^e A_e h_e}{420}\begin{bmatrix} 156 & -22h_e & 54 & 13h_e \\ -22h_e & 4h_e^2 & -13h_e & -3h_e^2 \\ 54 & -13h_e & 156 & 22h_e \\ 13h & -3h_e^2 & 22h_e & 4h_e^2 \end{bmatrix} + \frac{\rho^e I_e}{30h_e}\begin{bmatrix} 36 & -3h_e & -36 & -3h_e \\ -3h & 4h_e^2 & 3h_e & -h_e^2 \\ -36 & 3h_e & 36 & 3h_e \\ -3h_e & -h_e^2 & 3h_e & 4h_e^2 \end{bmatrix} \tag{6.1.42}$$

When rotary inertia is neglected, we omit the second part of the mass matrix in (6.1.42).

*Timoshenko Beam Theory*

The equations of motion of the Timoshenko beam theory are [see Reddy (2002), pp. 193–196]

$$\rho A\frac{\partial^2 w}{\partial t^2} - \frac{\partial}{\partial x}\left[GAK_s\left(\frac{\partial w}{\partial x} + \Psi\right)\right] = 0 \tag{6.1.43a}$$

$$\rho I\frac{\partial^2 \Psi}{\partial t^2} - \frac{\partial}{\partial x}\left(EI\frac{\partial \Psi}{\partial x}\right) + GAK_s\left(\frac{\partial w}{\partial x} + \Psi\right) = 0 \tag{6.1.43b}$$

where $G$ is the shear modulus ($G = E/[2(1+\nu)]$) and $K_s$ is the shear correction factor ($K_s = 5/6$). Note that Eq. (6.1.43$b$) contains the rotary inertia term. Once again, we assume periodic motion and write

$$w(x,t) = W(x)e^{-i\omega t}, \quad \Psi(x,t) = S(x)e^{-i\omega t} \tag{6.1.44}$$

and obtain the eigenvalue problem from Eqs. (6.1.43$a$) and (6.1.43$b$)

$$-\frac{d}{dx}\left[GAK_s\left(\frac{dW}{dx} + S\right)\right] - \omega^2\rho A W = 0 \tag{6.1.45a}$$

$$-\frac{d}{dx}\left(EI\frac{dS}{dx}\right) + GAK_s\left(\frac{dW}{dx} + S\right) - \omega^2\rho I\, S = 0 \tag{6.1.45b}$$

For equal interpolation of $W(x)$ and $S(x)$

$$W(x) = \sum_{j=1}^{n} W_j^e \psi_j^e(x), \quad S(x) = \sum_{j=1}^{n} S_j^e \psi_j^e(x) \tag{6.1.46}$$

where $\psi_j^e$ are the $(n-1)$ order Lagrange polynomials, the finite element model is given by

$$\left(\begin{bmatrix} [K^{11}] & [K^{12}] \\ [K^{21}] & [K^{22}] \end{bmatrix} - \omega^2\begin{bmatrix} [M^{11}] & [0] \\ [0] & [M^{22}] \end{bmatrix}\right)\begin{Bmatrix} \{W\} \\ \{S\} \end{Bmatrix} = \begin{Bmatrix} \{F^1\} \\ \{F^2\} \end{Bmatrix} \tag{6.1.47}$$

where $[K^e]$ is the stiffness matrix and $[M^e]$ is the mass matrix

$$K_{ij}^{11} = \int_{x_a}^{x_b} GAK_s \frac{d\psi_i^e}{dx}\frac{d\psi_j^e}{dx}dx$$

$$K_{ij}^{12} = \int_{x_a}^{x_b} GAK_s \frac{d\psi_i^e}{dx}\psi_j^e\, dx = K_{ji}^{21}$$

$$K_{ij}^{22} = \int_{x_a}^{x_b} \left( EI \frac{d\psi_i^e}{dx} \frac{d\psi_j^e}{dx} + GAK_s \psi_i^e \psi_j^e \right) dx$$

$$M_{ij}^{11} = \int_{x_a}^{x_b} \rho A \psi_i^e \psi_j^e \, dx, \quad M_{ij}^{22} = \int_{x_a}^{x_b} \rho I \psi_i^e \psi_j^e \, dx$$

$$F_j^1 = Q_{2i-1}, \quad F_i^2 = Q_{2i} \tag{6.1.48a}$$

$$Q_1^e \equiv -\left[ GAK_s \left( S + \frac{dW}{dx} \right) \right] \Big|_{x_a}, \quad Q_2^e \equiv -\left( EI \frac{dS}{dx} \right) \Big|_{x_a}$$

$$Q_3^e \equiv \left[ GAK_s \left( S + \frac{dW}{dx} \right) \right] \Big|_{x_b}, \quad Q_4^e \equiv \left( EI \frac{dS}{dx} \right) \Big|_{x_b} \tag{6.1.48b}$$

For the choice of linear interpolation functions, Eq. (6.1.47) has the explicit form (after rearranging the nodal variables)

$$[K^e] = \left( \frac{2E_e I_e}{\mu_0 h_e^3} \right) \begin{bmatrix} 6 & -3h_e & -6 & -3h_e \\ -3h_e & h_e^2(1.5+6\Lambda_e) & 3h_e & h_e^2(1.5-6\Lambda_e) \\ -6 & 3h_e & 6 & 3h_e \\ -3h_e & h_e^2(1.5-6\Lambda_e) & 3h_e & h_e^2(1.5+6\Lambda_e) \end{bmatrix}$$

$$[M^e] = \frac{\rho^e A_e}{6} \begin{bmatrix} 2 & 0 & 1 & 0 \\ 0 & 2r_e & 0 & r_e \\ 1 & 0 & 2 & 0 \\ 0 & r_e & 0 & 2r_e \end{bmatrix}, \quad r_e = \frac{I_e}{A_e} \tag{6.1.49a}$$

$$\Lambda_e = \frac{E_e I_e}{G_e A_e K_s h_e^2}, \quad \mu_0 = 12\Lambda_e \tag{6.1.49b}$$

For Hermite cubic interpolation of $W(x)$ and related quadratic approximation of $S(x)$ [i.e., *interdependent interpolation element* (IIE)], the resulting mass matrix is cumbersome and depends on the stiffness parameters ($E$ and $G$). We will not consider it here [see Reddy (1999*b*, 2000)].

**Example 6.1.2**

Consider a uniform beam of rectangular cross section ($B \times H$), fixed at $x = 0$ and free at $x = L$ (i.e., a cantilever beam). We wish to determine the first four flexural frequencies of the beam.

The boundary conditions of the structure are

$$W(0) = 0, \quad \frac{dW}{dx} = 0, \quad \left[ EI \frac{d^2W}{dx^2} \right]_{x=L} = 0, \quad \left[ EI \frac{d^3W}{dx^3} \right]_{x=L} = 0 \tag{6.1.50a}$$

in the Euler–Bernoulli beam theory and

$$W(0) = 0, \quad S(0) = 0, \quad \left[ EI \frac{dS}{dx} \right]_{x=L} = 0, \quad \left[ GAK_s \left( \frac{dW}{dx} + S \right) \right]_{x=L} = 0 \tag{6.1.50b}$$

in the Timoshenko beam theory. The first two terms in each case are the essential (or geometric) boundary conditions and the last two are the natural (or force) boundary conditions.

The number of eigenvalues we wish to determine dictates the minimum number of elements to be used to analyze the structure. First, consider the Euler–Bernoulli beam element. Since two primary degrees of freedom are specified ($U_1 = U_2 = 0$), a one-element mesh will have only two unknown degrees of freedom ($U_3$ and $U_4$). Hence, we can determine only two natural frequencies. Thus, a minimum of two Euler–Bernoulli beam elements are needed to determine four natural frequencies. If we use the reduced integration Timoshenko beam element, a mesh of two linear elements can only represent the first two mode shapes of the cantilever beam (see Fig. 6.1.4) because there are only two independent deflection degrees of freedom that are unspecified. In order to represent the first four mode shapes using the *reduced integration element* (RIE), we must use at least four linear elements or two quadratic elements. However, the four computed frequencies may not be the lowest four.

For illustrative purpose, first we consider the one-element mesh of the Euler–Bernoulli beam element. We have

$$\left( \frac{2EI}{L^3} \begin{bmatrix} 6 & -3L & -6 & -3L \\ -3L & 2L^2 & 3L & L^2 \\ -6 & 3L & 6 & 3L \\ -3L & L^2 & 3L & 2L^2 \end{bmatrix} - \omega^2 \frac{\rho AL}{420} \begin{bmatrix} 156 & -22L & 54 & 13L \\ -22L & 4L^2 & -13L & -3L^2 \\ 54 & -13L & 156 & 22L \\ 13L & -3L^2 & 22L & 4L^2 \end{bmatrix} \right.$$

$$\left. - \omega^2 \frac{\rho I}{30L} \begin{bmatrix} 36 & -3L & -36 & -3L \\ -3h & 4L^2 & 3L & -L^2 \\ -36 & 3L & 36 & 3L \\ -3L & -L^2 & 3L & 4L^2 \end{bmatrix} \right) \begin{Bmatrix} W_1 \\ \Theta_1 \\ W_2 \\ \Theta_2 \end{Bmatrix} = \begin{Bmatrix} Q_1 \\ Q_2 \\ Q_3 \\ Q_4 \end{Bmatrix}$$

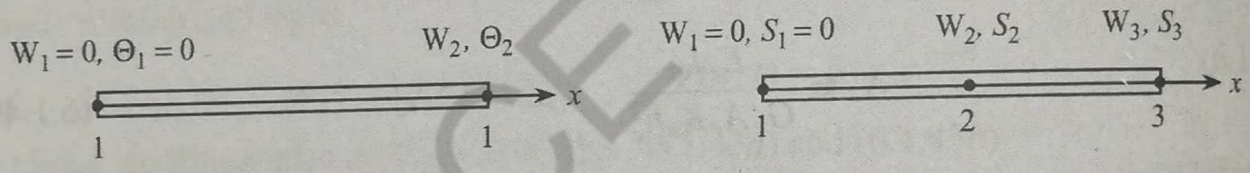


$$W(x) = W_1\phi_1(x) + \Theta_1\phi_2(x) + W_2\phi_3(x) + \Theta_2\phi_4(x)$$

$$\left.\begin{aligned} W(x) &= W_1^e \Psi_1^e(x) + W_2^e \Psi_2^e(x) \\ S(x) &= S_1^e \Psi_1^e(x) + S_2^e \Psi_2^e(x) \end{aligned}\right\} \text{Per element}$$

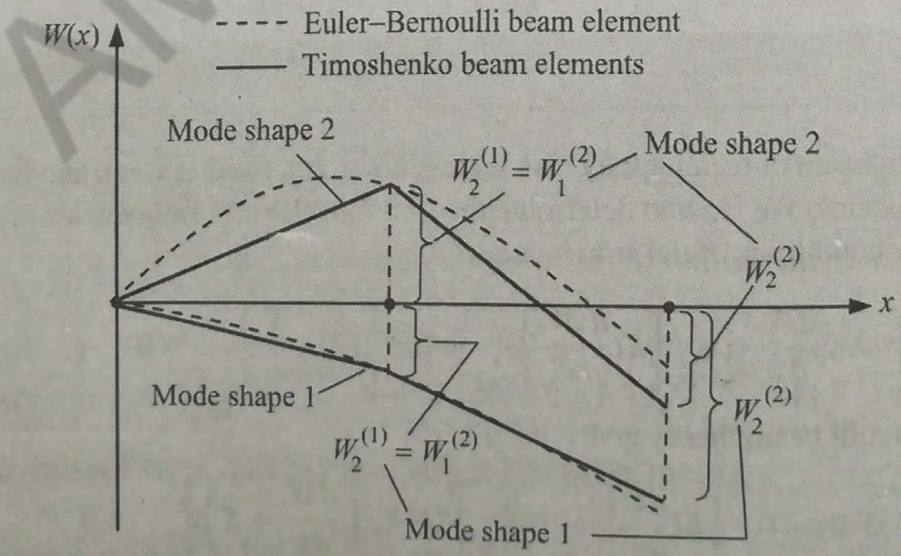


**Figure 6.1.4** Two possible nonzero mode shapes of a cantilever beam that can be represented by a mesh of two linear Timoshenko beam elements (or one Euler–Bernoulli beam element).

The specified displacement and force degrees of freedom are $W_1 = 0$, $\Theta_1 = 0$, $Q_3 = 0$, and $Q_4 = 0$. Hence, the condensed equations are

$$\left(\frac{2EI}{L^3}\begin{bmatrix} 6 & 3L \\ 3L & 2L^2 \end{bmatrix} - \omega^2 \frac{\rho AL}{420}\begin{bmatrix} 156 & 22L \\ 22L & 4L^2 \end{bmatrix} - \omega^2 \frac{\rho I}{30L}\begin{bmatrix} 36 & 3L \\ 3L & 4L^2 \end{bmatrix}\right)\begin{Bmatrix} W_2 \\ \Theta_2 \end{Bmatrix} = \begin{Bmatrix} 0 \\ 0 \end{Bmatrix}$$

Setting the determinant of the coefficient matrix in the above equation to zero, we obtain a quadratic characteristic equation in $\omega^2$.

First, consider the case in which the rotary inertia is neglected. The characteristic equation for this case is

$$15120 - 1224\lambda + \lambda^2 = 0, \quad \lambda = \frac{\rho AL^4}{EI}\omega^2$$

whose roots are

$$\lambda_1 = 12.48 \quad \lambda_2 = 1211.52, \quad \text{or} \quad \omega_1 = \frac{3.5327}{L^2}\sqrt{\frac{EI}{\rho A}}, \quad \omega_2 = \frac{34.8069}{L^2}\sqrt{\frac{EI}{\rho A}}$$

The exact frequencies are $\bar{\omega}_1 = 3.5160$ and $\bar{\omega}_2 = 22.0345$, where $\bar{\omega}_i = \omega_i(L^2\sqrt{\rho A/EI})$. The eigenvector components are computed from the first of the condensed equations

$$W_2^{(i)} = -L\left(\frac{1260 - 11\lambda_i}{420 - 13\lambda_i}\right)\Theta_2^{(i)}, \quad i = 1, 2$$

Hence, the eigenvectors are

$$\begin{Bmatrix} W_2 \\ \Theta_2 \end{Bmatrix}^{(1)} = \begin{Bmatrix} 0.7259L \\ -1.0000 \end{Bmatrix}, \quad \begin{Bmatrix} W_2 \\ \Theta_2 \end{Bmatrix}^{(2)} = \begin{Bmatrix} 0.1312L \\ -1.0000 \end{Bmatrix}$$

For the case in which rotary inertia is not neglected, we write $\rho I = \rho A\,(H^2/12)$ and take $H/L = 0.01$. The characteristic equation is

$$15112 - 1223.406\lambda + \lambda^2 = 0, \quad \lambda = \frac{\rho AL^4}{EI}\omega^2$$

whose roots are

$$\lambda_1 = 12.4797, \quad \lambda_2 = 1210.926 \quad \text{or} \quad \omega_1 = \frac{3.5327}{L^2}\sqrt{\frac{EI}{\rho A}}, \quad \omega_2 = \frac{34.7984}{L^2}\sqrt{\frac{EI}{\rho A}}$$

The exact frequencies are $\bar{\omega}_1 = 3.5158$ and $\bar{\omega}_2 = 22.0226$, where $\bar{\omega}_i = \omega_i(L^2\sqrt{\rho A/EI})$.

Next, we consider the one-element mesh of the Timoshenko beam element (RIE). We have

$$\left(\frac{2EI}{\mu_0 L^3}\begin{bmatrix} 6 & -3L & -6 & -3L \\ -3L & L^2\Xi_1 & 3L & L^2\Xi_2 \\ -6 & 3L & 6 & 3L \\ -3L & L^2\Xi_2 & 3L & L^2\Xi_1 \end{bmatrix} - \omega^2\frac{\rho AL}{6}\begin{bmatrix} 2 & 0 & 1 & 0 \\ 0 & 2r & 0 & r \\ 1 & 0 & 2 & 0 \\ 0 & r & 0 & 2r \end{bmatrix}\right)\begin{Bmatrix} W_1 \\ S_1 \\ W_2 \\ S_2 \end{Bmatrix} = \begin{Bmatrix} Q_1 \\ Q_2 \\ Q_3 \\ Q_4 \end{Bmatrix}$$

where $K_s = 5/6$, $r = I/A = H^2/12$, and

$$\Xi_1 = 1.5 + 6\Lambda, \quad \Xi_2 = 1.5 - 6\Lambda, \quad \Lambda = \frac{EI}{GAK_sL^2} = \frac{1+\nu}{5}\frac{H^2}{L^2}, \quad \mu_0 = 12\Lambda$$

The specified displacement and force degrees of freedom are $W_1 = 0$, $S_1 = 0$, $Q_3 = 0$, and $Q_4 = 0$; and the condensed equations are

$$\left(\frac{2EI}{\mu_0 L^3}\begin{bmatrix} 6 & 3L \\ 3L & L^2(1.5+6\Lambda) \end{bmatrix} - \omega^2\frac{\rho AL}{6}\begin{bmatrix} 2 & 0 \\ 0 & 2r \end{bmatrix}\right)\begin{Bmatrix} W_2 \\ S_2 \end{Bmatrix} = \begin{Bmatrix} 0 \\ 0 \end{Bmatrix}$$

Setting the determinant of the coefficient matrix to zero, we obtain the characteristic equation

$$\bar{\lambda}^2 - 3\left(1 + 3s^2 + 12s^2\Lambda\right)\bar{\lambda} + 108s^2 = 0, \quad \bar{\lambda} = \frac{\rho A L^4 \Lambda}{EI}\omega^2$$

where $s$ is the length-to-height ratio, $s = L/H$.

When the rotary inertia is neglected, we have

$$\bar{\lambda} = \frac{12\Lambda}{1 + 4\Lambda}$$

To further simplify the expression, we assume $\nu = 0.25$ and obtain

$$\omega^2 = \frac{12}{(1 + H^2/L^2)} \frac{EI}{\rho A L^4}$$

and

$$\frac{L}{H} = 100: \quad \omega = \frac{3.4639}{L^2}\sqrt{\frac{EI}{\rho A}}; \qquad \frac{L}{H} = 10: \quad \omega = \frac{3.4469}{L^2}\sqrt{\frac{EI}{\rho A}}$$

The exact frequency is $\bar{\omega} = 3.5158$ for $L/H = 100$ and $\bar{\omega} = 3.5092$ for $L/H = 10$, where $\bar{\omega}_i = \omega_i(L^2\sqrt{\rho A/EI})$. If the rotary inertia is included, we obtain

$$\frac{L}{H} = 100: \quad \omega = \frac{3.4639}{L^2}\sqrt{\frac{EI}{\rho A}}; \qquad \frac{L}{H} = 10: \quad \omega = \frac{3.4413}{L^2}\sqrt{\frac{EI}{\rho A}}$$

The frequencies obtained by the Euler–Bernoulli beam elements and Timoshenko beam elements (RIE) are shown in Table 6.1.2 for two different values of the length-to-height ratio $L/H$. The value $L/H = 100$ makes the effect of shear deformation negligible, and we obtain essentially the same result as in the Euler–Bernoulli beam theory. Since the frequencies are normalized, $\bar{\omega} = \omega L^2\sqrt{(\rho A/EI)}$, it is necessary only to select the values of $\nu$ and $L/H$. For

**Table 6.1.2** Natural frequencies of a cantilever beam according to Timoshenko beam theory (TBT) and Euler–Bernoulli beam theory (EBT) $[\bar{\omega} = \omega L^2(\rho A/EI)^{1/2}]$.

| | $L/H = 100$ | | | | $L/H = 10$ | | | |
|---|---|---|---|---|---|---|---|---|
| Mesh | $\bar{\omega}_1$ | $\bar{\omega}_2$ | $\bar{\omega}_3$ | $\bar{\omega}_4$ | $\bar{\omega}_1$ | $\bar{\omega}_2$ | $\bar{\omega}_3$ | $\bar{\omega}_4$ |
| 4L | 3.5406 | 25.6726 | 98.3953 | 417.1330 | 3.5137 | 24.1345 | 80.2244 | 189.9288 |
| 8L | 3.5223 | 22.8851 | 68.8937 | 151.8431 | 3.4956 | 21.7004 | 60.6297 | 119.2798 |
| 16L | 3.5174 | 22.2350 | 63.3413 | 127.5434 | 3.4908 | 21.1257 | 56.4714 | 104.6799 |
| 2Q | 3.5214 | 23.3226 | 78.3115 | 328.3250 | 3.4947 | 22.0762 | 67.0884 | 181.0682 |
| 4Q | 3.5161 | 22.1054 | 63.3271 | 133.9828 | 3.4895 | 21.0103 | 56.4572 | 108.6060 |
| 8Q | 3.5158 | 22.0280 | 61.7325 | 121.4458 | 3.4892 | 20.4421 | 55.2405 | 100.7496 |
| EBT† | 3.5158 | 22.0226 | 61.6179 | 120.6152 | 3.4892 | 20.9374 | 55.1530 | 100.2116 |
| TBT† | 3.5158 | 22.0315 | 61.6774 | 120.8300 | 3.5092 | 21.7425 | 59.8013 | 114.2898 |
| EBT‡ | 3.5160 | 22.0345 | 61.6972 | 120.9019 | 3.5160 | 22.0345 | 61.6972 | 120.9019 |

† Rotary inertia is included (Exact).

‡ Rotary inertia is neglected; the results are independent of the ratio $L/H$ (Exact).

computational purposes, we take $\nu = 0.25$; also, note that

$$GAK = \frac{E}{2(1+\nu)} BH\frac{5}{6} = \frac{4EI}{H^2}, \quad \rho I = \frac{H^2 \rho A}{12}$$

where $B$ and $H$ are the width and height, respectively, of the beam.

We note from Table 6.1.2 that the finite element results converge with $h$-refinement (i.e., when more of the same kind of elements are used) and also with $p$-refinement (i.e., when higher-order elements are used). The $p$-refinement shows more rapid convergence of the fundamental (i.e., first) frequency. Note that the effect of shear deformation is to reduce the magnitude of natural frequency when compared to the EBT. In other words, the assumed infinite shear rigidity makes the EBT over-predict the magnitude of frequencies. The first four mode shapes of the cantilever beam, as obtained using the 16-element mesh of linear elements, are shown in Fig. 6.1.5.

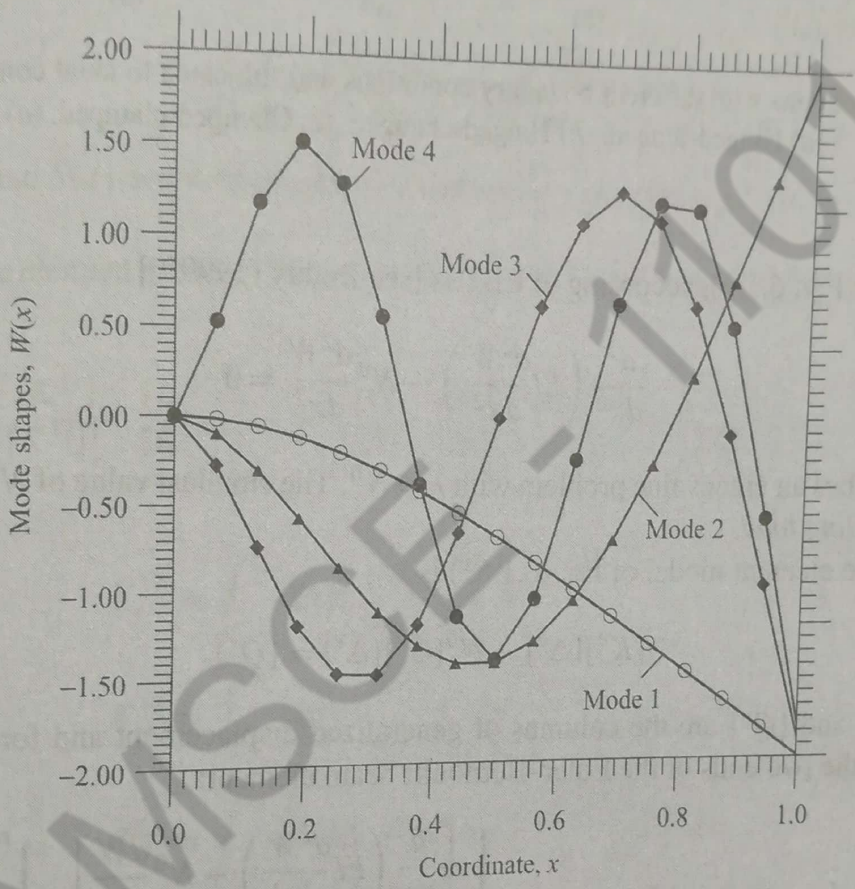


**Figure 6.1.5** First four natural mode shapes of a cantilever beam, as predicted using a 16-element mesh of linear Timoshenko beam elements ($L/H = 10$).



In closing the discussion on natural vibration, it is noted that when the symmetry of the system is used to model the problem, only symmetric modes are predicted. It is necessary to model the whole system in order to obtain all the modes of vibration.

## Stability (Buckling) of Beams

*EBT*

The study of buckling of beam-columns also leads to an eigenvalue problem. For example, the equation governing onset of buckling of a column subjected to an axial compressive